出國報告(出國類別：進修)

美國海軍研究院電機工程博士班返國心得報告

服務機關：國防部軍備局中山科學研究院
姓名職稱：馮柏凱 少校技士
派赴國家：美國
報告日期：103 年 1 月 28 日
出國時間：98 年 12 月 30 日至 102 年 12 月 22 日

摘要

海軍研究院創建於西元 1909 年並於 1951 年遷至西岸加州蒙特利現址，該校為美軍培育軍官研究發展尖端軍事系統的最高學府，其中主要分為四大系所：工程應用科學研究所(Graduate School of Engineering and Applied Science, GSEAS)、作戰資訊研究所(Graduate School of Operational and Information Science, GSOIS)、國際研究所(School of International Graduate Studies, SIGS)以及企業公共政策研究所(Graduate School of Business and Public Policy, GSBPP)；本次進修項目為電機工程博士班(Electrical Engineering，PhD)，該項隸屬於工程應用科學研究所，專業領域包含控制，微波，電腦，電路，訊號處理及通訊等學門。教學重點除教導電機領域的專業知識外並廣泛著墨於電子作戰整合概念，本次進修著重於電子戰領域的前端，訊號傳輸與接收的重要元件---分散式相位陣列天線。

奉准出國文令：國人管理字第 0980014048 號令

『美國海軍研究院電機工程博士班返國心得報告』

報告人：國防部軍備局中山科學研究院 馮柏凱少校

受訓班隊名稱：

(一) 中文：電機工程博士班

(二) 英文：Electrical Engineering (PhD)

受訓起迄日期：98 年 12 月 30 日至 102 年 12 月 20 日

返國日期：102 年 12 月 22 日

受訓地點及校名：

(一) 中文：美國加州蒙特瑞海軍研究院

(二) 英文：Naval Postgraduate School, Monterey, California

目次

一、目的

本次在美國海軍研究院進修電機工程博士學位，主要以修習相位陣列天線、雷達、微波等相關課程為主，意在延續碩士所學的電子戰專業領域（應用面），並由修課習得電機專業領域的基礎原理（理論面），希望於畢業後返回工作崗位能將理論與實務相結合，提昇工作成效。

二、 過程

首先，職將簡短介紹該校運作方式，接著描述該校電機工程博士班的入學及修業過程的要求，最後是畢業的規定及挑戰，提供後續有意至該校進修人員做為參考依據。美國海軍研究院採學季制，每季為三個月，學校會依據學員專長及離校時間長短，視情況給予一個學季的 refresh 課程，主要為基本學科複習。因參加受訓學員可能已離校一段時間，為使各學員能順利銜接後續專業課程，所以學校會安排第一學季做基本學科概念講述，像是微積分、工程數學等。

Refresh 課程結束後，緊接著就是專業課程教授，以電機工程博士班為例，實質上是沒有任何修課要求的，但是因為在進入正式論文研究之前會有三次測驗，分別是 screening exam（筆試）, written qualifying exam（筆試）和 oral qualifying exam（口試），所以修課便成為準備測驗的方式之一。電機領域有分為七個專業（track），包含微波、通訊、電子、電腦、數位訊號處理、控制、網路等。要參加 screening exam 的學員，必須選擇其中三個專業作為主要測驗項目，職選擇微波、通訊和數位訊號處理為主要測驗項目。決定主要測驗項目後，接著就必須廣泛且仔細地研讀各專業所表列的基礎科目，才有希望順利通過 screening exam。對大部分的人來說，修課是準備 screening exam 必要方法，尤其是對跨領域（專業不在電機領域）的人來說，因為進入博士學程的第一關 screening exam 所測驗的是相關專業的廣度及細節，修課可以獲得所需的廣度，而自身詳盡的研讀有助於細節的瞭解，

兩者並行是通過第一關測驗的主要方式。

在順利通過第一關後，學員始可自行尋求至少五位教授，組成所謂的委員會（PhD committee），其中一位為主任委員，也就是指導教授，但通常，除指導教授是由學員自行選擇外，其他委員大多由指導教授建議相關領域的教授擔任。因為委員會成員之間溝通協調的好壞，對於接下去的兩個測驗、論文研究過程和論文口試的順利與否，有著關鍵的影響，所以指導教授通常會推薦與他本身有合作或關係良好的教授來擔綱。

第二關，也就是 written qualifying exam（筆試），測驗內容就不像 screening exam 那樣廣泛但是會更深入，範圍和方式可以和委員會的成員討論，測驗的目的在確認學員對將來所要從事研究的領域，有深度的瞭解和分析研究的能力。

通過第二關後，將進入第三關 oral qualifying exam（口試），測驗範圍和第二關類似，不同點在於是以口試方式進行，主要目的是因為除了分析研究能力外，表達和講述的能力也是作為一個研究人員不可或缺的基本能力，其中的重點在於能在白板講述或描繪考試委員所提的問題，並利用相關專業知識尋求解決之道。理論推導也是此次測驗的重點項目，所以先前的練習（邊想、邊說、邊寫）就會是測驗成功與否的關鍵。

如能順利通過前文所述的三個測驗，緊接著就是論文研究的重點期。但在開始之前，學員必須提出論文題目和初步研究成果（proposal），並向委員會進行口頭報告，待委員會正式同意後，始得開始進行論文研究。通常這個時期會花費一年左右的時間，因為需要廣泛地閱讀和論文題目相關的文獻資料並撰寫電腦程式進行初步模擬，才能歸納整理出新的方法或理論來進行進一步研究。完成 proposal 後，博士候選人的資格也就拿到了。

完成博士學位的最後一關即是論文口試，通常是安排在畢業前三個月，規定是必須開放給所有想要參與的人進行旁聽及提問（口試前兩週必須公告），流程是先針對研究成果進行口頭報告，再來就是開放提問。一旦

順利完成，最後就是綜整各委員意見，進行論文修正，完成後就正式取得博士學位了。

此次進修完成博士論文一篇，題目為分散式數位陣列天線（Distributed Digital Subarray Antennas）。主要是為了探討可行的方式，將位於同一結構上不同系統的陣列天線聯合起來使用，目的是為了提高天線的增益值（Gain）及 SNR (signal-to-noise ratio)。但是當數個分散在不同位置的陣列天線一同運作時，grating lobe 的產生會造成系統的誤判，也會導致能量的損失。Grating lobe 的存在所造成的問題如圖一所示。

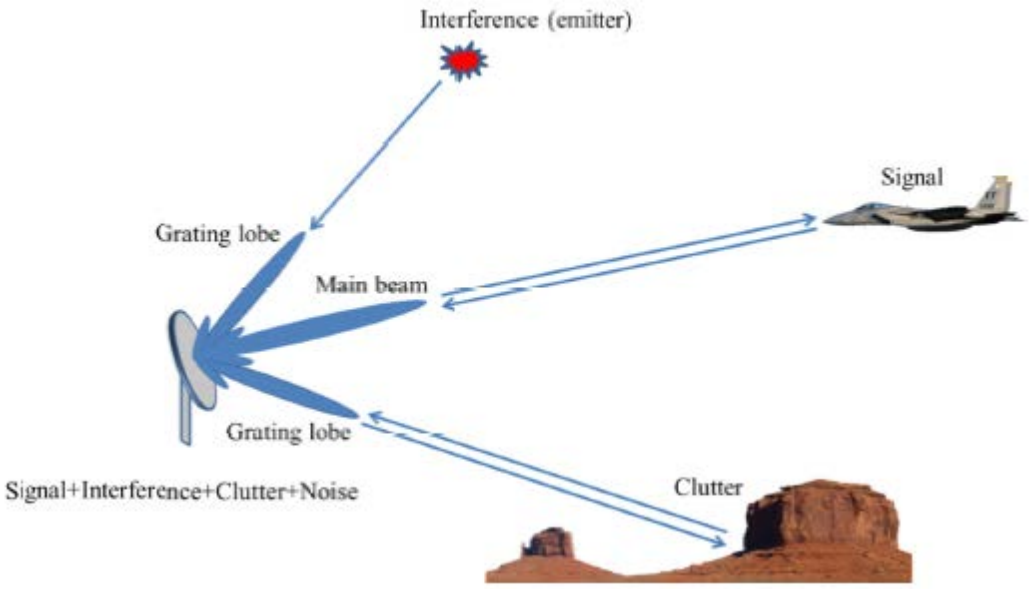

圖一、需求訊號、干擾、clutter 及接收雜訊的描述。

所以論文中探討傳統消除 grating lobe 的方式和結合一種以上的方法來消除 grating lobe，分析其效用及利用模擬的方式來展現研究的結果。圖二為線性的分散式陣列天線模型，其中黑點部分為實體天線，白點部分為虛擬天線。

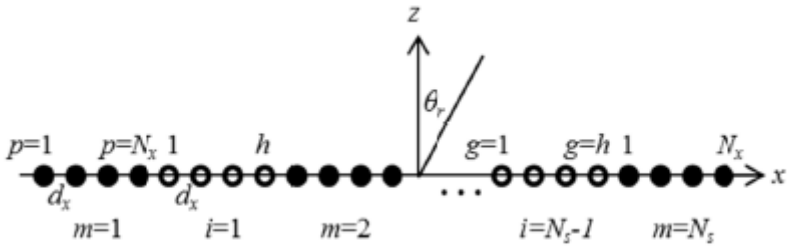

圖二、分散式陣列天線模型，黑點為實體天線，白點為虛擬天線。

圖三為傳送端模擬的結果。實驗結果證實，同時利用多種傳統消除 grating lobe 的方式，可以更有效地降低 grating lobe 的強度。相關代號解釋如下：

P：週期性分散式數位陣列天線

SR：依序旋轉

RD：隨機陣列位置

RS：隨機陣列大小

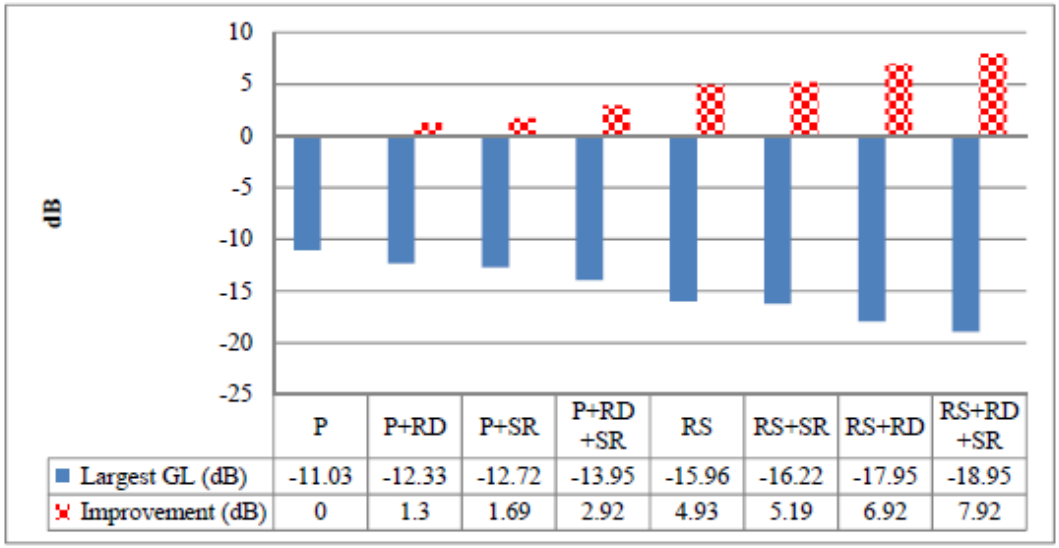

	P	P+RD	P+SR	P+RD +SR	RS	RS+SR	RS+RD	RS+RD +SR
Largest GL (dB)	-11.03	-12.33	-12.72	-13.95	-15.96	-16.22	-17.95	-18.95
Improvement (dB)	0	1.3	1.69	2.92	4.93	5.19	6.92	7.92

圖三、比較各種傳統消除 grating lobe 的方式及其組合應用的成效。

在接收端，我們提出一項新的方法，可以非常有效地降低 grating lobe，因此可以改善 SCR（signal-to-clutter ratio）和 SIR（signal-to-interference ratio）。

我們用虛擬的資料（虛擬陣列天線）補滿各個實體陣列天線之間的空間，由此，我們可以把這整個實體含虛擬陣列天線視為一個完整且連續的陣列天線。因為各元件間的距離小於波長的一半，grating lobe 就不會出現。圖四的紅色圖形為僅含實體分散式陣列天線的 radiation pattern，grating lobes 清晰可見。藍色圖形為採用新方法後所產生的 radiation pattern，grating lobe 問題可以有效解決。

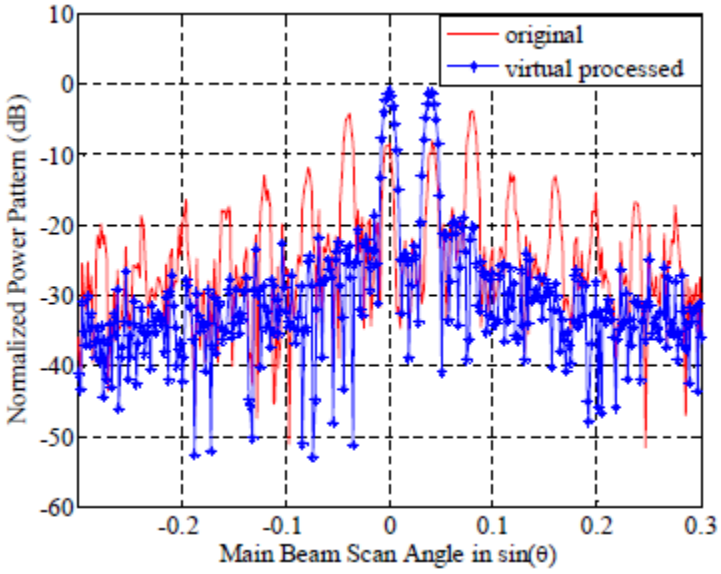

圖四、分散式陣列天線之 radiation pattern 和虛擬陣列填入後之 radiation pattern 結果比較。

論文的另一個貢獻是發展出一套新的訊號角度估算法則，取名為 Modified Matrix Pencil Method 和 Three-Step Modified Matrix Pencil Method，可以適用於分散式陣列天線的情況並有效提升其估算準確度。經由一系列的模擬及推導，歸納出了角度估算的誤差和固定系統誤差的關係在不同的訊號雜訊比之下的曲線，如圖五所示。

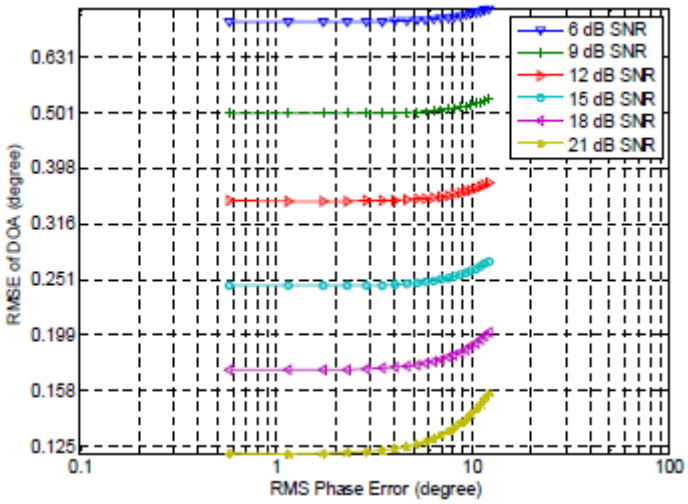

圖五、角度估算的誤差和固定系統誤差的關係在不同的訊號雜訊比之下的曲線。

三、心得

承蒙長官厚愛，職得以先後在海軍研究院進修電戰碩士和電機工程博士，兩次的進修都讓我收穫良多，除了專業知識的獲得之外，國際人脈的建立更是額外的收穫。

博士班的訓練讓我瞭解到，越是站在知識的前緣，越需要謙卑，因為人外有人，天外有天，尊重專業才是王道。另外，教育的本質不是直接給予答案，而是在學習如何去提問，然後去尋找自己的答案。

四、建議事項

美國海軍研究院為美軍培養高科技研發人才的最高學府，其教職員大多具備豐富的國防科技研發經驗並曾經或現正參與尖端武器系統的開發工作。建議能建立雙方常態性邀訪的機制，以延續此一難得的跨國人脈，為國防科技交流增添另一條不可或缺的管道。

NAVAL POSTGRADUATE SCHOOL

MONTEREY, CALIFORNIA

DISSERTATION

DISTRIBUTED DIGITAL SUBARRAY ANTENNAS

by

Bo-Kai Feng

December 2013

Dissertation Supervisor: David C. Jenn

Approved for public release; distribution is unlimited

THIS PAGE INTENTIONALLY LEFT BLANK

REPORT DOCUMENTATION PAGE			Form Approved OMB No. 0704-0188
Public reporting burden for this collection of information is estimated to average 1 hour per response, including the time for reviewing instruction, searching existing data sources, gathering and maintaining the data needed, and completing and reviewing the collection of information. Send comments regarding this burden estimate or any other aspect of this collection of information, including suggestions for reducing this burden, to Washington headquarters Services, Directorate for Information Operations and Reports, 1215 Jefferson Davis Highway, Suite 1204, Arlington, VA 22202-4302, and to the Office of Management and Budget, Paperwork Reduction Project (0704-0188) Washington DC 20503.			
1. AGENCY USE ONLY *(Leave blank)*	**2. REPORT DATE** December 2013	**3. REPORT TYPE AND DATES COVERED** Dissertation	
4. TITLE AND SUBTITLE DISTRIBUTED DIGITAL SUBARRAY ANTENNAS		**5. FUNDING NUMBERS**	
6. AUTHOR(S) Bo-Kai Feng			
7. PERFORMING ORGANIZATION NAME(S) AND ADDRESS(ES) Naval Postgraduate School Monterey, CA 93943-5000		**8. PERFORMING ORGANIZATION REPORT NUMBER**	
9. SPONSORING / MONITORING AGENCY NAME(S) AND ADDRESS(ES) N/A		**10. SPONSORING / MONITORING AGENCY REPORT NUMBER**	
11. SUPPLEMENTARY NOTES The views expressed in this thesis are those of the author and do not reflect the official policy or position of the Department of Defense or the U.S. Government. IRB Protocol number _____N/A_____.			
12a. DISTRIBUTION / AVAILABILITY STATEMENT Approved for public release; distribution is unlimited		**12b. DISTRIBUTION CODE**	

13. ABSTRACT (maximum 200 words)

A system that incorporates distributed digital subarrays working cooperatively as a single array can potentially increase the output signal-to-noise ratio and provide better spatial resolution compared with using the subarrays individually. However, collectively combining periodic widely separated subarrays results in unacceptable grating lobes, and these lobes cannot be suppressed using traditional windowing methods. In this research, we focus on distributed subarray antennas that are comprised of subarrays that can operate individually or collectively. We develop techniques for grating lobe suppression on both the transmitting and receiving sides of the distributed array system. Traditional solutions and new methods are examined in detail via numerical simulation to quantify the performance limitations when applied in combination. One contribution of this research is a hybrid approach that uses a combination of suppression techniques on both the transmitting and receiving sides. Another contribution is the development of new receiving processing methods to suppress grating lobes and improve the signal-to-clutter ratio and signal-to-interference ratio. A final contribution shows the relationship between thermal noise, array errors, and the grating lobe suppression effectiveness. The consideration of array errors addresses the issue of array calibration and synchronization, which are critical concerns when multiple arrays operate coherently.

14. SUBJECT TERMS Digital Distributed Subarray Antenna, Virtual Filling, Random Array			**15. NUMBER OF PAGES** 125
			16. PRICE CODE
17. SECURITY CLASSIFICATION OF REPORT Unclassified	**18. SECURITY CLASSIFICATION OF THIS PAGE** Unclassified	**19. SECURITY CLASSIFICATION OF ABSTRACT** Unclassified	**20. LIMITATION OF ABSTRACT** UU

NSN 7540-01-280-5500

Standard Form 298 (Rev. 2-89)
Prescribed by ANSI Std. 239-18

THIS PAGE INTENTIONALLY LEFT BLANK

Approved for public release; distribution is unlimited

DISTRIBUTED DIGITAL SUBARRAY ANTENNAS

Bo-Kai Feng
Major, Taiwan Army
B.S., Chung Cheng Institute of Technology, 1999
M.S., Naval Postgraduate School, 2006

Submitted in partial fulfillment of the
requirements for the degree of

DOCTOR OF PHILOSOPHY IN ELECTRICAL ENGINEERING

from the

NAVAL POSTGRADUATE SCHOOL
December 2013

Author: Bo-Kai Feng

Approved by:

David C. Jenn
Professor of Electrical and Computer Engineering
Dissertation Committee Chair and Dissertation Supervisor

Lawrence J. Ziomek
Professor of Electrical and Computer Engineering

Roberto Cristi
Professor of Electrical and Computer Engineering

Ric A. Romero
Assistant Professor of Electrical and Computer Engineering

Gamani Karunasiri
Professor of Physics

Approved by: R. Clark Robertson, Chair, Electrical and Computer Engineering

Approved by: Douglas Moses, Vice Provost for Academic Affairs

THIS PAGE INTENTIONALLY LEFT BLANK

ABSTRACT

A system that incorporates distributed digital subarrays working cooperatively as a single array can potentially increase the output signal-to-noise ratio and provide better spatial resolution compared with using the subarrays individually. However, collectively combining periodic widely separated subarrays results in unacceptable grating lobes, and these lobes cannot be suppressed using traditional windowing methods. In this research, we focus on distributed subarray antennas that are comprised of subarrays that can operate individually or collectively. We develop techniques for grating lobe suppression on both the transmitting and receiving sides of the distributed array system. Traditional solutions and new methods are examined in detail via numerical simulation to quantify the performance limitations when applied in combination. One contribution of this research is a hybrid approach that uses a combination of suppression techniques on both the transmitting and receiving sides. Another contribution is the development of new receiving processing methods to suppress grating lobes and improve the signal-to-clutter ratio and signal-to-interference ratio. A final contribution shows the relationship between thermal noise, array errors, and the grating lobe suppression effectiveness. The consideration of array errors addresses the issue of array calibration and synchronization, which are critical concerns when multiple arrays operate coherently.

THIS PAGE INTENTIONALLY LEFT BLANK

TABLE OF CONTENTS

THIS PAGE INTENTIONALLY LEFT BLANK

LIST OF FIGURES

THIS PAGE INTENTIONALLY LEFT BLANK

LIST OF TABLES

THIS PAGE INTENTIONALLY LEFT BLANK

LIST OF ACRONYMS AND ABBREVIATIONS

AESA	active electronically scanned array
BW	beamwidth
DAS	distributed array system
dB	decibel
DBF	digital beamforming
DDSA	digital distributed subarray antenna
DOA	direction-of-arrival
DSA	distributed subarray antenna
DSP	digital signal processing
ESPRIT	estimation of signal parameters via rotational invariance techniques
EW	electronic warfare
FFT	fast fourier transform
GL	grating lobe
HFSWR	high frequency surface wave radar
I	in-phase
MFAR	multi-function array radar
MP	matrix pencil
MS	multiple snapshots
MSS	multiple single-snapshot
MUSIC	multiple signal classification
MWN	minimum weighted norm
PDF	probability density function
Q	quadrature

RMS	root mean square
RMSE	root mean square error
SIGINT	signal intelligence
SCR	signal-to-clutter ratio
SIR	signal-to-interference ratio
SLL	side lobe level
SNR	signal-to-noise ratio
SS	single snapshot
Super-SVA	super spatially variant apodization
SVD	singular value decomposition
VHF	very high frequency
WSNs	wireless sensor networks

EXECUTIVE SUMMARY

Complete digital control of amplitude and phase at the element level of an array allows great flexibility in beamforming. Modern radar and communications systems incorporate phased arrays with wider bandwidths, allowing for the possibility that several systems on the same platform can share arrays. A system that incorporates distributed digital subarrays (DDSAs) working cooperatively as a single array (thus forming an array of subarrays) can potentially increase the output signal-to-noise ratio (SNR) and provide better spatial resolution compared with using the subarrays individually.

Another factor impacting architecture is the platform design philosophy for military applications, which has changed dramatically with the advent of stealth technology and requires reduced platform signatures. Due to the stealth requirement, it is difficult to find an available area sufficient for a large array on board a ship, so it might be necessary to use several relatively small noncontiguous (separated) areas (subarrays) and then process the received signal coherently.

Traditional periodically distributed subarrays (subarrays whose centers are equally spaced) form a long baseline and are capable of very accurate angular location of targets. However, collectively combining periodic widely separated subarrays results in unacceptable grating lobes, and these lobes cannot be suppressed using traditional windowing methods. Grating lobes appear in the visible region if the subarrays are nearly periodic, and they are unwanted because of the ambiguities that accompany them. Even if the individual array patterns have no grating lobes, conventional beamforming with periodic DDSAs will have an output response with grating lobes, which is unacceptable for most applications.

In this research, we focus on distributed subarray antennas that are comprised of subarrays that can operate individually or collectively. It is assumed that no grating lobes appear in the visible region for each subarray when scanned. We develop techniques for grating lobe suppression on both the transmitting and receiving sides of the distributed array system (DAS). Traditional solutions and new methods will be examined in detail

via numerical simulation to quantify the performance limitations when applied in combination.

In Figure 1, we summarize the effectiveness of the conventional methods and their combinations on grating lobe suppression for this specific arrangement without amplitude tapering. The improvements shown are computed relative to the periodic DDSA. For concise presentation, we define the shorthand notation of each method as below:

P: periodic DDSA. RD: random subarray displacement.

SR: sequential subarray rotation. RS: random subarray sizes.

In Figure 1, it can be seen that the combination of methods has the greatest improvement relative to using the conventional methods individually. However, it is worth noting that an optimization process is needed for each new DDSA arrangement to achieve maximum grating lobe reduction.

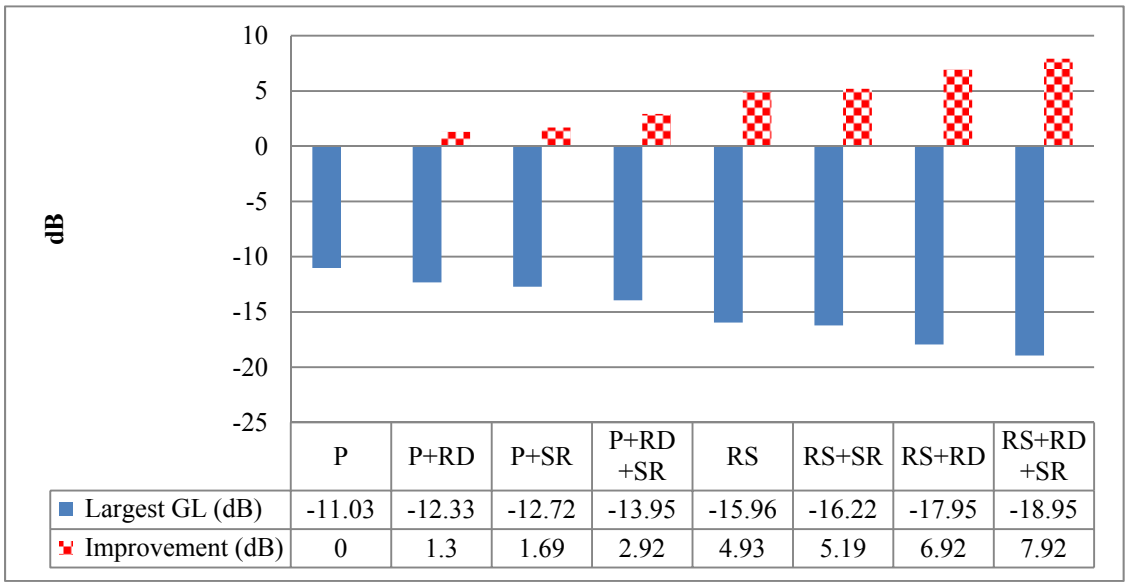

	P	P+RD	P+SR	P+RD +SR	RS	RS+SR	RS+RD	RS+RD +SR
Largest GL (dB)	-11.03	-12.33	-12.72	-13.95	-15.96	-16.22	-17.95	-18.95
Improvement (dB)	0	1.3	1.69	2.92	4.93	5.19	6.92	7.92

Figure 1. Summary of the effectiveness on grating lobe suppression using conventional approaches individually and in combination.

One contribution of this research is a hybrid approach that uses a combination of suppression techniques on both the transmitting and receiving sides. The result is an

improved two-way pattern performance. For comparison purposes, a two-way pattern of the periodic DDSA is shown in Figure 2. The two-way pattern shown in Figure 3 is generated by multiplying the transmitting pattern (random subarray sizes) by the receiving pattern (random subarray sizes and virtual filling). The side lobe level has gone down to less than -50 dB without affecting the mainbeam.

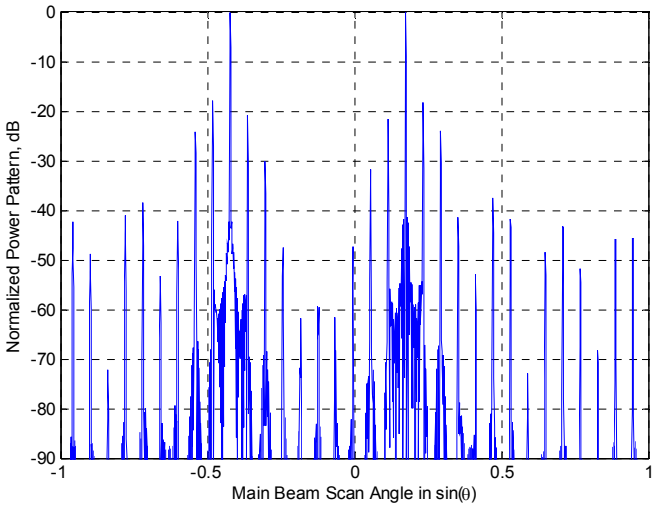

Figure 2. Periodic DDSA two-way pattern of signals from 10° and -25° related to the broadside.

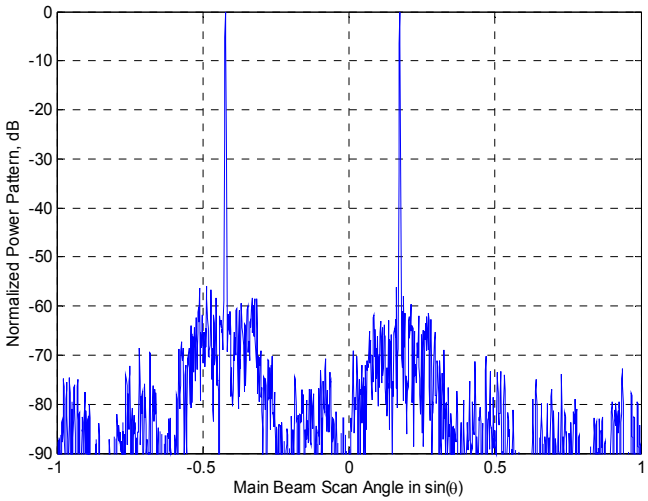

Figure 3. Random subarray sizes DDSA two-way pattern of signals from 10° and -25° related to the broadside.

Another contribution is the development of new receiving processing methods to suppress grating lobes and improve the signal-to-clutter ratio (SCR) and signal-to-interference ratio (SIR). We propose virtual filling of the gaps between the subarrays to eliminate the grating lobes on the receiving side so that the response of a single large contiguous array is synthesized. Therefore no grating lobes will appear as long as element spacing within all subarrays is less than one half of the wavelength. Furthermore, amplitude tapering can be applied to the synthesized array to reduce interference and clutter. Consider a five-subarray DDSA with thirty elements in each subarray and an element spacing of 0.42λ. The subarray length is 12.6λ. The gaps are also (arbitrarily) set to 12.6λ. One unit amplitude signal is incident from 0° with a phase of $\pi/5$. A second interference signal is coming in at 2.3° with a phase $-4\pi/5$. In Figure 4, the average synthesized array response with an SNR per element of 6 dB (single snapshot) in the direction of both signals is the same as that of a contiguous array as the weights are changed to scan the main beam in a region of direction cosine space ($\sin\theta$). A 20 dB Taylor amplitude distribution is applied. As can be seen, the high response of the interfering signal that occurs at grating lobe locations has been eliminated.

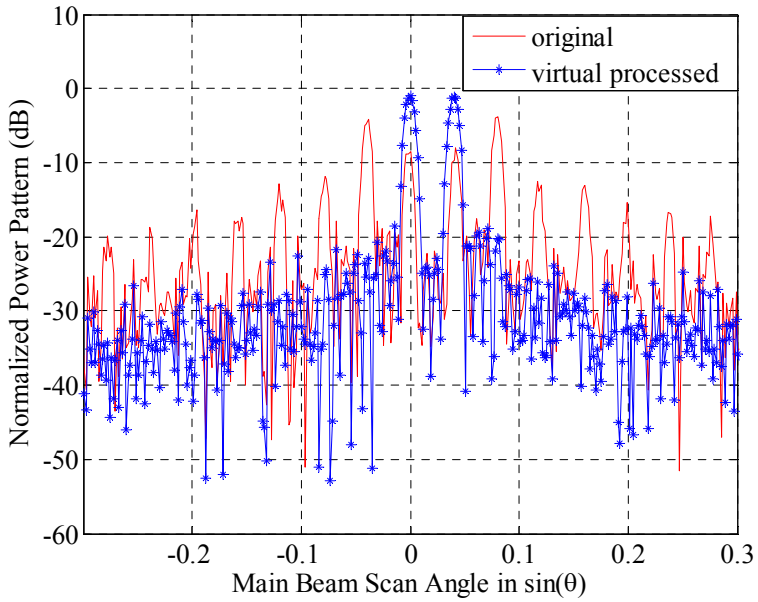

Figure 4. Comparison of original and synthesized antenna response after virtual filling for an element level SNR of 6 dB. Taylor amplitude taper ($\bar{n}$ =5, SLL=–20 dB) has been applied.

A final contribution shows the relationship (and hence tradeoffs) between thermal noise, array errors, and the grating lobe suppression effectiveness. The consideration of array errors addresses the issue of array calibration and synchronization, which are critical concerns when multiple arrays operate coherently. A five-subarray DDSA model is used to examine the effects of fixed errors to the direction-of-arrivals (DOAs) estimation and filling method. Each subarray is comprised of 10 elements with element spacings equal to 0.45λ. Subarray center distances are 10λ. Fixed errors are uniformly distributed from -21° to 21° (root mean square (RMS) values from 0° to 12.1°), and the SNR is varied from 6 dB to 21 dB at each element. Two signals with equal magnitude and non-coherent phases ($\pi/5$ and $-4\pi/5$) from DOAs of -10° and 15° relative to broadside are impinging on the DDSA.

The receiving pattern for 6 dB SNR for the ideal contiguous array of the same aperture size as DDSA, original DDSA and virtual filling method are compared in Figure 5. A huge improvement in terms of grating lobes and sidelobe suppression can be observed after applying the virtual filling method.

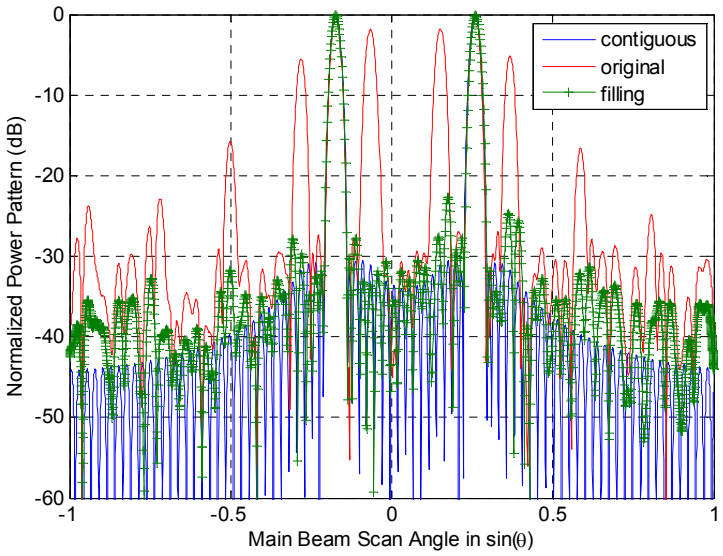

Figure 5. Pattern comparison of contiguous, original DDSA and virtual filling. Assuming no fixed errors and with 6 dB SNR at each element. Taylor amplitude taper ($\bar{n}$ =5, SLL=–30 dB) has been applied.

In order to quantify the effect of fixed errors on the DOA estimations, a plot that compares the root mean square error (RMSE) of the DOA versus RMS phase error for different SNR levels is shown in Figure 6.

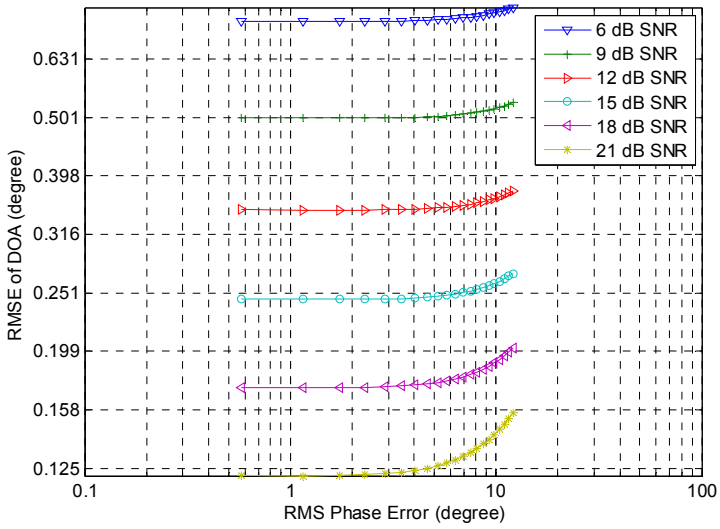

Figure 6. RMSE of DOA versus RMS phase errors from 0° to 12.1° for different element SNR.

Many of the sources of the fixed errors can be compensated for by pre-calculation or pre-measurement, but there will still be some residual errors after correction. We consider phase errors up to 21° and examine how they degrade the radiation pattern. Figure 7 has a plot of the pattern of the worst case (21° fixed error) at 6 dB SNR. By comparing Figure 7 with Figure 5, we see that the effect of the fixed error on the receiving pattern is to increase the side lobe level and lower the main beam by 0.6 dB due to the increase of RMSE of the DOA.

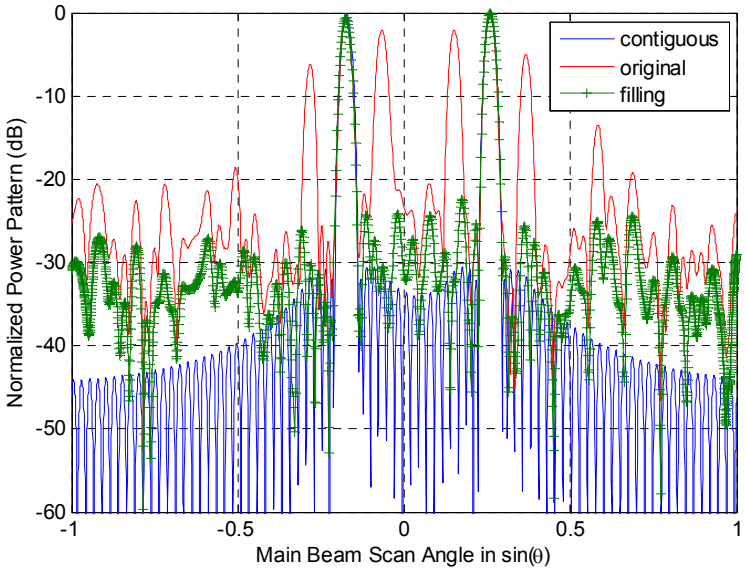

Figure 7. Pattern comparison of contiguous, original DDSA and virtual filled DDSA for 21° fixed error and with 6 dB SNR at each element. Taylor amplitude taper ($\bar{n}$ =5, SLL= –30 dB) has been applied.

THIS PAGE INTENTIONALLY LEFT BLANK

ACKNOWLEDGMENTS

I would like to thank my wife, Hsiang-Hsiang; my son, Benson; and my daughter, Angela, for their consistent support and the sacrifice of many hours together so I could complete this work.

And I would like to express my sincere appreciation to Professor David Jenn for his mentoring and guidance that made the challenging dissertation process very rewarding. My committee members, Professor Lawrence J. Ziomek, Professor Roberto Cristi, Professor Ric A. Romero, and Professor Gamani Karunasiri have all provided significant insights and improvements to this dissertation, for which I am grateful.

THIS PAGE INTENTIONALLY LEFT BLANK

I. INTRODUCTION

The phased array is generally the antenna architecture of choice for most modern high-performance radar and communication systems. Phased arrays consist of a collection of individual antennas that are geometrically arranged and excited (phased) so as to provide the desired radiation characteristics.

Traditionally antenna arrays have been constructed with a large number of radiating elements distributed over a given confined surface with an average distance to the nearest neighbor no larger than $\lambda/2$. Advanced Active Electronically Scanned Array (AESA) systems, which structurally integrate the arrays into the platform, have opened up the possibility of antenna systems consisting of separated subarray apertures where the aperture is split into two or more subarrays and separated by a relatively large distance. Within each subarray the average distance between the radiating elements is still not larger than $\lambda/2$ but the distances between the phase centers of the subarrays are much larger than that. An increase in angular measurement performance can potentially be gained by increasing the measurement base by dividing the aperture into two or more subarrays and pulling them apart. This should improve both angular accuracy and resolution [1, 2].

Also, when multiple systems on the same platform are using arrays with increased bandwidths, these systems can share arrays. Another factor impacting architecture is the platform design philosophy for military applications, which has changed dramatically with the advent of stealth technology and requires reduced platform signatures. Due to the stealth requirement, it is difficult to find an available area sufficient for a large array on board a ship, so it might be necessary to use several relatively small noncontiguous (separated) areas (subarrays) and then process the received signal coherently.

"Hastily formed" subarray systems are reconfigurable and expandable arrays for emergencies that can be deployed on the sides of hills, buildings, or trucks. Some of these applications are illustrated in Figure 1.

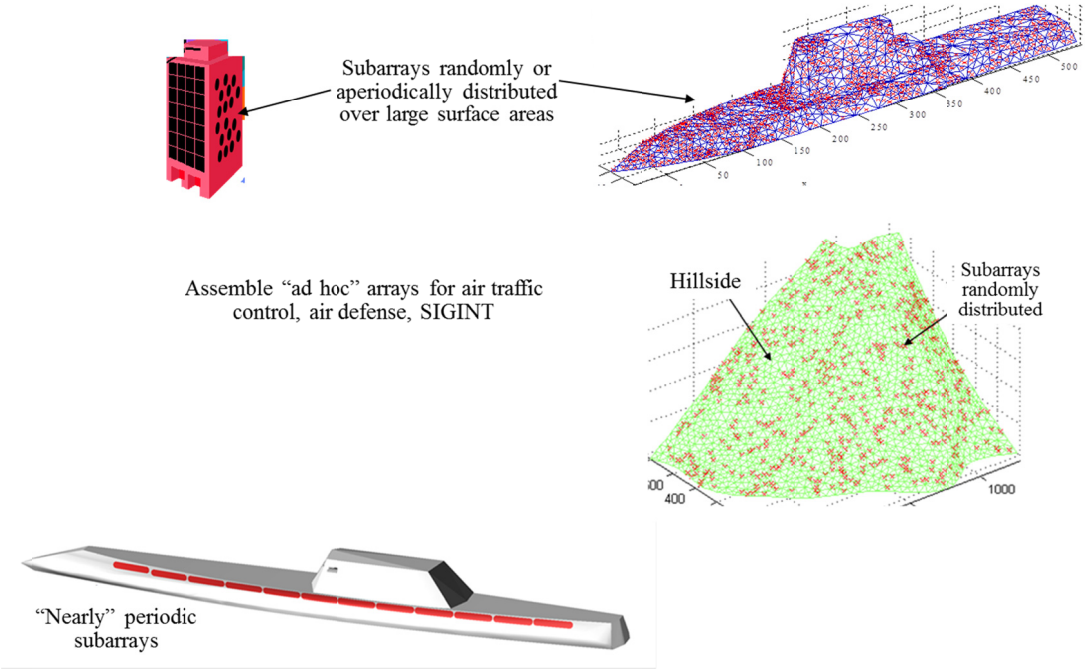

Figure 1. Assembled "ad hoc" arrays for air traffic control, air defense, signal intelligence (SIGINT).

A. PERIODIC DISTRIBUTED SUBARRAYS

Traditional periodically distributed subarrays (subarrays whose centers are equally spaced) form a long baseline and are capable of very accurate angular location of targets [3, 4]. However, collectively combining periodic widely separated subarrays results in unacceptable grating lobes, and these lobes cannot be suppressed using traditional windowing methods. Grating lobes appear in the visible region if the subarrays are nearly periodic, and they are unwanted because of the ambiguities that accompany them. Besides that, the interference power from another emitter can severely degrade the system performance when the emitter is in the direction of a grating lobe. Similar degradation can occur when a sector of clutter return, which consists of reflections of transmitted power from obstacles, is received through the grating lobes. The depiction of the desired signal, interference, clutter and receiver noise can be seen in Figure 2. The signal-to-interference ratio (SIR), the signal-to-clutter ratio (SCR) and the signal-to-noise ratio (SNR) are defined as the signal power over the interference power, the signal power over the clutter power, and the signal power over the noise power, respectively.

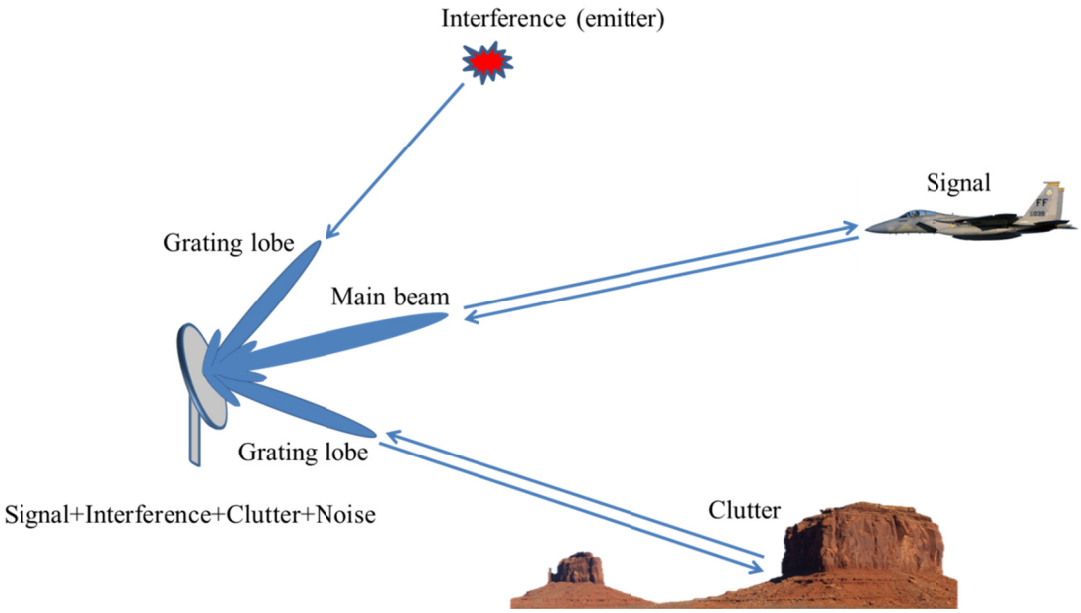

Figure 2. An illustration of the desired signal, interference, clutter and receiver noise.

It is possible to suppress the grating lobes through control of the subarray factor. In other words, the nulls of the subarray pattern are placed at angles where the grating lobes occur. However, the resulting constraints are severe. Some additional improvement is achieved if separate transmitting and receiving antennas are used, and grating lobes are allowed for only one of the two antennas. The main limitation is that the configurations of the transmitting and receiving antennas need to be different, and hence more space is required [5].

B. RANDOM AND APERIODIC DISTRIBUTED SUBARRAYS

Another approach to reducing grating lobes is randomization of the subarray positions. A contiguous random fractal array is an example that utilizes randomness to suppress the grating lobes [6]. An aperiodic array is somewhere between periodic and random arrays. For a linear array with unequal element spacing, it is possible to mitigate large grating lobes because of the "space tapering" effect from the non-uniform element spacing [7].

C. DIGITAL ANTENNAS

Digital antennas are widely used today because of their flexibility in signal processing and suitability for low profile array design compared to their analog counterparts [8]. An example of digital array antenna architecture is shown in Figure 3. The important feature of this architecture is that element level baseband in-phase (*I*) and quadrature (*Q*) data are available to a central array processor (digital beamformer). A digital antenna architecture allows for a wide range of waveform control and digital beamforming on both the transmitting and receiving sides.

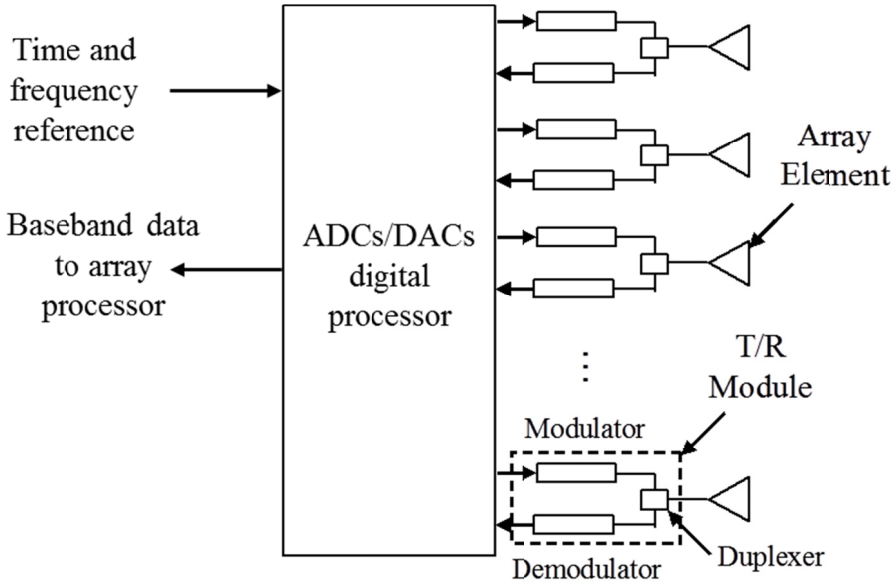

Figure 3. Generic digital antenna architecture.

When subarrays are used together in a digital antenna system there are several beamforming options. The first is to let them act independently (with or without a common time and phase reference). The system can schedule the antenna resources to improve the performance [9]. For example, a radar may add a second array to increase the scan volume or reduce the frame time.

A second approach is to use the antennas collectively as if they are elements of a larger array, i.e., they act as subarrays in a large array [10]. This arrangement could be

referred to this as a "synthetic array." Depending on the performance requirements and subarray locations and orientation, not all subarrays need to be used at the same instance.

D. GEOMETRICAL ARRANGEMENT

The geometrical arrangement and individual capabilities of the subarrays greatly affect the potential performance of the synthetic array. Fundamental array parameters include:

- The number of subarrays.
- The size of the subarrays and their shapes.
- Element types and polarization.
- Scan capability (maximum scan angle, scan rates and planes of scan).
- Physical arrangement (the distribution of elements and subarrays in space).
    - Linear, planar, volumetric.
    - Periodic, aperiodic or random.
    - Rotation and tilt relative to a global reference.

Based on the physical arrangement, periodic array structures can be linear, planar or volumetric. Linear and planar structures are most often used because they are relatively easy to design, manufacturing and integrate into platforms, and they can provide any desirable beamwidth and gain. In this research we shall assume that all of the arrays are planar, but they can be tilted, rotated and have different numbers of elements and element spacings. An example of distributed linear array of N_s subarrays in the x-y plane is shown in Figure 4. We consider only rectangular subarrays; the extension to other shapes (e.g., circular) is straightforward.

Each subarray is capable of operating independently (i.e., it can scan independently), and its element level I and Q data are available to a central beamformer/processor. A primary interest in this research is to develop beamforming

techniques on the receiving side because there is more flexibility in processing the received data. The flexibility of the hardware on the transmitting side is generally more limited.

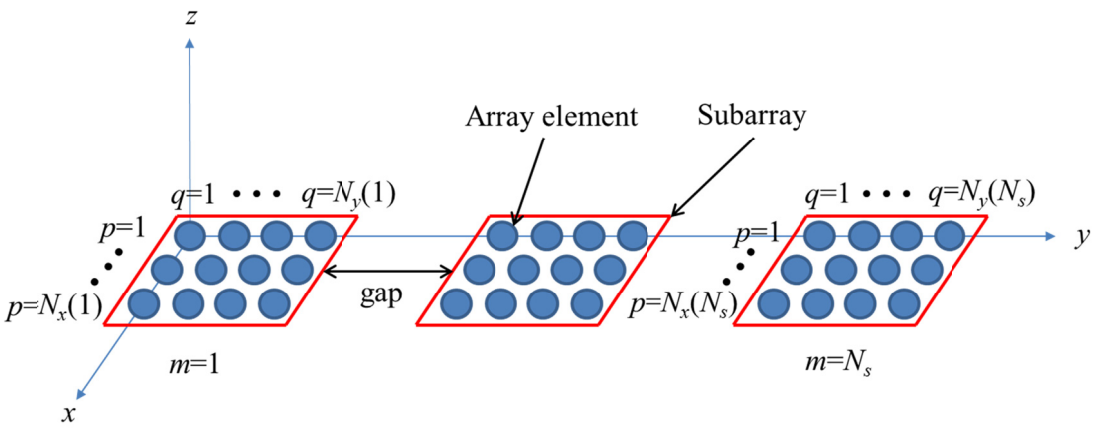

Figure 4. Distributed linear array structure.

Periodic spacing of array elements along a line or over a plane has been a major way of creating a phased array antenna for decades. As long as the element spacing for the array is less than a half wavelength, grating lobes will not exist in the far field radiation pattern when scanned. An advantage of using periodic structures is that lobe and null locations of the radiation pattern are predictable, and they result in lower manufacturing and replacement/maintenance cost. Also, pattern synthesizing and beamforming are relative easy compared to that of non-periodic structures.

A disadvantage of the periodic array structure is that grating lobes become a problem for element spacing larger than a half wavelength. Because the pattern is determined by the element spacing in wavelengths, narrow bandwidth is not uncommon. Generally speaking, the aperture size must be increased, and more radiation elements (larger area) are needed to decrease the beamwidth. Larger spacing is also used to reduce the number of elements in an array to reduce cost, weight and volume.

For military applications, stealth is one of the crucial issues that cannot be ignored for today's warfare. A revolutionary idea that could provide the potential of using the entire length and width of a large ship as the aperture is to let the stealth designed ship

structure dictate where the subarrays can be placed. The aperture can be used collectively or individually for various purposes such as communication, surveillance, guidance and control, and even threat imaging [5]. This idea of having integrated subarray elements in the ship's hull forming the aperture for the radar is not entirely new [11], but there are problems associated with a distributed array system (DAS) such as those shown in Figure 1. Not only are there grating lobes due to the subarray spacing, but the distribution of frequency and time references, and calibration and error correction are significant challenges.

E. DISSERTATION OBJECTIVE

Very few researchers have looked at using a large number of arrays collectively, in particular, if the subarrays are not identical. The conventional approaches to reducing grating lobes have mainly been applied to individual arrays but not to multiple arrays with gaps. Likewise, random methods are often applied to the distribution of elements within an array but not between subarrays.

A primary objective of this research is to investigate the wide variety of processing techniques that can be applied with digital distributed subarray antennas for grating lobe suppression. Many radar, communication and electronic warfare (EW) systems' performance and capabilities can be improved by using multiple antennas (or equivalently one large synthetic antenna). Potential improvements are the increase in signal-to-noise ratio, high angular resolution, wider bandwidth, and reconfigurability.

In this research, we focus on distributed antennas that are comprised of subarrays that can operate individually or collectively. It is assumed that no grating lobes appear in the visible region for each subarray when scanned. We develop techniques for grating lobe suppression on both the transmitting and receiving sides of the DAS. Traditional solutions and new methods will be examined in detail via numerical simulation to quantify the performance limitations when applied in combination. One contribution of this research is a hybrid approach that uses a combination of suppression techniques on both the transmitting and receiving sides. The result is an improved two-way pattern performance.

Another contribution is the development of new receiving processing methods to suppress grating lobes and improve the signal-to-clutter ratio and signal-to-interference ratio. A final contribution shows the relationship (and hence tradeoffs) between thermal noise, array errors, and the grating lobe suppression effectiveness. The consideration of array errors addresses the issue of array calibration and synchronization, which are critical concerns when multiple arrays operate coherently.

F. RELATED WORK

Steinberg and Yadin in 1982 [12] first introduced the concept of a distributed airborne array to make use of a large aperture to achieve higher angular resolution. Lin's 1983 paper [3] was the first to consider using coherently internetted mini-radars to accomplish surveillance and tracking efficiently. Lin's 2003 thesis [5] adapted the concept of distributed subarray antennas and proposed it for both Multi-function Array Radar (MFAR) and Very High Frequency (VHF) applications. By combining distributed subarrays on the available areas of a constrained platform, the MFAR or VHF distributed subarray antennas (DSAs) can achieve the maximum resolution and potential reductions in cost and complexity.

Many methods have been employed to reduce or eliminate the grating lobes for DSAs, but all have their limitations and disadvantages. (We refer to these collectively as "traditional" or "conventional" techniques.) Within a single array, a common approach is to place subarray nulls at grating lobe locations using overlapping subarrays [13], but this severely limits the array geometry. Another approach is to rotate or tilt the subarrays, thereby reducing the periodicity [14]. The grating lobe level varies as $20\log(1/N_s)$, where N_s is the number of subarrays. To be effective, this method requires a large number of subarrays. Random or fractal element spacings within the subarrays and randomizing the number of elements between subarrays have been used [15]. Again, large numbers of elements and subarrays are needed for truly random behavior, and only modest grating lobe suppression is achieved [16]. (For a 128 element linear array, the improvement is about 6 dB.) Multiplicative beamforming has also been applied to suppress grating

lobes [17], but the resultant loss in SNR-gain (an average of 6 dB) is the main drawback of this method [18].

All of these methods adopts only a single solution for grating lobe suppression, and their effectiveness is generally not good. An alternative approach to improving the grating lobe suppression is a hybrid method, which includes both a physical treatment in tandem with digital signal processing (DSP). On the transmitting side "mild" randomization of subarrays is used to lower the grating lobes. On the receiving side, we propose virtual filling of the gaps between the distributed subarrays to eliminate the grating lobes on the receiving side so that the response of a single large contiguous array is synthesized. This approach was recently suggested in [19] to fill gaps in the array matrices for super-resolution direction-of-arrival (DOAs) estimation. They use minimum weighted norm (MWN) and super spatially variant apodization (Super-SVA) for virtual filling, which requires significant computational power and large numbers of time snapshots (time samples). Super-SVA performance degradation occurs for coherent signals.

For the virtual filling method, DOA estimation is crucial to synthesizing the virtual element weights. Super resolution techniques that are based on the eigen-structure of the input covariance matrix, such as multiple signal classification (MUSIC) [20], root-MUSIC [21] and estimation of signal parameters via rotational invariance techniques (ESPRIT) [22], are used to generate the high resolution DOA estimates. However, an extra step of spatial smoothing is needed for correlated or coherent signals, and a large number of snapshots are required for acceptable accuracy. Sarkar [23] utilized the matrix pencil (MP) method to get the DOA of the signals in a coherent multi-path environment. In the MP method, based on the spatial samples of the data, the analysis is done on each snapshot, and therefore non-stationary environments can be handled easily. In recent years, the MP method has received more attention due to its computational simplicity and accuracy in noisy environments. Comparative studies with other DOA estimation algorithms can be found [24-32].

However, traditional MP is designed for the single periodic array and cannot be used directly for DSA configurations. Therefore, to meet the needs of this research, we

have developed a modified MP method for DSA and devised an enhanced three-step modified MP method for further improvement in the resolution of DOA estimation.

G. ORGANIZATION OF THE DISSERTATION

First a survey of fundamental grating lobe reduction approaches commonly used on single sparse arrays (i.e., the "conventional" or "traditional" approaches) is presented. Then these methods are extended and applied to the DSA problem with numerical simulations to assess their effectiveness. Next the virtual filling solution is applied on the receiving side, and finally the impact on the two-way (transmitting and receiving) pattern is examined.

An introduction to general formulation for the pattern of a DSA is discussed in Chapter II. Because the radiation pattern is primarily impacted by the physical arrangement of radiation elements, i.e., array lattices, some special cases are discussed. They include planar arrays of identical subarrays in a rectangular grid with and without random displacements.

There are a number of traditional approaches to lowering the grating lobes in a single sparse periodic array, and these are discussed in Chapter III. Also included in this chapter is an overview of combined solution approaches and the various advantages and disadvantages of these traditional solutions.

Grating lobe suppression with traditional methods is considered in Chapter IV. The physical arrangement of subarrays and the multiplicative beamforming method are discussed in detail, and simulation results are provided for each. Because of the limited performance of each method, a hybrid approach which combines several different traditional methods is proposed and evaluated in this chapter.

The new filling method for receiving beamforming is considered in Chapter V. The DOA estimation technique for non-stationary environments is studied and tailored for the DSA models. This is done first from the classical MP method. Next MP is modified to be used for DSA problems. These MP studies comprise the basis of the

proposed filling methods for grating lobe suppression, even though they could stand alone as a separate research problem.

Potential applications of proposed methods are discussed in Chapter VI. An extended three-step MP method, which improves the estimation accuracy, is presented. To complete a system-wide study, both the transmitting and receiving sides must be considered. By combining random subarray sizes on the transmitting side and the virtual filling method on the receiving side, a novel two-way DSA pattern with suppressed grating lobes is achieved.

THIS PAGE INTENTIONALLY LEFT BLANK

II. THEORETICAL BACKGROUND

A. A GENERAL FORMULATION FOR THE PATTERN OF DISTRIBUTED DIGITAL SUBARRAYS

To begin we present the general formulation of radiation patterns for distributed digital subarrays (DDSAs). These formulas apply to any arbitrary three-dimensional arrangement of arrays. Formulas for special cases such as planar and random subarrays will also be covered in this chapter. The spherical coordinate system that is used throughout is shown in Figure 5.

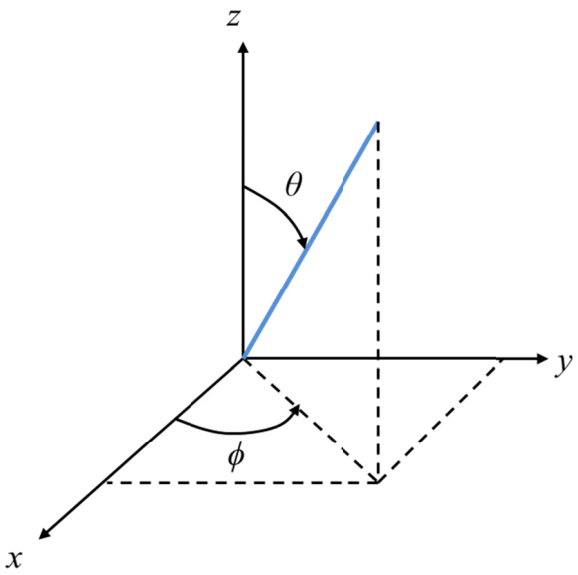

Figure 5. Spherical coordinate system for DDSA.

1. General Formulas

In Figure 6, an illustration of the general array geometry is shown. The subarrays are defined by:

N_s = number of subarrays,

m = subarray index, $m = 1, 2, ..., N_s$, and

$x_s(m), y_s(m), z_s(m)$ = coordinates of subarray m in the global system.

The subarrays can be rotated and tilted with respect to the global origin. In the global system (θ, ϕ) the direction cosines are

$$\begin{aligned} u &= \sin\theta\cos\phi \\ v &= \sin\theta\sin\phi \\ w &= \cos\theta. \end{aligned} \tag{1}$$

The scan direction in global coordinates is (θ_s, ϕ_s), with direction cosines

$$\begin{aligned} u_s &= \sin\theta_s \cos\phi_s \\ v_s &= \sin\theta_s \sin\phi_s \\ w_s &= \cos\theta_s. \end{aligned} \tag{2}$$

In the local subarray m coordinate system (θ_m, ϕ_m) the direction cosines are

$$\begin{aligned} u_m &= \sin\theta_m \cos\phi_m \\ v_m &= \sin\theta_m \sin\phi_m \\ w_m &= \cos\theta_m, \end{aligned} \tag{3}$$

and the scan angle direction cosines in the local subarray coordinate system are

$$\begin{aligned} u_{sm} &= \sin\theta_{sm} \cos\phi_{sm} \\ v_{sm} &= \sin\theta_{sm} \sin\phi_{sm} \\ w_{sm} &= \cos\theta_{sm}. \end{aligned} \tag{4}$$

A rotation matrix can be used to obtain the subarray direction cosines from the global ones, and vice versa.

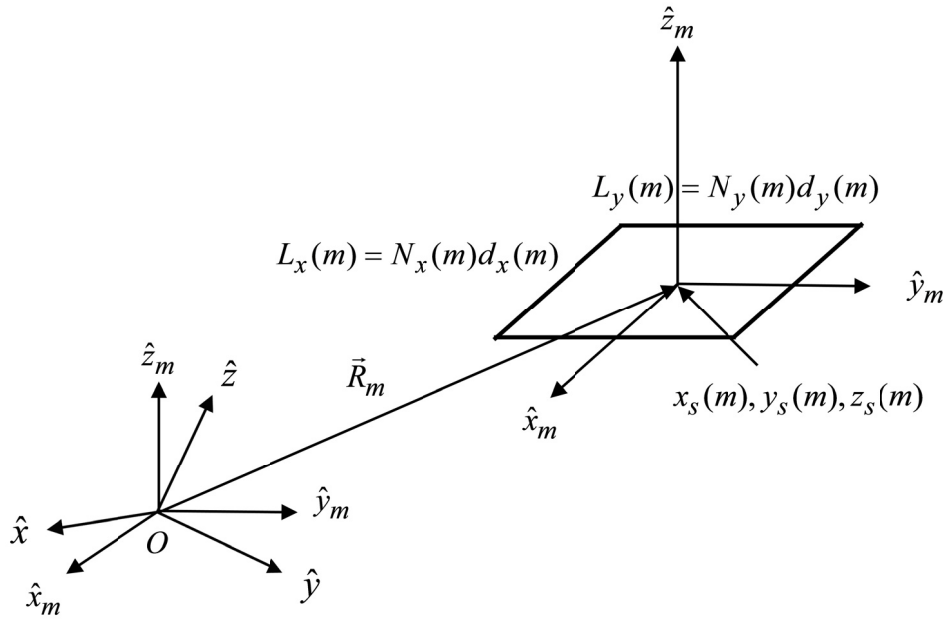

Figure 6. Subarray *m* and its local coordinate system relative to the global origin.

Consider planar rectangular subarrays with all arrays in the local $z = 0$ plane. The element spacing of the subarrays can be different, but the spacing within each subarray is equal. The number of elements in the subarrays can vary. Define:

$N_x(m), N_y(m) =$ number of elements in the local *x* and *y* directions for subarray *m*,

$N(m) = N_x(m)N_y(m) =$ total number of elements in subarray *m*,

$d_x(m), d_y(m) =$ spacing between elements for subarray *m*,

$L_x(m) = N_x(m)d_x(m) =$ length of the m^{th} subarray in its *x* direction, and

$L_y(m) = N_y(m)d_y(m) =$ length of the m^{th} subarray in its *y* direction.

We also define $k = 2\pi/\lambda$, where λ is the wavelength at the frequency of operation.

The complex pattern of the m^{th} subarray is given by the sum ($e^{j\omega t}$ time dependence assumed and suppressed)

$$F_s(m) = \sum_{p=1}^{N_x(m)} \sum_{q=1}^{N_y(m)} a(m,p,q)\, e^{j\psi(m,p,q)} \exp\left[jk(x(m,p)u_m + y(m,q)v_m) \right] \qquad (5)$$

where

$$w(m,p,q) = a(m,p,q)e^{j\psi(m,p,q)} \tag{6}$$

is the complex weight (amplitude a and phase ψ) at element p, q of subarray m applied for scanning, side lobe control, beam shaping and error compensation. For equally spaced elements, with each subarray centered at its local origin

$$\begin{aligned} x(m,p) &= \frac{2p-(N_x(m)+1)}{2} d_x(m) = P(m,p)d_x(m) \\ y(m,q) &= \frac{2q-(N_y(m)+1)}{2} d_y(m) = Q(m,q)d_y(m) \end{aligned} \tag{7}$$

so that

$$F_s(m) = \sum_{p=1}^{N_x(m)} \sum_{q=1}^{N_y(m)} w(m,p,q) \exp\left[jk(P(m,p)d_x(m)u_m + Q(m,q)d_y(m)v_m) \right]. \tag{8}$$

Note that when receiving, the exponential factor would be obtained from the element baseband I and Q samples:

$$I(m,p,q) + jQ(m,p,q) \equiv \exp\left[jk(P(m,p)d_x(m)u_m + Q(m,q)d_y(m)v_m) \right]. \tag{9}$$

The array factor (constructed from the centers of each subarray) is

$$F_a = \sum_{m=1}^{N_s} \exp\left[jk\left(x_s(m)u + y_s(m)v + z_s(m)w\right) \right]. \tag{10}$$

The total distributed array factor is given by

$$\begin{aligned} F &= \sum_{m=1}^{N_s} F_s(m) \exp\left[jk\left(x_s(m)u + y_s(m)v + z_s(m)w\right) \right] \\ &= \sum_{m=1}^{N_s} \left\{ \sum_{p=1}^{N_x(m)} \sum_{q=1}^{N_y(m)} w(m,p,q) \exp\left[jk(P(m,p)d_x(m)u_m + Q(m,q)d_y(m)v_m) \right] \right\} \\ &\qquad \times \exp\left[jk\left(x_s(m)u + y_s(m)v + z_s(m)w\right) \right]. \end{aligned} \tag{11}$$

If the weights are separable in the x and y coordinates such that

$$w(m,p,q) = w_x(m,p)w_y(m,q), \tag{12}$$

then

$$F = \sum_{m=1}^{N_s} \left\{ \sum_{p=1}^{N_x(m)} w_x(m,p) \exp\left[jkP(m,p) d_x(m) u_m \right] \sum_{q=1}^{N_y(m)} w_y(m,q) \exp\left[jkQ(m,q) d_y(m) v_m \right] \right\} \times \exp\left[jk\left(x_s(m)u + y_s(m)v + z_s(m)w \right) \right]. \tag{13}$$

Furthermore, if the amplitude weights are uniform ($w_x = w_y = 1$) and a linear phase is added to scan the beam in the local coordinate system (u_{sm}, v_{sm}), then

$$F = \sum_{m=1}^{N_s} \left\{ \frac{\sin\left[\frac{N_x(m)}{2} kd_x(m)\left(u_m - u_{sm}\right) \right]}{\sin\left[\frac{kd_x(m)}{2}\left(u_m - u_{sm}\right) \right]} \frac{\sin\left[\frac{N_y(m)}{2} kd_y(m)\left(v_m - v_{sm}\right) \right]}{\sin\left[\frac{kd_y(m)}{2}\left(v_m - v_{sm}\right) \right]} \right\} \times \exp\left[jk\left(x_s(m)u + y_s(m)v + z_s(m)w \right) \right]. \tag{14}$$

In order to linearize the phase across the entire array a scanning phase (u_s, v_s, w_s) should be added to the exponential factor in Eq. (14):

$$\exp\left\{ jk\left[x_s(m)(u - u_s) + y_s(m)(v - v_s) + z_s(m)(w - w_s) \right] \right\}. \tag{15}$$

However, these scanning phases could be added to the element weights as constant values for each subarray.

To complete the expression for the pattern an element factor must be added. In the local subarray coordinates (θ_m, ϕ_m) the element factor *S* for subarray *m* can be expressed as

$$\vec{S}(m, \theta_m, \phi_m) = S_\theta(m, \theta_m, \phi_m)\hat{\theta}_m + S_\phi(m, \theta_m, \phi_m)\hat{\phi}_m. \tag{16}$$

This allows for the possibility that elements are different for each subarray, which generally would not be the case. The final, most general expression for the total array pattern is

$$\vec{F}(u,v) = \sum_{m=1}^{N_s} F_s(m)\, \vec{S}(m, u_m, v_m) \times \exp\left\{ jk\left[x_s(m)(u - u_s) + y_s(m)(v - v_s) + z_s(m)(w - w_s) \right] \right\}. \tag{17}$$

The normalized power pattern is computed by

$$P_{\text{norm}}(u,v) = \frac{\left|\vec{F}(u,v)\right|^2}{\left|\vec{F}(u,v)\right|^2_{\max}} = \frac{\vec{F}(u,v) \bullet \vec{F}(u,v)^*}{\left|\vec{F}(u,v)\right|^2_{\max}}. \tag{18}$$

The array's gain pattern can be expressed as the peak gain times this normalized power pattern

$$G(u,v) = G_0 P_{\text{norm}}(u,v) \tag{19}$$

where G_0 is the main beam gain.

2. Special Case 1: Planar Array of Identical Subarrays in a Rectangular Grid

a. Specialized Formulas

The index *m* can be dropped from the subarray quantities if all subarrays are identical. As shown in Figure 7, let: $N_{sx}, N_{sy} =$ number of subarrays in the *x* and *y*-directions $(N_s = N_{sx}N_{sy})$, and $s_{x_0}, s_{y_0} =$ center-to-center spacing between subarrays in the *x* and *y* directions. Then

$$\begin{aligned} x_s(p) &= \left[\frac{2p-(N_{sx}+1)}{2}\right] s_{x_0} = P(p)s_{x_0} \\ y_{s(q)} &= \left[\frac{2q-(N_{sy}+1)}{2}\right] s_{y_0} = Q(q)s_{y_0}. \end{aligned} \tag{20}$$

The subscript *m* can also be dropped from the direction cosines because all subarrays are aligned with the global coordinate system. Now the array factor can be reduced to closed form

$$\begin{aligned} F_a &= \sum_{p=1}^{N_{sx}} \sum_{q=1}^{N_{sy}} \exp\left[jk\left(P(p)s_{x_0}(u-u_s) + Q(q)s_{y_0}(v-v_s)\right)\right] \\ &= \frac{\sin\left[\frac{N_{sx}}{2} ks_{x_0}(u-u_s)\right]}{\sin\left[\frac{ks_{x_0}}{2}(u-u_s)\right]} \frac{\sin\left[\frac{N_{sy}}{2} ks_{y_0}(v-v_s)\right]}{\sin\left[\frac{ks_{y_0}}{2}(v-v_s)\right]}. \end{aligned} \tag{21}$$

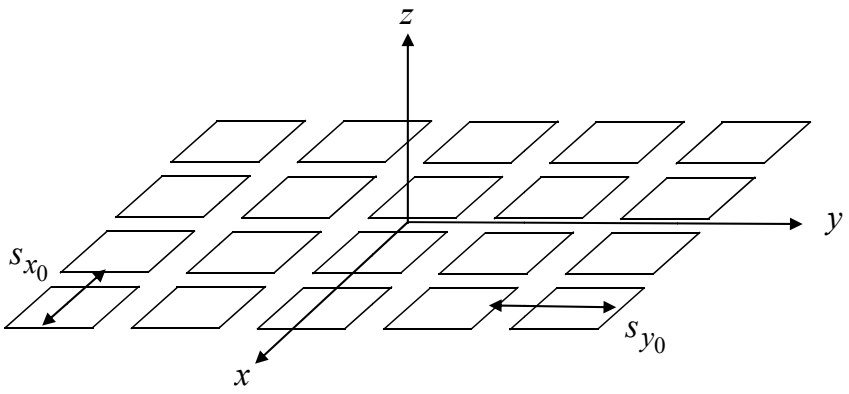

Figure 7. Periodic array in a rectangular grid.

The total complex pattern is constructed from the product of the subarray factor and array factor:

$$F = F_s \times F_a = \left\{ \frac{\sin\left[\frac{N_x}{2} kd_x (u - u_s)\right]}{\sin\left[\frac{kd_x}{2}(u - u_s)\right]} \frac{\sin\left[\frac{N_y}{2} kd_y (v - v_s)\right]}{\sin\left[\frac{kd_y}{2}(v - v_s)\right]} \right\} \times \left\{ \frac{\sin\left[\frac{N_{sx}}{2} ks_{x_0} (u - u_s)\right]}{\sin\left[\frac{ks_{x_0}}{2}(u - u_s)\right]} \frac{\sin\left[\frac{N_{sy}}{2} ks_{y_0} (v - v_s)\right]}{\sin\left[\frac{ks_{y_0}}{2}(v - v_s)\right]} \right\}. \quad (22)$$

b. Lattice Grating Lobes

The situation of interest is one where the element spacing is small enough so that individual subarray grating lobes do not occur for any scan angle. Any grating lobes that occur are due to the gaps between the subarrays in the rectangular grid (i.e., the lattice grating lobes, also called construction grating lobes). Several conventional techniques have been used to suppress the lattice grating lobes:

- Employ an array element that has nulls at the locations of the grating lobes: This approach is limited to a couple of wide angle grating lobes at best.
- Employ other periodic lattice configurations: For example, a triangular lattice shifts the grating lobes off of the principal planes

(in direction cosine space). Circular, hexagonal, octagonal, etc. grids have been used. Other shapes have also been investigated, such as fractal and spiral constructions.

- Adjust the subarray size and element spacing: Select the subarray spacing and element spacing so that subarray pattern nulls fall at the grating lobe locations. Again, there are limitations due to the constraints on the size of the subarrays and the gaps between them.
- Multiplicative beamforming: A single "master" subarray pattern is used to suppress grating lobes, and hence it reduces the design constraints. However, it has other implications on the beamforming performance that will be discussed in Chapter II, Section B. It can only be applied on the receiving side.
- Minor perturbation of the geometry: Minor changes in the geometry such as rotation and tilt of the subarrays can be used to reduce (but not eliminate) the grating lobes. The perturbations complicate the design, deployment and manufacturing of the array. The changes also reduce gain and increase average side lobe levels, but these consequences are usually tolerable.
- Aperiodic or random array configurations: If the array has no periodicity there will be no lattice grating lobes. Taken to the extreme this would be a random array, where the subarray locations are completely random. Most applications do not allow for randomly distributed locations. One exception would be a "randomly thinned" array because it is deployed over a well-defined area.

3. Special Case 2: Planar Array of Identical Subarrays in a Rectangular Grid with Random Displacements

In this case $x_s(m), y_s(m)$ are random numbers with a known probability density function (PDF), and hence a known average and variance. We will assume there is no displacement in the *z* direction, but a random deviation in *x* and *y* can occur for each subarray. It is assumed that the errors are small enough so that there is no overlap in the subarrays in their displaced positions. The spacing between subarrays can be written as a sum of the error free distance plus the random error in the *x* and *y* directions δ_x, δ_y, respectively. The PDF of δ_x, δ_y can be inferred by the method in which the subarrays are distributed. These are generally zero mean with variances $\overline{\delta_x^2}$ and $\overline{\delta_y^2}$.

The location of the subarray *p*, *q* is:

$$\begin{aligned} x_s(p,q) &= \frac{2p-(N_{sx}+1)}{2} s_{x_0} + \delta_x(p,q) = P(p)s_{x_0} + \delta_x(p,q) \\ y_s(p,q) &= \frac{2q-(N_{sy}+1)}{2} s_{y_0} + \delta_y(p,q) = Q(q)s_{y_0} + \delta_y(p,q). \end{aligned} \tag{23}$$

Note that x_s, y_s are now functions of both indices *p* and *q*. This is because the random *x* and *y* displacements must be assigned independently for each subarray (i.e., not just for rows and columns) so that the errors at subarrays are uncorrelated.

Now we compute the mean power pattern. To simplify the equations we consider only the *x* direction (which would be the case for a linear array along *x*). The result can easily be extended to the *y* direction by analogy. The mean power pattern is the expected value of the power pattern:

$$\begin{aligned} \overline{F(u) \bullet F(u)^*} &= \overline{\sum_{p=1}^{N_{sx}} \sum_{n=1}^{N_{sx}} \exp\left[jk\left(P(p)s_{x_0} + \delta_p\right)(u-u_s)\right] \exp\left[-jk\left(P(n)s_{x_0} + \delta_n\right)(u-u_s)\right]} \\ &= \sum_{p=1}^{N_{sx}} \sum_{n=1}^{N_{sx}} \exp\left[jk\, s_{x_0}\left(P(p)-P(n)\right)(u-u_s)\right] \overline{\exp\left[jk\left(\delta_p - \delta_n\right)(u-u_s)\right]}. \end{aligned} \tag{24}$$

We can define a new random variable $\Delta = k(\delta_p - \delta_n)(u - u_s)$. The mean and variance of this new random variable (0, $\overline{\Delta^2}$) can be determined from the mean and variance of δ_p and δ_n

$$\overline{\Delta^2} = k^2\left(\overline{\delta_p^2} + \overline{\delta_n^2}\right)\left(u - u_s\right)^2. \tag{25}$$

When p=n in Eq. (24) all exponents are zero and

$$\sum_{p\,=\,n}^{N_{sx}} \sum^{N_{sx}} (1) = N_{sx}. \tag{26}$$

Also, using the fact that the maximum value of F will be N_{sx}

$$\overline{\left|F(u)\right|^2}_{\text{norm}} = \frac{1}{N_{sx}^2}\left\{ N_{sx} + \sum_{p\neq\, n}^{N_{sx}} \sum^{N_{sx}} \exp\left[\, jk\, s_{x_0}\left(P(p) - P(n)\right)(u - u_s)\right] \overline{e^{j\Delta}} \right\}. \tag{27}$$

The expected value of the exponential is [33]

$$\overline{e^{j\Delta}} = \begin{cases} 1, & p = n \\ e^{-\overline{\Delta^2}}, & p \neq n. \end{cases} \tag{28}$$

Now, by adding and subtracting

$$\pm\, e^{-\overline{\Delta^2}} \sum_{p=\,n}^{N_{sx}} \sum^{N_{sx}} (1) \tag{29}$$

and using the + with the second term in the curly brackets in Eq. (27) to complete the sum, we get

$$\begin{aligned} \overline{\left|F_a(u)\right|^2}_{\text{norm}} &= \frac{1}{N_{sx}^2}\left[N_{sx} - e^{-\overline{\Delta^2}} N_{sx} + e^{-\overline{\Delta^2}} \left|F_{a_0}(u)\right|^2 \right] \\ &= e^{-\overline{\Delta^2}} \left|F_{a_0}(u)\right|^2 + \left[1 - e^{-\overline{\Delta^2}}\right]\frac{1}{N_{sx}}, \end{aligned} \tag{30}$$

where F_{a_0} is the normalized error free (unperturbed) pattern. As the error increases, the energy in the error free pattern is transferred to the second term, which represents random side lobe "noise."

Equation (30) extended to include the *y* dimension for a planar array is

$$\begin{aligned}\overline{\left|F_a(u,v)\right|^2}_{\text{norm}} &= \frac{1}{N_s^2}\left[N_s - e^{-\overline{\Delta^2}}N_s + e^{-\overline{\Delta^2}}\left|F_{a_0}(u,v)\right|^2\right] \\ &= e^{-\overline{\Delta^2}}\left|F_{a_0}(u,v)\right|^2 + \left[1 - e^{-\overline{\Delta^2}}\right]\frac{1}{N_s}.\end{aligned} \tag{31}$$

Note that the subarray and element factors still need to be included to get the total array pattern.

B. PERIODIC DISTRIBUTED DIGITAL SUBARRAYS

1. Background

As mentioned in Chapter I, more arrays are used on the same platform to facilitate the multi-function requirements of today's warfare. Those arrays might be distributed over the platform in the form of periodic spacing. Each array itself is an element of a periodic array (i.e., a subarray), and depending on the mission type, subarrays can be operated independently or collectively. However, collectively operated distributed subarrays provide a narrower main beam beamwidth, hence higher angular resolution and better SNR, compared to the sum of individually operated subarrays.

The pattern function for the case of a rectangular grid of subarrays was presented in Eq. (22). It was noted that a large spacing between subarray centers leads to a major disadvantage of this kind of arrangement, which is grating lobes.

In the following section, two methods are proposed to eliminate or suppress the grating lobes that appear in the periodic distributed subarrays. The first method, multiplicative beamforming, has been used in radio astronomy, dealing with subarrays with large element spacing in one of the two subarrays. The second method, subarray rotation, has been applied to contiguous arrays for grating lobe suppression.

2. Multiplicative Beamforming Applied to Distributed Subarrays

The multiplicative beamforming method has been primarily used on thinned arrays in order to use fewer antenna elements yet achieve high resolution. A major advance in this method was made by Davies and Ward [34], who introduced

interdependent amplitude tapers for two constituent subarrays to synthesize a desired low side lobe radiation pattern. The thinning rates that can be achieved are of the order of 80%. The performance of multiplicative receiving systems in real digital beamforming (DBF) radar measurements was studied in [17]. A compound interferometer is a multiplicative receiving array. Its product pattern can be made equal to the power pattern of a conventional linear array with uniform element weighting was shown in [35]. MacPhie [36] demonstrated the Mills Cross can be used to obtain a multiplicative pattern equal to the power pattern of a conventional planar array but with fewer elements. An improvement of the azimuthal resolution of high-frequency surface-wave radar (HFSWR) with this method has been demonstrated in [37]. Lili Xu et al. [38] utilized the concept of the multiplicative array to improve the performance of nulling antennas as well.

The primary idea of multiplicative beamforming is to use two subarrays, one with element spacing of $\lambda/2$ and the other a thinned array with element spacing larger than $\lambda/2$ as shown in Figure 8. The composite directional response of this thinned multiplicative array can be seen in Figure 9. These subarrays are built such that the zeros of the first subarray match the grating lobes of the second subarray. This processing implies the loss of SNR gain, defined as the ratio of the output SNR over the input SNR, as the energy in the grating lobes is canceled. It is only used on the receiving side because of the multiplication requirement [18, 37].

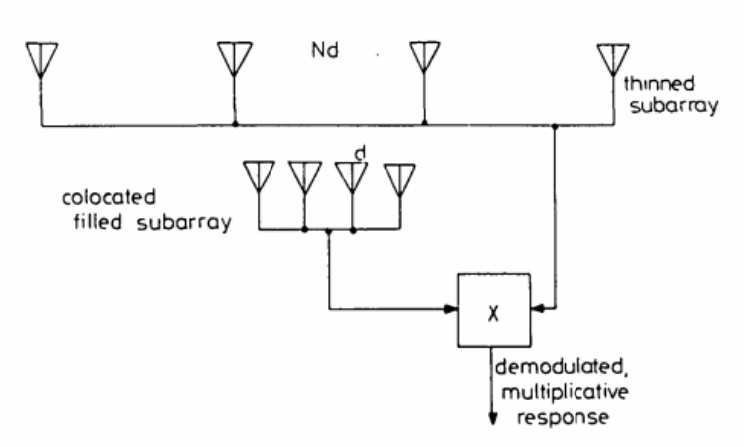

Figure 8. Thinned multiplicative array configuration with coincident subarrays (from [34]).

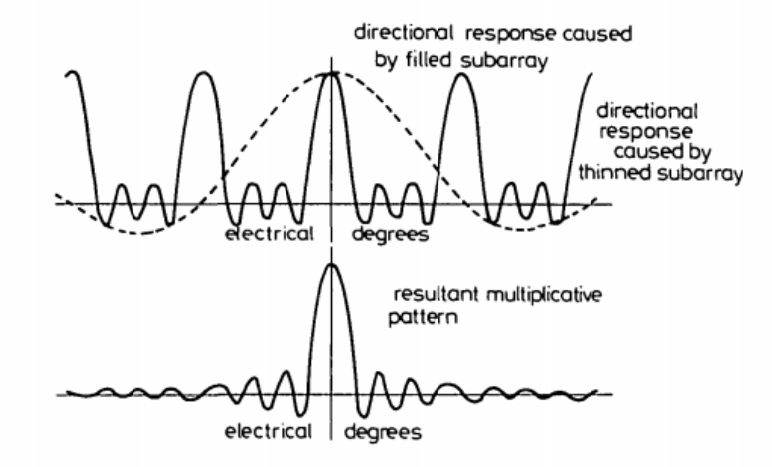

Figure 9. Composite directional responses from a thinned multiplicative array with coincident subarrays (from [34]).

The other limitation of this method is the problem of multiple target cross products which tend to provide confusing directional information for complex multi-target excitation of the array. However, if the signal sources are uncorrelated, this cross product averages to zero. For radar applications, the adoption of frequency agile transmissions or Doppler processing can serve to decorrelate the returns so that the cross products can be reduced by integration [34].

3. Distributed Subarray with Subarray Rotation

Non-uniform spacing between elements would remove grating lobes but normally at the cost of increased side lobes. Optimization methods that try to reduce the side lobes require substantial computation time and power [39]. Random designs become practical only when the number of elements is very large, typically 1000 or more. A new method proposed by Agrawal [14] can be used to suppress the grating lobes to a certain extent by simply rotating subarrays with respect to each other by specified angle. The subarray arrangement and the simulation results are shown in Figure 10 and Figure 11, respectively.

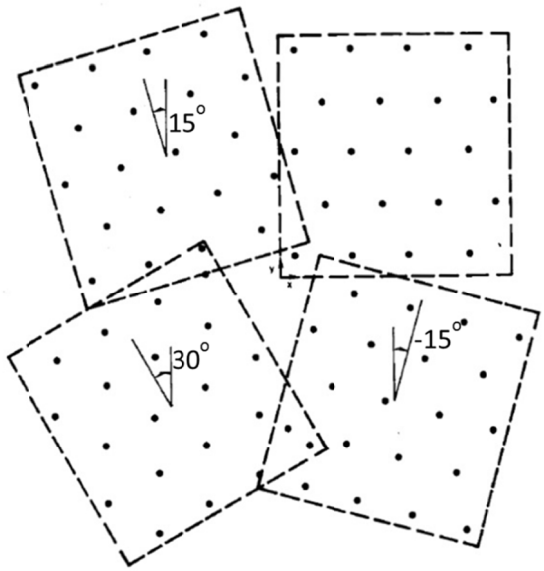

Figure 10. Eighty-element array with four subarrays rotated by 0°, 15°, 30° and 15° (from [14]).

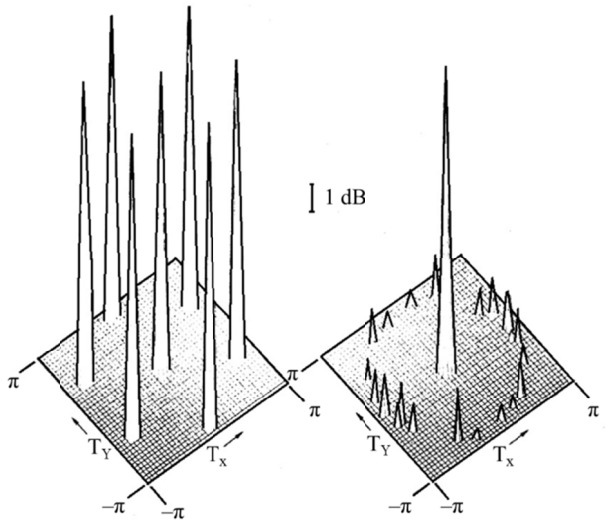

Figure 11. Computed radiation patterns: (a) Eighty-element array without subarray rotation. (b) Eighty-element array of Figure 10 ($d = 2.6\lambda$) (from [14]).

In this example, the array with a triangular lattice is divided into four subarrays. The element spacing d is equal to 2.6λ and hence grating lobes exist. By physically rotating subarrays by 0°, 15°, 30° and -15°, grating lobes, which remain at the same angular distance from the main beam, multiply in number by the number of subarrays while their amplitude is divided by the same number [14]. Kerby [40] examined the behaviors of the periodic array of random subarrays, arrays of periodically rotated random subarrays, and arrays of randomly rotated random subarrays and demonstrated the lowered side lobe level of the array factor by subarray rotation.

This approach can be extended to periodic distributed subarrays to lower the magnitude of the grating lobes.

C. APERIODIC AND RANDOM DISTRIBUTED DIGITAL SUBARRAYS

1. Background

Aperiodic and random arrays provide a possibility of using fewer elements than a periodic array to achieve the required side lobe level (SLL), beamwidth (BW) and directive gain. By breaking the periodicity, grating lobes can be mitigated or suppressed. Randomly thinning an array is one method used to accomplish this. For example, every element in a filled array can be assigned a number between 0 and 1 from a uniform PDF. If the array is to be thinned by 50% then elements with numbers less than 0.5 could be removed.

Antenna arrays with randomly spaced elements have been studied in [41]. The probabilistic properties of an antenna array when its elements are placed at random over an aperture according to a given distribution were presented. It was found that the required number of elements is closely related to the desired side lobe level and is almost independent of the aperture dimension. The resolution or the beamwidth depends mainly on the aperture size. The directive gain is proportional to the number of elements used if

the average spacing is large. As a consequence the number of elements required is considerably less than one with uniform spacing.

In practice, taking the manufacturing deviations and element position errors due to external forces into account, no subarrays are identical. Those "errors" are usually random variables and can only be characterized in terms of probabilities or distributions. Thus, in a sense, all practical arrays have some randomness, but the errors are controlled so that they are small compared to the wavelength.

Another advantage of random phased arrays is the potential for bandwidth improvement, i.e., wideband operation. Aperiodicity is generally recognized as one effective way to extend the useful bandwidth of antenna arrays. Random arrays can be designed with very little pattern variation and no grating lobes over wide frequency ranges [42]. Goffer, et al. [43] discussed the implementation of divided arrays with random sizes and random locations of their centers in order to avoid periodicity. Closed-form expressions for the average array factor, the average power pattern and its variance are presented.

However, lack of periodicity makes manufacturing more complex and costly. Maintenance will be another issue if truly random arrays are used. A periodic array with random subarrays has been proposed as a way to reduce the manufacturing cost but retain some properties of random array [40]. We would like to further lower the manufacturing cost and increase the functionality of each subarray by using periodic subarrays with random location perturbations or periodic subarrays with random sizes.

2. Random Array

Collaborative beamforming for wireless sensor networks (WSNs) has been used to increase the transmission range of individual sensor nodes [44]. A random array of subarrays can be considered as a wired sensor network. The individual signals from sensor nodes arrive coherently and add constructively in the intended direction. The radiated power is concentrated in a certain direction and reduces the power in other

directions. The beam pattern characteristics of collaborative beamforming have been recently derived in [45] using the random array theory and assuming that sensor nodes in one cluster of the WSN are uniformly distributed over a circular disk.

Another paper derived the beam pattern for the WSN with Gaussian distributed sensor nodes [46]. The average power pattern for N uniformly distributed nodes is [45, 46]:

$$P_{av}(\phi) = \frac{1}{N} + \left(1 - \frac{1}{N}\right)\left|2\frac{J_1(\alpha(\phi))}{\alpha(\phi)}\right|^2 \tag{32}$$

where $J_n(x)$ is the n^{th} Bessel function of the first kind. The radius of the disk normalized by the wavelength is $\alpha(\phi) \triangleq 4\pi\tilde{R}\sin(\phi/2)$ and $\tilde{R} \triangleq R/\lambda$. For Gaussian distributed nodes:

$$P_{av}(\phi) = \frac{1}{N} + \left(1 - \frac{1}{N}\right)\left|e^{-\frac{\alpha^2\sigma^2}{2}}\right|^2 \tag{33}$$

where $\alpha = 4\pi\sin(\phi/2)$ and $\sigma^2 = \sigma_0^2/\lambda^2$ is the normalized variance of the Gaussian distribution.

The average power pattern of a uniformly distributed WSN is shown in Figure 12. Several values of $\tilde{R}$ with $N = 16$ and 256 are plotted for comparison. As can be observed, the side lobe approaches $1/N$ as the beam angle moves away from the main beam as predicted by Eq. (32). As N increases, the peak side lobe level goes down. The main beam width is inversely proportional to $\tilde{R}$.

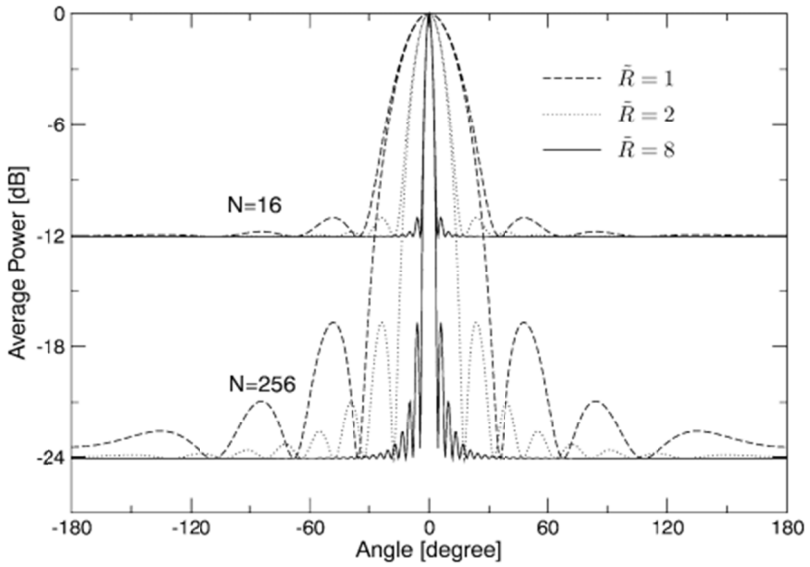

Figure 12. Average beam pattern with different $\tilde{R}$ and $N=16$ and 256 (from [45]).

3. Random Distributed Subarrays

a. Periodic Subarrays with Random Displacements

A random array has been suggested for grating lobe reduction at the expense of higher side lobes in a WSN. We would like to extend the idea from using a single isotropic antenna to a subarray at each node location. The random distribution of subarrays will follow a certain PDF, for example, uniform, Gaussian, truncated Gaussian, Rayleigh, truncated Rayleigh, etc.

By applying the same concept of pattern multiplication from periodic distributed subarrays, we can easily find the average radiation pattern from the single subarray pattern and the randomly distributed construction array pattern. The average array radiation pattern formulas can be multiplied by a single subarray pattern (if all subarrays are identical), and the final pattern for the random distributed subarrays can be obtained. However, in order to use the random properties effectively, the number of subarrays has to be large enough.

b. Periodic Subarrays with Random Sizes and Random Displacements

Subarraying within a single contiguous array has been applied to minimize the number of true time delay units for broadband application. Ideally, a true time delay unit at each element is preferred for a broadband array. However, practical limitations like cost, weight and complexity make it impossible to be realized. Therefore, subarraying becomes the option to improve the inherent bandwidth limitation of a phased array. The design with contiguous equal size subarrays results in high side lobes, grating lobes, gain reduction and squinting in the pointing angle [43]. A typical periodic array model with random subarray sizes and subarray centers was presented in [47] and is shown in Figure 13.

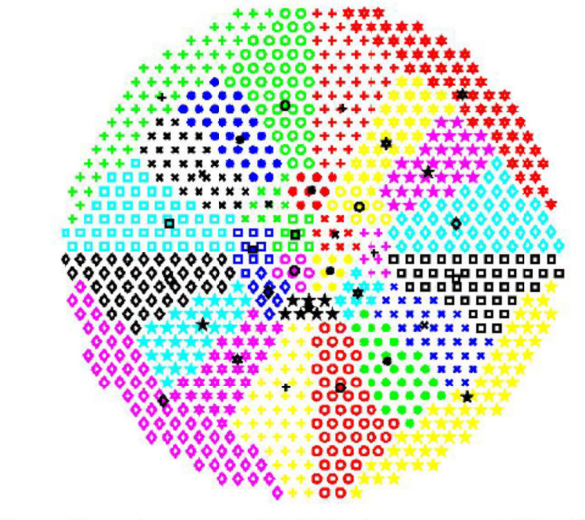

Figure 13. Generic array with 902 elements and 32 subarrays and corresponding subarray centers (from [47]).

For an example of the reduction possible, see Figure 14. A radiation pattern of a linear array of 128 elements, equally divided into 32 contiguous subarrays of four elements each, is depicted. For a steering angle of 40°, grating lobes can be clearly seen due to the periodicity in the array. The desired (average) radiation pattern of the same array, but randomly divided and distributed, is shown in Figure 15. The elimination of the grating lobes and the reduction of the side lobes are expected, since the periodicity

in the array was removed. Also these are applications where the number of elements in the subarrays is different and could be selected randomly from a discrete distribution.

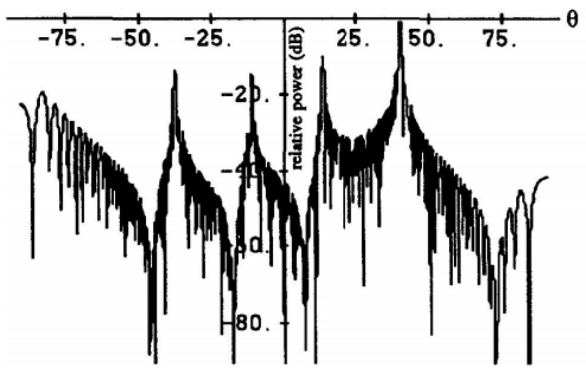

Figure 14. Pattern of a uniformly divided array, 128 elements divided into 32 subarrays of four elements each, steering to 40° (from [43]).

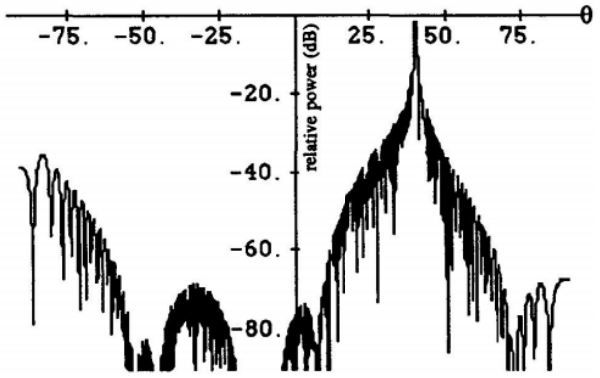

Figure 15. Average pattern of a randomly divided array (from [43]).

D. SUMMARY AND CONCLUSIONS

Basic formulas for the DDSA radiation pattern were presented in this chapter. Both periodic and aperiodic or random arrangements were considered, and general equations are derived. Several methods of potential interest for grating lobe suppression, including subarray rotation, multiplicative beamforming and randomness, were discussed in this chapter as well.

THIS PAGE INTENTIONALLY LEFT BLANK

III. PROBLEM STATEMENT AND SOLUTION APPROACH

A. DISTRIBUTED SUBARRAYS

The capabilities of the digital distributed subarray antennas, such as higher angular resolution and gain compared with using single arrays individually, were mentioned in Chapter I. Some challenges that accompany DDSAs include the grating lobe problem, calibration, and time and frequency synchronization. Among the three, the calibration (including error correction) and position location problems are an active area of investigation (e.g., for distributed sensor networks, distributed arrays, etc.) and several methods have been presented in the literature to address the problems [48-52]. Timing and frequency/phase synchronization are required for coherent DDSA operation as well [53-56]. For our applications of interest, all arrays are on a common structure (e.g., a ship or a building), and thus distributing reference signals is relatively straightforward. The mitigation of grating lobes, the presence of which significantly affects the performance of a DDSA, has received relatively little attention in the past [4, 57, 58].

Grating lobes for a periodic DDSA come from the widely spaced subarray centers. The only method to lower the grating lobes on the transmitting side is to break up the periodicity of the subarray centers. However, on the receiving side there are more options available because digital signal processing can be applied.

B. SOLUTION APPROACHES

For our research, individual subarrays should be able to operate independently, which means that subarray grating lobes will not exist (i.e., the element spacing should be less than $\lambda/2$ for the elements in every subarray). Hence, thinning within the subarrays will not be an option for our approach. From pattern multiplication, we know that the radiation pattern of a periodic distributed subarray can be expressed in terms of the multiplication of a single subarray factor and the construction factor (the array factor, composed of the centers of each subarray). Grating lobes come from the construction factor because of the large spacing between subarrays. The objective is to eliminate or suppress the grating lobes from the construction factor, so they are at the desired side

lobe level. From the formulas presented in Chapter II, we know that the total array factor is the product of the individual subarray pattern and the construction pattern. Two grating lobe reduction approaches are apparent. One is to reduce the construction lobes by breaking the periodicity. The other is to suppress the grating lobes with the subarray pattern.

We first look at some traditional methods for grating lobe suppression of a sparse array. Few of the traditional methods have been applied to distributed subarrays; therefore, the methods are extended to DDSAs, and their effectiveness is examined by numerical simulations. Due to limited effectiveness in suppressing DDSA grating lobes by traditional methods, we investigate a new approach which utilizes the power of digital signal processing to eliminate the grating lobes and further lower the side lobes on the receiving pattern. It is demonstrated that a combination of the traditional methods on the transmitting side together with the digital processing on the receiving side provide significant two-way pattern improvement.

1. Traditional Solutions

a. Sequential Subarray Rotation

As described in Chapter II, subarray rotation is capable of suppressing the grating lobes of a sparse periodic array. The main idea is to relocate the grating lobes in direction cosine space so that the magnitudes of the lobes will not accumulate. However, subarray rotation complicates the hardware design and introduces other problems, such as gain loss if the rotation angles are too large. The grating lobe suppression efficiency degrades as the subarray gap size increases as well.

b. Multiplicative Beamforming

Multiplicative beamforming on the receiving side was introduced in Chapter II. The grating lobes can be suppressed by multiplication of the main and auxiliary array outputs. Careful design is needed to place the nulls of the auxiliary array on top of the grating lobes of the main array. Multiplicative beamforming can only be

used on the receiving side and the overall SNR-gain tends to be lower due to the cancellation of energy in the grating lobes.

c. Aperiodic or Random Subarray Sizes

Random subarraying has been proposed for a contiguous subarray antenna to reduce the grating lobes due to the subarray steering or when the phase center distances between subarrays are too wide. Randomizing the subarray sizes can only lower the grating lobe to a moderate level if the subarray centers are still periodic.

d. Aperiodic or Random Displacement

An aperiodic or random array has no grating lobes because there is no strong periodicity. For the DDSA case, aperiodic or random displacement of identical subarrays is an option for lowering the grating lobes. However, as in the case of aperiodic or random subarray sizes, the degree of grating lobe reduction is only moderate.

2. Overview of Proposed Solution

a. Combination of Fundamental Solutions

Fundamental solutions provide at most moderate (several dB) of grating lobe suppression. Multiplicative beamforming can only be applied on the receiving side. Subarray rotation works better for small subarray spacings. A combination of these fundamental methods might provide better results compared with their individual use. Manufacturing complexity is another important factor that needs to be taken into account when designing a combined solution.

b. Virtual Filling Method

The virtual filling method can only be used on the receiving side. The idea is to fill the gaps of a DDSA with virtual elements so that no grating lobes appear in the visible region. After filling the gaps between subarrays virtually, the “filled” array can be treated as contiguous, and therefore some advantages that come with a larger contiguous aperture array are obtained.

c. Combination of Fundamental Solutions with Virtual Filling Method

Since the virtual filling method is applicable when receiving only, a combination of fundamental solutions is employed on the transmitting side. For a radar application, a two-way pattern is generated by multiplying the transmitting pattern with the receiving pattern. Improvement in terms of lower side lobes and grating lobes is possible after the pattern multiplication.

IV. GRATING LOBE SUPPRESSION WITH CONVENTIONAL SOLUTIONS

In this chapter we apply the conventional methods to DDSAs and examine them individually to evaluate their effectiveness.

A. MULTIPLICATIVE BEAMFORMING

The DDSA model shown in Figure 16 was created for investigating multiplicative beamforming on the receiving side. Arrays 1 through 5 are 4 by 7 rectangular subarrays with element spacings equal to half a wavelength. Spacings between centers for subarrays 1 through 5 is six wavelengths. Two auxiliary subarrays denoted 6 (8 by 1) and 7 (1 by 12) are used to do the pattern multiplications for $\phi = 90^{\circ}$ and $\phi = 0^{\circ}$ planes, respectively. The center locations of subarrays 6 and 7 are (45λ, 10λ) and (60λ, 20λ), respectively. Distances between the primary DDSA (1 through 5) and auxiliary subarrays (6 and 7) are not critical.

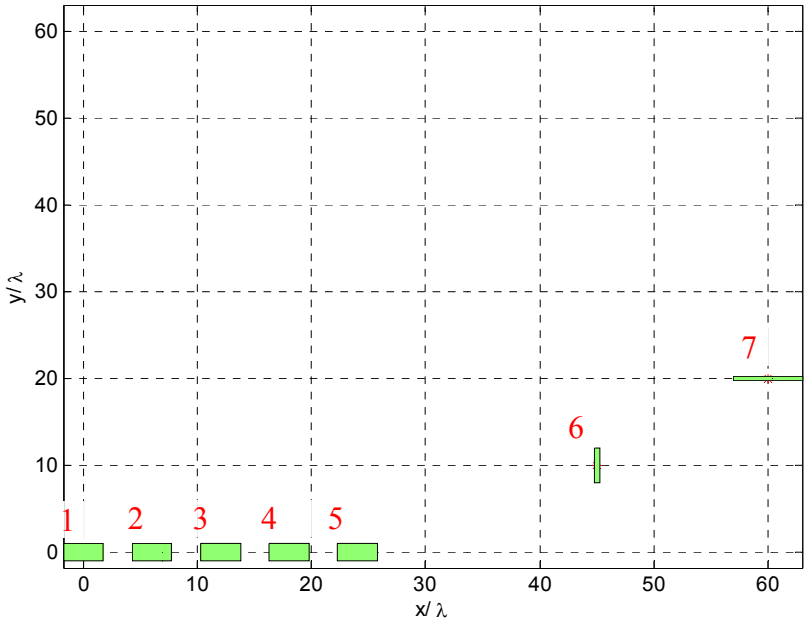

Figure 16. Multiplicative beamforming DDSA model.

Unlike traditional multiplicative beamforming using one regular and one sparse array, we would like to have subarrays that can work individually or collaboratively if needed. Therefore, sparse arrays are not an option for our model.

The radiation pattern of the primary DDSA (arrays 1 through 5) is shown in Figure 17 for the $\phi = 0^{\circ}$ plane. By multiplying the pattern of the primary DDSA with the pattern of the auxiliary subarray (number 7), grating lobes are suppressed dramatically as seen in Figure 18.

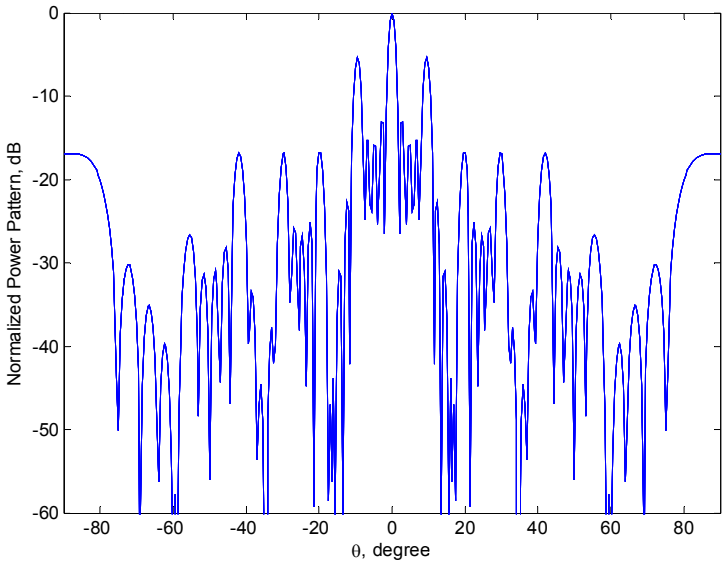

Figure 17. Primary DDSA pattern (subarrays 1 through 5) in the $\phi = 0^{\circ}$ plane.

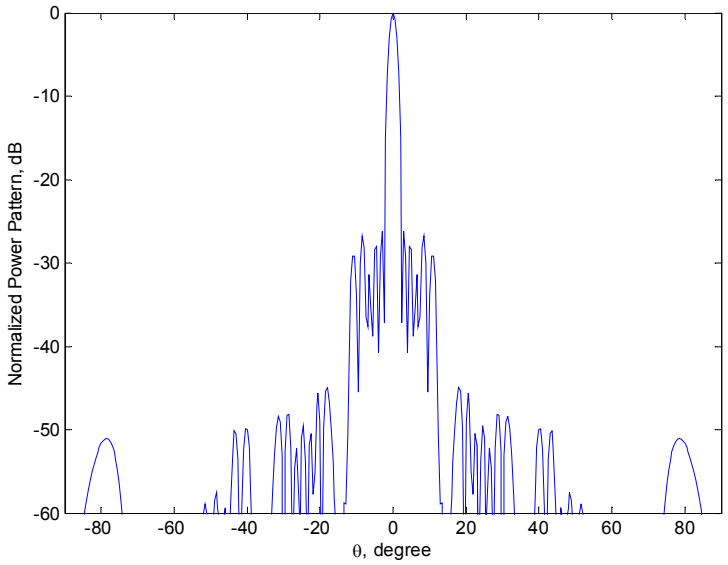

Figure 18. Multiplicative beamforming pattern of arrays 1 through 5 and auxiliary number 7 with Taylor amplitude taper ($\bar{n}$ =5, SLL= –26 dB) on arrays 1 through 5 in the $\phi = 0^{\circ}$ plane.

The same methodology can be applied to the elevation pattern ($\phi = 90^{\circ}$). The original $\phi = 90^{\circ}$ pattern and the multiplicative processed pattern are shown in Figure 19 and Figure 20, respectively. Not only has the side lobe level been suppressed, but the mainbeam beamwidth is reduced.

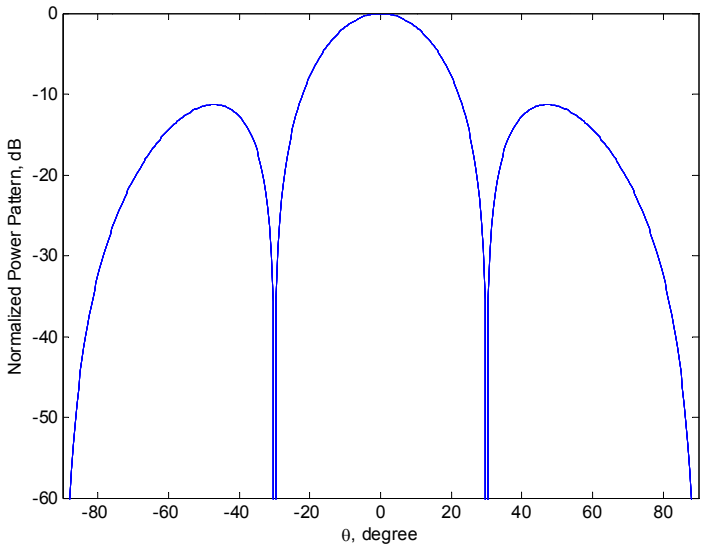

Figure 19. Primary DDSA pattern of arrays 1 through 5 in the $\phi = 90^{\circ}$ plane.

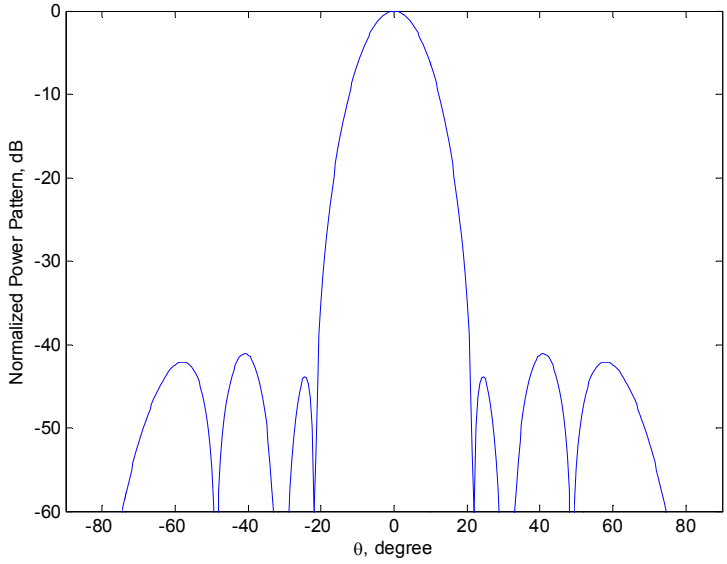

Figure 20. Multiplicative beamformed pattern of arrays 1 through 5 and auxiliary number 6 with a Taylor amplitude taper ($\overline{n}$ =5, SLL= −30 dB) on 6 in the $\phi = 90^{\circ}$ plane.

B. CONVENTIONAL ARRAY GEOMETRY SOLUTIONS

For attacking the grating lobe problem on the transmitting side, introducing randomness is one of the possible approaches. We consider subarrays with random displacements, rotations and sizes. The goal is to reduce the grating lobes that come from the periodic spacing between subarrays. Simulation models shown in this section are the ones with the lowest grating lobes based on one hundred Monte Carlo trials of which the maximum grating lobes are identified for all trials. It should be noted that for other numbers of trials, the best arrangement might be different.

Suppose we would like to design a periodic distributed digital subarray antenna. Each subarray is a periodic array with ten elements along *x* and four elements along *y,* with an element spacing of $\lambda/2$ in both dimensions. Subarrays are separated by 1.5λ. From Figure 21 and Figure 22 can be seen the physical layout and radiation pattern, respectively. Grating lobes occur due to the periodic gaps between subarrays.

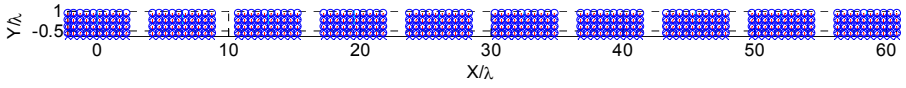

Figure 21. Physical layout of a periodic distributed linear array composed of ten identical planar subarrays whose centers are equally spaced. The gap between subarrys is 1.5λ.

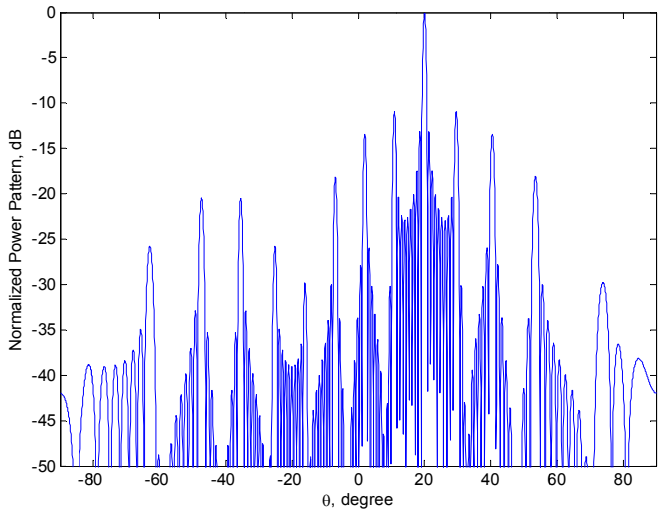

Figure 22. Radiation pattern of the periodic distributed subarray antenna shown in Figure 21.

1. Sequential Subarray Rotation

One can use subarray rotation to mitigate or suppress the grating lobes. In this example, each subarray is rotated 3° sequentially, as shown in Figure 23. From Figure 24 one can see the effect of subarray rotation, which is that the grating lobes are suppressed.

A Taylor amplitude taper ($\overline{n}$ =5, SLL= -20 dB) was used to lower the side lobes as shown in Figure 25.

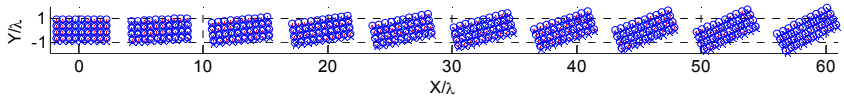

Figure 23. Physical layout of the periodic distributed subarray with subarray rotation.

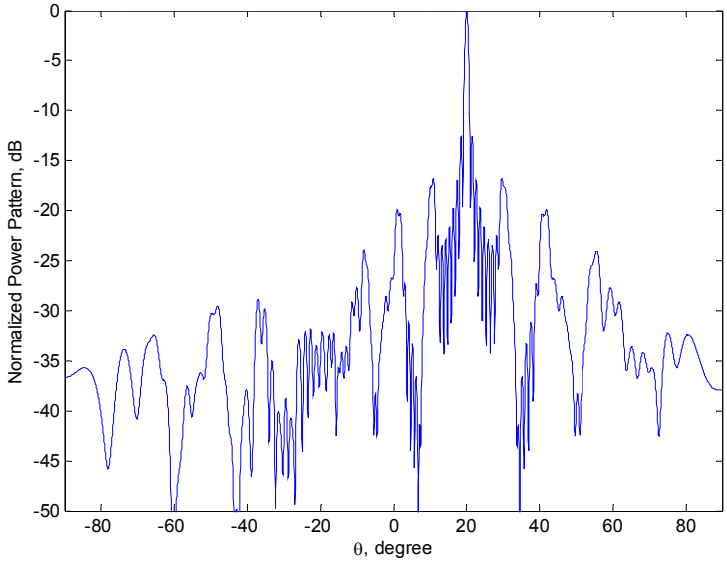

Figure 24. Radiation pattern of the array shown in Figure 23.

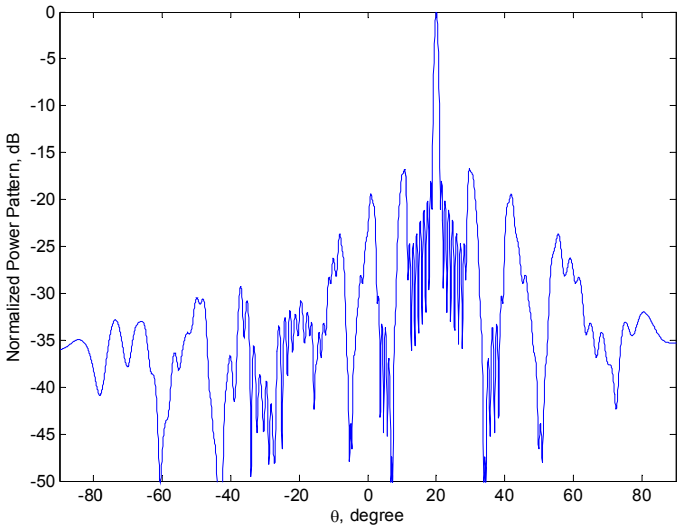

Figure 25. Radiation pattern of the array shown in Figure 23 with Taylor amplitude tapering ($\bar{n}$ =5, SLL= –20 dB).

2. Random Subarray Sizes

Next we consider randomly changing the subarray sizes, yet keeping the total number of elements along x and y the same as in the previous example for comparison purposes. A Rayleigh distribution is arbitrarily chosen as the PDF for the randomization process. However, it is worth noting that the larger the differences between the sizes of the subarrays the better the grating lobe suppression capability, which means it is preferable to have subarray sizes distributed over a wider range. The physical layout is shown in Figure 26. By doing subarray size randomization, grating lobes drop to –16 dB as shown in Figure 27.

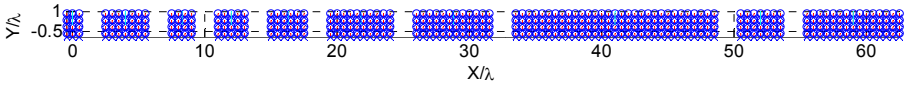

Figure 26. Physical layout of the random sized distributed subarrays with total number of elements along *x* and *y* the same as for the periodic case.

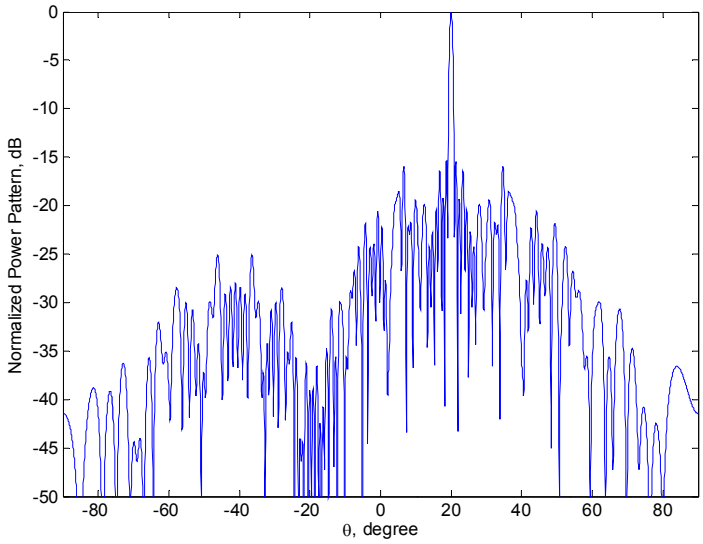

Figure 27. Radiation pattern of the array shown in Figure 26.

3. Random Subarray Displacement and Sizes

The next step is to add random positions for each subarray on top of their random sizes. From Figure 28 and Figure 29, one can see the physical layout and the radiation pattern of this array, respectively. As can be seen in Figure 29, the peak grating lobe level has been lowered by around 1.5 dB by doing random locations.

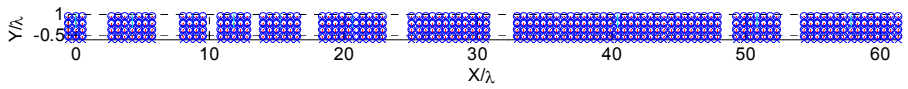

Figure 28. Physical layout of the array with random subarray sizes and random subarray locations.

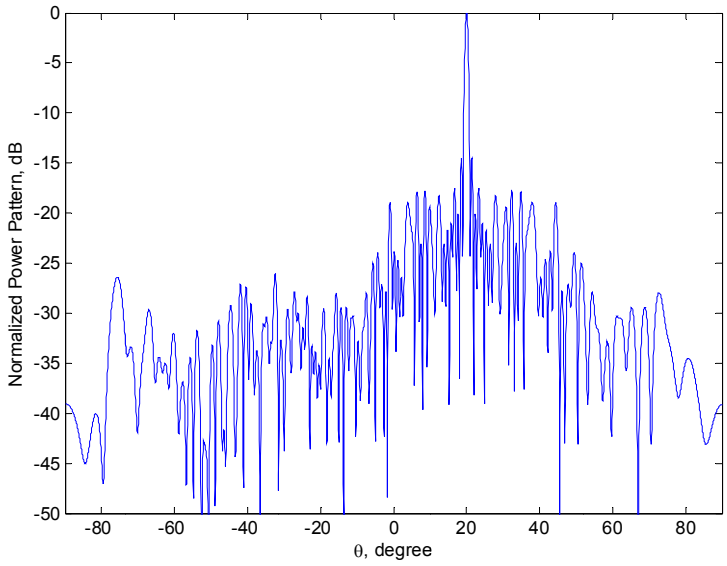

Figure 29. Radiation pattern of the array shown in Figure 28.

4. Combination of Random Subarray Displacements, Sizes and Sequential Rotations

As a final step we can use the subarray rotation idea from periodic distributed subarrays. We choose sequential rotations instead of random rotations for two reasons. First, sequential rotations are guaranteed to move grating lobes to desired locations in direction cosine space. Random rotations might move them to nearby locations which can

reinforce the grating lobes. Secondly, sequential rotation is favorable in terms of manufacturing complexity.

The layout of the final array with random sizes, position, and sequential rotations (2° sequentially) is shown in Figure 30. The radiation pattern can be seen in Figure 31. The peak grating lobe is approximately -19 dB, which has only 1 dB of improvement compared to the non-rotated case. Therefore, this added complexity is likely not worth the effort. After applying the Taylor amplitude tapering ($\bar{n}$ =5, SLL=-20 dB), the final pattern is shown in Figure 32.

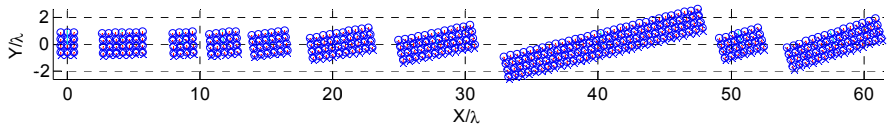

Figure 30. Physical layout of the subarray with random subarray sized and random subarray locations and sequential subarray rotations.

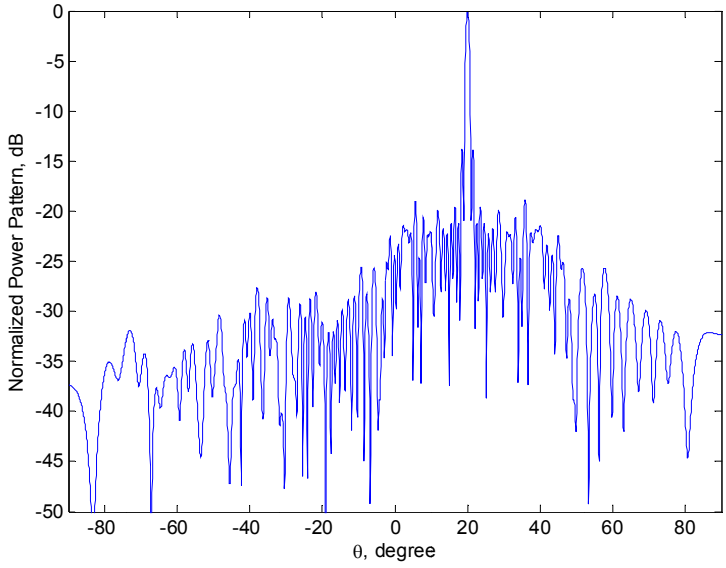

Figure 31. Radiation pattern of the array shown in Figure 30.

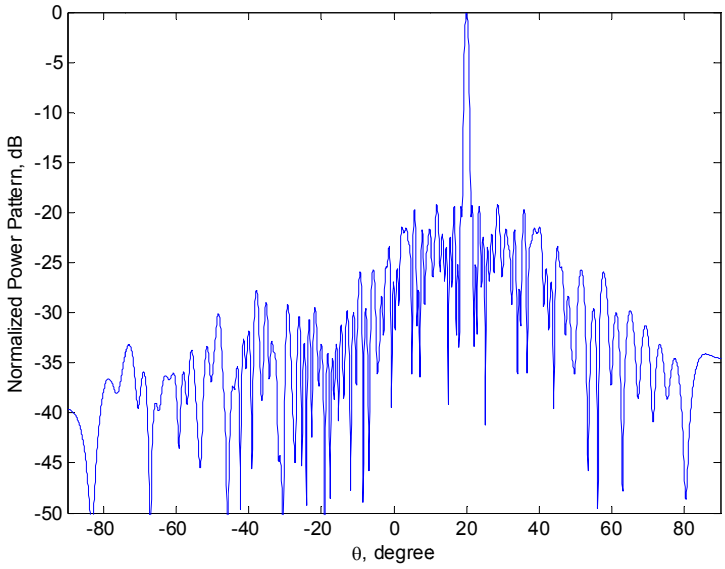

Figure 32. Radiation pattern of the array shown in Figure 30 with Taylor amplitude tapering ($\overline{n}$ =5, SLL=-20 dB) in the $\phi = 0^{\circ}$ plane.

In Figure 33, we summarize the effectiveness of the conventional methods and their combinations on grating lobe suppression for this specific arrangement without amplitude tapering. The improvements shown are computed relative to the periodic DDSA. For concise presentation, we define the shorthand notation of each method as below:

P: periodic DDSA.

RD: random subarray displacement.

SR: sequential subarray rotation.

RS: random subarray sizes.

In Figure 33, it can be seen that the combination of methods has the greatest improvement relative to using the conventional methods individually. However, it is worth noting that an optimization process is needed for each new DDSA arrangement to achieve maximum grating lobe reduction.

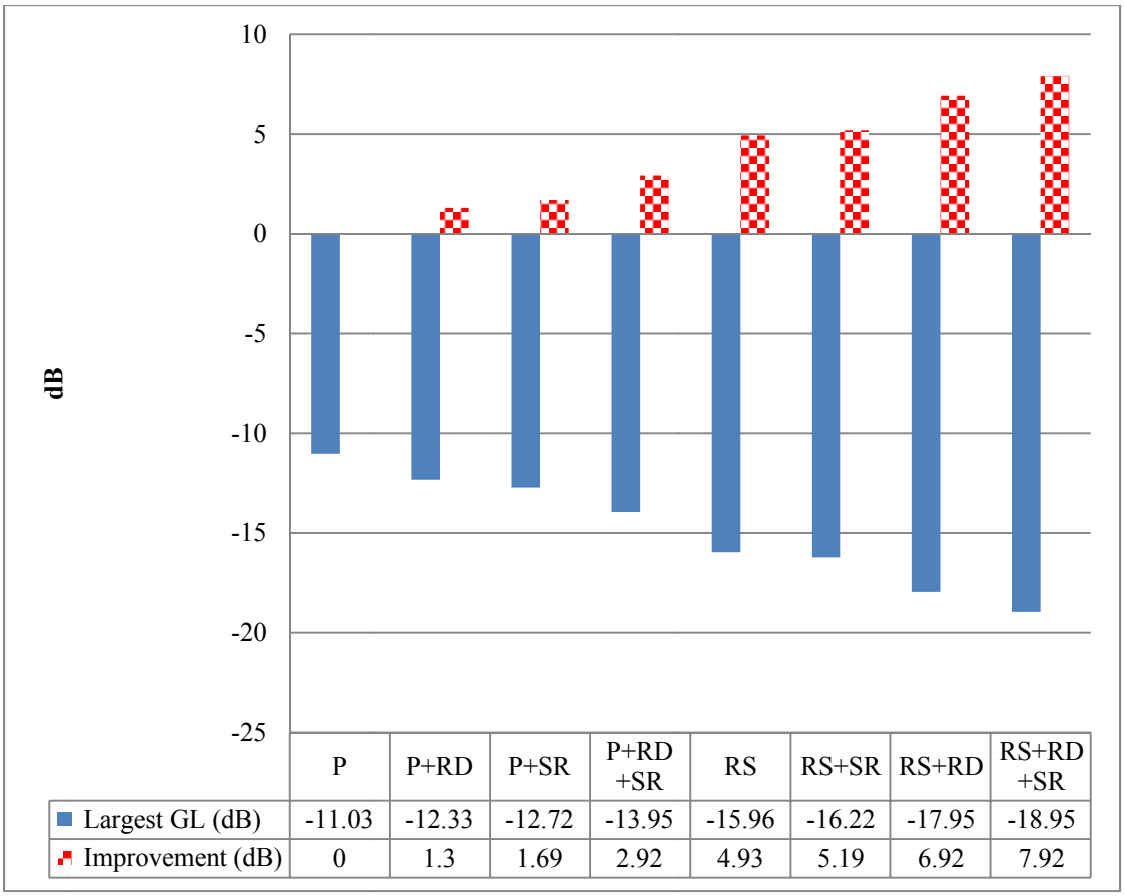

	P	P+RD	P+SR	P+RD +SR	RS	RS+SR	RS+RD	RS+RD +SR
Largest GL (dB)	-11.03	-12.33	-12.72	-13.95	-15.96	-16.22	-17.95	-18.95
Improvement (dB)	0	1.3	1.69	2.92	4.93	5.19	6.92	7.92

Figure 33. Summary of the effectiveness on grating lobe suppression using conventional approaches individually and in combination.

C. SUMMARY AND CONCLUSIONS

In this chapter, several conventional methods for grating lobe suppression were examined. To further improve the grating lobe suppression results, a combination of the conventional methods was introduced and simulated. As can be seen from the simulation results, each method provides some additional grating lobe suppression. By combining the methods, grating lobes are further lowered by approximately 8 dB (from −11 dB to −19 dB). However, disadvantages such as polarization loss, hardware complexity, gain loss and limited suppression ability for large separations restrict the use of these methods, and therefore, tradeoffs need to be made accordingly.

THIS PAGE INTENTIONALLY LEFT BLANK

V. GRATING LOBE SUPPRESSION WITH VIRTUAL FILLING

Complete digital control of amplitude and phase at the element level of an array allows great flexibility in beamforming. Modern radar and communications systems are incorporating phased arrays with wider bandwidths, allowing for the possibility that several systems on the same platform can share arrays. A system that incorporates DDSAs working cooperatively as a single array (thus forming an array of subarrays) can potentially increase the output SNR and provide better spatial resolution compared with using the subarrays individually. However, even if the individual array patterns have no grating lobes, conventional beamforming with periodic subarrays will have an output response with grating lobes, which is unacceptable for most applications.

In this chapter, we propose virtual filling of the gaps between the subarrays to eliminate the grating lobes on the receiving side so that the response of a single large contiguous array is synthesized. Therefore no grating lobes will appear as long as element spacing within all subarrays is less than one half of the wavelength. Furthermore, amplitude tapering can be applied to the synthesized array to reduce interference and clutter. The number of virtual elements that can be used to fill between or extend outside the real elements is restricted by the accuracy of the estimated parameters.

Multiple signals that impinge on the array can be either desired (e.g., radar target return) or undesired (e.g., interference or clutter). If the subarrays are widely separated, then closely spaced grating lobes occur, and there will be many angles where the undesired signal has a large response as the main beam is scanned. We would like an output response for the synthetic array that mimics the response of a contiguous array so that the mainbeam is in the direction of the desired signal and the interference is in a low side lobe. This response can be synthesized by filling in the gaps between the arrays with virtual elements. Here, methods are used to estimate the virtual element weights from the in-phase and quadrature baseband signals received by the real elements. The information needed to reconstruct the contiguous array response is the signal DOAs, magnitudes and phases.

In Section A, the DDSA model is introduced. Because DOA estimation is crucial to synthesizing the virtual element weights, Section B discusses how some single snapshot (SS) DOA algorithms perform with regard to this problem. In particular, the modified MP algorithm is found to have improved resolution for closely spaced signals relative to the Fast Fourier Transform (FFT) method. A multiple snapshot (MS) algorithm is also described in Section B. In Section C, we present formulas for estimating signal amplitudes and phases based on the DOAs. The dependence on element level SNR of the synthesized array response is formulated. Noise and other errors are considered in Section D.

A. DDSA MODEL

For simplicity we consider a linear array of N_s identical subarrays. Each subarray contains N_x elements that are equally spaced d_x along the *x* axis as shown in Figure 34. The gap between subarrays is $D = h\,d_x$ where *h* is an integer greater than zero (i.e., the gap is an integer multiple of the element spacing as shown in Figure 34).

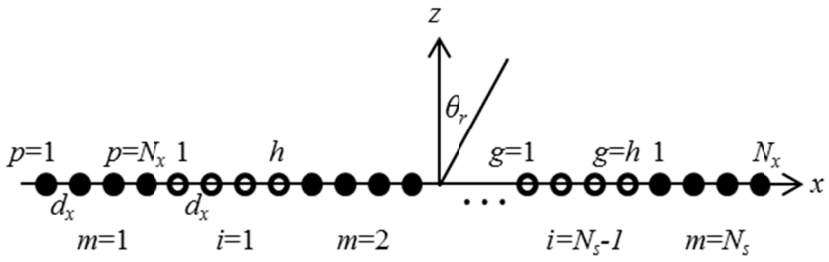

Figure 34. Linear distributed digital subarray model. Black filled dots are real elements and non-filled dots are virtual elements.

If the entire array is centered at the origin, the location of element p in subarray m is

$$x(m,p) = \left[p - \frac{N_s N_x + (N_s - 1)h + 1}{2} + (m-1)(N_x + h) \right] d_x \equiv P(m,p) d_x \qquad (m = 1, 2, ..., N_s;\ p = 1, 2, ..., N_x). \tag{34}$$

If there are $K \le N_s N_x$ signals incident on the array from angles θ_r $(r = 1, 2, ..., K)$ with complex voltages $V_r e^{j\alpha_r}$ the element outputs can be expressed in phasor form as:

$$A(m,p) = \sum_{r=1}^{K} V_r \exp(-jkP(m,p) d_x \sin\theta_r + j\alpha_r) \equiv I(m,p) + jQ(m,p). \tag{35}$$

B. DOA ESTIMATION

Numerous DOA estimation algorithms are available, but the MP method performs particularly well for single snapshot noisy data. It utilizes singular value decomposition (SVD) to divide the matrix space into signal and noise subspaces. By discarding the eigenvector corresponding to the noise signal, the noise effect can be reduced, and hence, the estimation accuracy can be improved.

From measurement of the I and Q at the elements, the signal parameters θ_r and $V_r e^{j\alpha_r}$ can be estimated. Thermal noise is accounted for by adding a complex noise to the $A(m,p)$ in Eq. (35). The noise leads to an error in the parameter estimates, which in turn results in a distortion of the synthesized antenna response.

1. Matrix Pencil Method

General formulas of the classical MP method used to estimate the DOAs are presented. A single one-dimensional (1-D) uniform linear array model is shown in Figure 35.

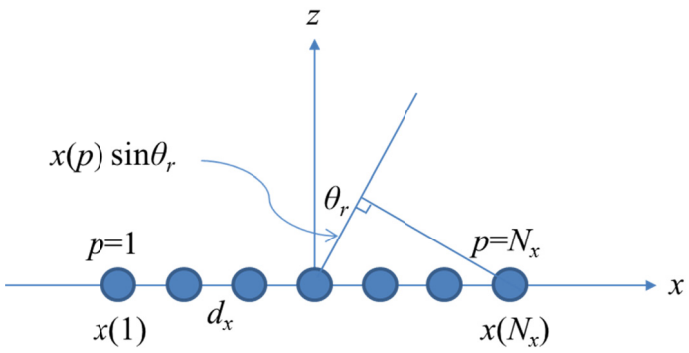

Figure 35. Linear array model.

For a linear array centered at the origin, locations of each element can be represented similar to Eq. (34) as:

$$x(p) = \left[p - \frac{N_x + 1}{2} \right] d_x \equiv P(p) d_x \qquad (p = 1, 2, ..., N_x). \tag{36}$$

The sum of K complex signals received at each element can be modeled as follows:

$$\begin{aligned} A(p) &= \sum_{r=1}^{K} V_r \exp(-jkP(p)d_x \sin\theta_r + j\alpha_r) \\ &\equiv I(p) + jQ(p) \end{aligned} \tag{37}$$

where $V_r e^{j\alpha_r}$ is the complex magnitude associated with signal r, θ_r is the direction-of -arrival of signal r with respect to the z direction.

In the noisy environment, we use SVD directly with received complex signals in the form of Hankel structure matrix of dimension $(N_x - L + 1) \times L$, in which L is the pencil parameter chosen between $N_x/2$ and $N_x/3$ for optimum noise removal [23]. The Hankel structure matrix **A** is

$$\mathbf{A} = \begin{pmatrix} A(1) & A(2) & \cdots & A(L) \\ A(2) & A(3) & \cdots & A(L+1) \\ \vdots & \vdots & \ddots & \vdots \\ A(N_x - L + 1) & A(N_x - L + 2) & \cdots & A(N_x) \end{pmatrix}_{(N_x - L + 1) \times L} . \tag{38}$$

The SVD of **A** can be represented as:

$$\mathbf{A} = \mathbf{W}\mathbf{\Psi}\mathbf{U}^H \tag{39}$$

where **W** and **U** are unitary matrices whose columns are eigenvectors of $\mathbf{A}\mathbf{A}^H$ and $\mathbf{A}^H\mathbf{A}$, respectively. **Ψ** is a diagonal matrix containing the singular values of **A**. If the number of signals (K) is known, we can select the largest K singular values and their corresponding eigenvectors, and form a new signal matrix $\tilde{\mathbf{W}}$ which contains only the signal subspace eigenvectors and has most of the noise effects removed.

Next, by solving the following eigenvalue problem, the DOAs can be estimated:

$$\begin{aligned} (\tilde{\mathbf{W}}_1^{\dagger}\tilde{\mathbf{W}}_2)\mathbf{v} &= \Lambda_r\mathbf{v} \qquad\qquad r = 1, ..., K \\ \tilde{\mathbf{W}}_1^{\dagger} &= (\tilde{\mathbf{W}}_1^H\tilde{\mathbf{W}}_1)^{-1}\tilde{\mathbf{W}}_1^H \end{aligned} \tag{40}$$

where **v** is the eigenvector, and Λ_r is the eigenvalue of $\tilde{\mathbf{W}}_1{}^{\dagger}\tilde{\mathbf{W}}_2$, $\tilde{\mathbf{W}}_1$ and $\tilde{\mathbf{W}}_2$ are $\tilde{\mathbf{W}}$ with the last and first row deleted, respectively. The symbol † is the Moore-Penrose pseudo inverse as defined in Eq. (40). We then can extract the DOAs from Λ_r using the following equation:

$$\hat{\theta}_r = \sin^{-1}\left\{\frac{\mathrm{Im}\left[\ln(\Lambda_r)\right]}{kd}\right\}. \tag{41}$$

2. Modified Matrix Pencil Method for DDSA

a. Single-Snapshot MP Method

We propose an extension of the MP method that is tailored to the DDSA by arranging the Hankel matrices of each subarray from top to bottom sequentially. Let $\mathbf{Y}_m$ be the Hankel matrix for subarray m

$$\mathbf{Y}_m = \begin{pmatrix} A(m,1) & \cdots & A(m,L) \\ \vdots & \ddots & \vdots \\ A(m,N_x-L+1) & \cdots & A(m,N_x) \end{pmatrix}_{[(N_x-L+1)]\times L} \tag{42}$$

so that for a single snapshot

$$\mathbf{Y}_{SS} = \begin{pmatrix} \mathbf{Y}_1 \\ \vdots \\ \mathbf{Y}_{N_s} \end{pmatrix}_{[(N_x-L+1)N_s]\times L} . \tag{43}$$

b. Multiple Single-Snapshot MP Method

Due to rapidly advancing technology, receivers are capable of high sampling rates. Therefore, a multiple single-snapshot (MSS) MP method is relatively straightforward, and it is shown in this section to have good thermal noise removal capability in terms of DOA estimations. Based on the simulation results, thirty single snapshots will be enough for acceptable DOA estimation. Using more single snapshots improves the estimation accuracy at the expense of longer waiting time and a requirement for more computational power.

A multiple single-snapshot method is based on the single-snapshot formulas described in the previous section. By averaging the estimated DOAs from snapshots, the thermal noise effects on DOA estimations can be reduced dramatically.

c. Multiple Snapshots

In principle, MP requires only a single snapshot, but it can be extended to multiple snapshots, thus resulting in a lower root mean square error (RMSE) [28].

The multiple snapshot MP can be considered as a concatenation of multiple columns of single snapshot MP. If $\mathbf{Y}_{m,b}$ is the Hankel matrix for snapshot b $(b = 1,2,...,B)$ of subarray m

$$\mathbf{Y}_{m,b} = \begin{pmatrix} A_b(m,1) & \cdots & A_b(m,L) \\ \vdots & \ddots & \vdots \\ A_b(m,N_x-L+1) & \cdots & A_b(m,N_x) \end{pmatrix}_{(N_x-L+1)\times L} \tag{44}$$

then for multiple snapshots

$$\mathbf{Y}_{MS} = \begin{pmatrix} \mathbf{Y}_{1,1} & \cdots & \mathbf{Y}_{1,B} \\ \vdots & \ddots & \vdots \\ \mathbf{Y}_{N_s,1} & \cdots & \mathbf{Y}_{N_s,B} \end{pmatrix}_{[(N_x-L+1)N_s]\times(LB)} . \tag{45}$$

Note that computational time increases with the number of snapshots. Some advantages of using multiple snapshots are to stabilize the DOA estimation for a small number (one or two) of subarrays cases at lower SNR (0 to 4 dB). The RMSE of DOA estimation tends to decrease when the number of snapshots increases. However, in terms of DOA estimation, the average of multiple single-snapshots will provide more accurate results compared to multiple snapshot case as in Eq. (45). This is because the noise effects will be reduced again by averaging.

d. Simulation Results

After the matrices for the DDSA are formed, the standard MP procedure for finding the DOAs of signals in the noisy environment is applied [32].

The improved performance of the angle estimates from the modified MP method was verified using a Monte Carlo simulation with 100 trials. First, a signal is incident from 30° with phase $\pi/5$ radian onto a DDSA comprised of five eight-element linear arrays with an element spacing of 0.42λ. The spacing between subarrays is 3.36λ. The advantage of using the modified MP method can be observed in Figure 36. It can be seen that for one subarray (i.e., small $N_s N_x$) at low SNR, the RMSE of the DOA is high. As expected, employing more subarrays makes the estimates much more accurate.

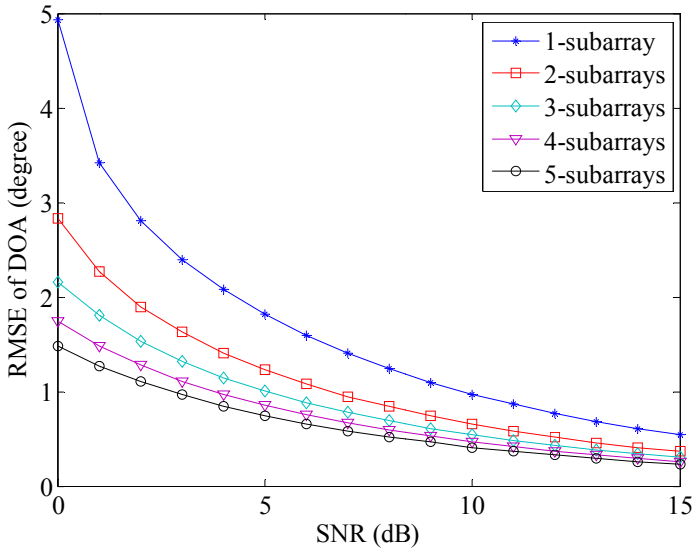

Figure 36. RMSE of DOA for one signal vs. SNR per element for various numbers of subarrays. Each subarray has eight elements spaced 0.42λ, and gaps are equal to the subarray size.

Next, we increase the number of elements in the DDSAs from eight to eighty. The gaps are now $80d = 33.6\lambda$ long. Also the number of signals is increased to two: one from 30° and a second from 31°. The phases of the signals are $\pi/5$ and $-4\pi/5$, respectively. From the curves in Figure 37 and Figure 38, it can be seen that increasing the number of DDSAs provides much smaller RMSE even at low SNR (0 dB) for the two signals. If the FFT method [59] were used at the subarray level, the beamwidth would be too wide to resolve the two closely spaced signals. As for the single target case, using more subarrays in the processing results in much more stable and accurate results, which will be crucial for effective "filling."

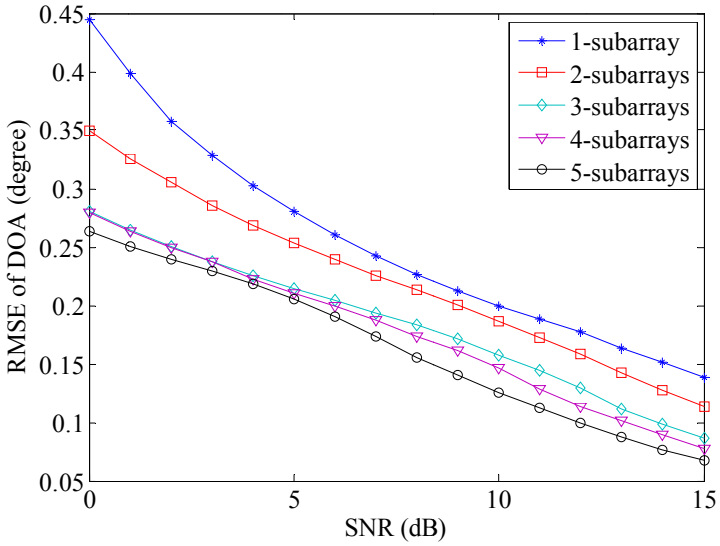

Figure 37. RMSE of DOA for signal 1 vs. SNR per element for various numbers of subarrays. Each subarray has eighty elements spaced 0.42λ, and gaps are equal to the subarray size.

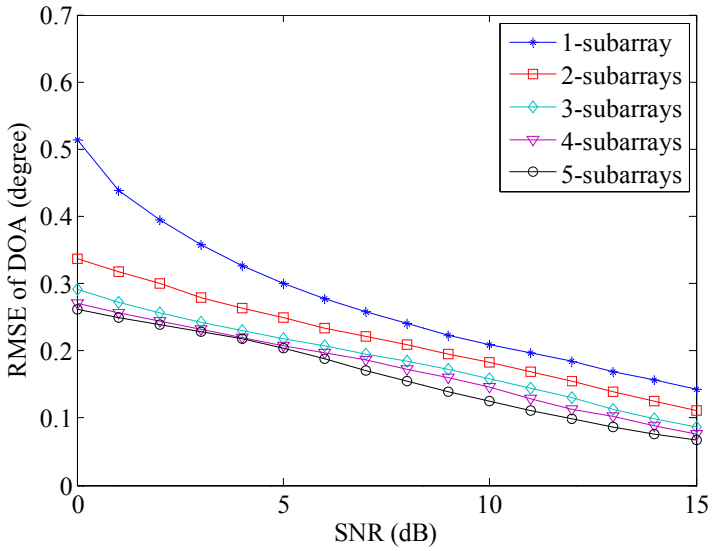

Figure 38. RMSE of DOA for signal 2 vs. SNR per element for various numbers of subarrays. Each subarray has eighty elements spaced 0.42λ, and gaps are equal to the subarray size.

C. VIRTUAL FILLING METHOD

1. Introduction

The sum of *K* complex signals from the source $V_r e^{j\alpha_r}$ from angle $\hat{\theta}_r$ at the output of the elements of subarray *m* can be written as

$$A(m,p) = \sum_{r=1}^{K} V_r \exp(-jkP(m,p)d_x \sin\hat{\theta}_r)\exp(j\alpha_r) \qquad (p = 1,...,N_x) \tag{46}$$

Casting these in matrix form gives

$$\mathbf{E}_m\ \mathbf{V} = \mathbf{A}_m \tag{47}$$

where

$$\mathbf{E}_m = \begin{pmatrix} e^{-jkP(m,1)d\sin\hat{\theta}_1} & \cdots & e^{-jkP(m,1)d\sin\hat{\theta}_K} \\ \vdots & \ddots & \vdots \\ e^{-jkP(m,N_x)d\sin\hat{\theta}_1} & \cdots & e^{-jkP(m,N_x)d\sin\hat{\theta}_K} \end{pmatrix}_{N_x\times K} \tag{48}$$

$$\mathbf{V} = \begin{pmatrix} V_1 e^{j\alpha_1} \\ \vdots \\ V_K e^{j\alpha_K} \end{pmatrix}_{K\times 1} \tag{49}$$

$$\mathbf{A}_m = \begin{pmatrix} A(m,1) \\ \vdots \\ A(m,N_x) \end{pmatrix}_{N_x\times 1} . \tag{50}$$

To estimate signal magnitudes and phases, a least squares method can be used that employs all subarray element outputs [23]. They are assembled column wise and solved to obtain estimates of the complex signals $\hat{\mathbf{V}}$:

$$\begin{pmatrix} \hat{\mathbf{V}}_1 \\ \vdots \\ \hat{\mathbf{V}}_K \end{pmatrix}_{K\times 1} = \begin{pmatrix} \mathbf{E}_1 \\ \vdots \\ \mathbf{E}_{N_s} \end{pmatrix}^{\dagger}_{N_s N_x\times K} \begin{pmatrix} \mathbf{A}_1 \\ \vdots \\ \mathbf{A}_{N_s} \end{pmatrix}_{N_s N_x\times 1} . \tag{51}$$

Note that adding subarrays increases the total number of elements and thus the number of signals that can be handled.

Now the estimated signal magnitudes $\hat{V}_r$ and phases $\hat{\alpha}_r$ can be used to create virtual complex data to "fill" the gaps between subarrays. The location of virtual element g in gap i (between subarrays i and i+1) is

$$\begin{aligned} x(i,g) &= \left(g - \frac{(N_s-2)N_x + (N_s-1)h + 1}{2} + (i-1)(N_x+h) \right) d_x \\ &\equiv Z(i,g)d_x \quad (g = 1,2,...,h;\ i = 1,2,...,N_s-1) \end{aligned} \tag{52}$$

The complex data for filling is given by the same formula as for the real data in Eq. (46)

$$B(i,g) = \sum_{r=1}^{K} \hat{V}_r \exp(-jkZ(i,g)d_x \sin\hat{\theta}_r) \exp(j\hat{\alpha}_r). \tag{53}$$

Combining the real and virtual data gives the response of the synthesized array

$$\mathbf{F} = \left[\left(\mathbf{A}_1\right)_{1\times N_x} \left(\mathbf{B}_1\right)_{1\times h} \cdots \left(\mathbf{B}_{N_s\text{-}1}\right)_{1\times h} \left(\mathbf{A}_{N_s}\right)_{1\times N_x} \right]_{1\times[N_sN_x+(N_s-1)h]} \tag{54}$$

where the **B** partitions are comprised of the terms given by Eq. (53). **F** represents the complex outputs of the synthesized array in the K signal directions. Multiplying by the desired beamforming weights and summing gives the array response.

2. Simulation Results

Consider a five-subarray DDSA with 30 elements in each subarray and an element spacing of 0.42λ. The subarray length is 12.6λ. The gaps are also (arbitrarily) set to 12.6λ. One unit amplitude signal is incident from 0° with a phase of $\pi/5$. A second interference signal is coming in at 2.3° with a phase $-4\pi/5$. The pattern is shown in Figure 39 as the weights are changed to scan the main beam in a region of direction cosine space ($\sin\theta$). A 20 dB Taylor amplitude distribution is applied. As can be seen, the high response of the interfering signal that occurs at grating lobe locations has been eliminated. The synthesized array response in the direction of both signals is the same as that of a contiguous array.

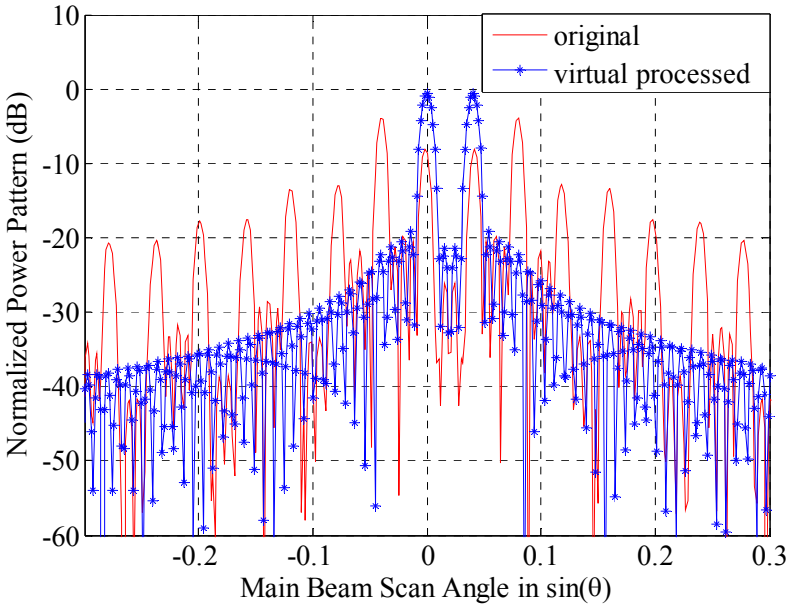

Figure 39. Comparison of original and synthesized antenna responses of 5 subarrays each with 30 elements, for signals (noiseless) incident from 0° and 2.3°.

The average synthesized array response for the same case shown in Figure 39 can be seen in Figure 40, but with an SNR per element of 6 dB (single snapshot). The results of a Monte Carlo simulation of thirty trials (equivalent to thirty single snapshots) using Eq. (43) for the five-subarray two-signal case used to generate Figure 40 are summarized in Table 1.

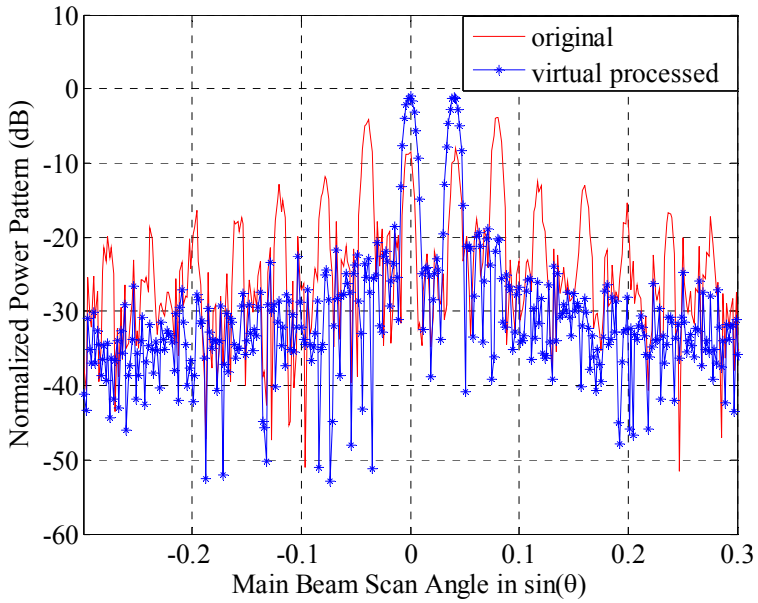

Figure 40. Comparison of original and synthesized antenna response after virtual filling for an element level SNR of 6 dB. Taylor amplitude taper ($\overline{n}$ =5, SLL= –20 dB) has been applied.

Table 1. Exact and estimated signal parameters for virtual processing.

Parameter	**Actual**		**Estimated (mean)**		**Estimated (variance)**	
	Signal 1	**Signal 2**	**Signal 1**	**Signal 2**	**Signal 1**	**Signal 2**
DOA (degrees)	0	2.3	0.0356	2.2965	0.1808	0.2878
Amplitude (Volts)	1	1	0.9630	0.9533	0.002	0.0034
Phase (radians)	0.6283	2.5133	0.6371	2.5045	0.0018	0.002

The effectiveness of the virtual approach relies on having accurate angle estimates for the signals of interest, which in turn requires a high effective array SNR (i.e., large $N_s N_x$ if the SNR per element is low; high SNR if the total number of elements $N_s N_x$ is small). The SNR per element can be increased by adding a low noise amplifier or

increasing the gain of the array element. It is also possible to improve the DOA estimates with multiple snapshots or by averaging multiple single snapshots.

D. NOISE AND OTHER ERRORS

For a real application, factors such as noise and errors cause performance degradation of a system. Thermal noise appears in almost all receivers and is commonly considered as the primary error source in the receiver. Low noise amplifiers are usually used to increase the SNR. Other errors including array element positioning error, mutual coupling error, manufacturing imperfections and calibration errors are considered as fixed errors that can be measured in advance and possibly be compensated. We model the thermal noise at the element level by specifying the element SNR. Not only is it random between elements, but it is also random from snapshot to snapshot. On the other hand, fixed errors are modeled as random variables that are fixed between snapshots/trials.

Next, a five-subarray DDSA model is used to examine the effects of fixed errors to the DOAs estimation and filling method. Each subarray is comprised of ten elements with element spacings equal to 0.45λ. Subarray center distances are 10λ. Fixed errors are uniformly distributed from -21° to 21° (root mean square (RMS) values from 0° to 12.1°), and the SNR is varied from 6 dB to 21 dB at each element. Two signals with equal magnitude and non-coherent phases ($\pi/5$ and $-4\pi/5$) from DOAs of -10° and 15° relative to broadside are impinging on the DDSA.

The receiving pattern for 6 dB SNR for the ideal contiguous array of the same aperture size as DDSA, original DDSA and virtual filling method are compared in Figure 41. A huge improvement in terms of grating lobes and sidelobe suppression can be observed after applying the virtual filling method.

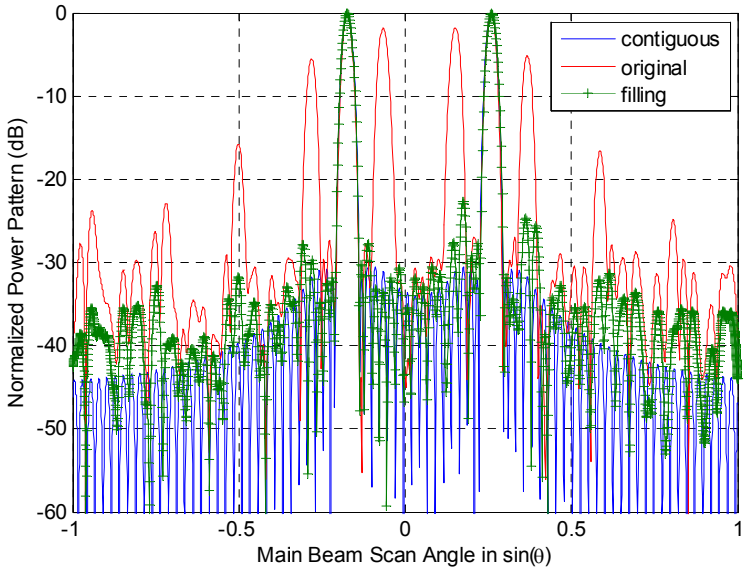

Figure 41. Pattern comparison of contiguous, original DDSA and virtual filling. Assuming no fixed errors and with 6 dB SNR at each element. Taylor amplitude taper ($\bar{n}$ =5, SLL=−30 dB) has been applied.

In order to quantify the effect of fixed errors on the DOA estimations, a plot that compares the RMSE of the DOA versus RMS phase error for different SNR levels is shown in Figure 42. The formula used to calculate the average RMSE of the DOA for the K signals is

$$RMSE = \sqrt{\frac{\sum_{r=1}^{K}\left[\left(\hat{\theta}_r - \theta_r\right)^2\right]}{K}} \tag{55}$$

where $\hat{\theta}_r$ is the estimated angle, and θ_r is the true angle of signal r. Two conclusions can be made based on the information provided by the plot:

1. The most efficient way to improve the RMSE of the DOA is to increase the SNR at each element.

2. For RMS phase errors less than 6° which correspond to a fixed error of -10.5° to 10.5°, the effect on DOA estimation can be ignored for all SNRs.

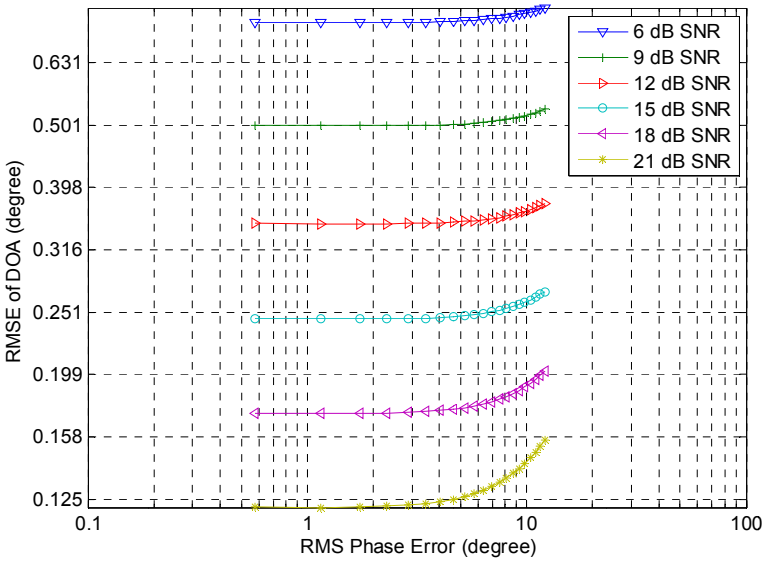

Figure 42. RMSE of DOA versus RMS phase errors from 0° to 12.1° for different element SNR.

Many of the sources of the fixed errors can be compensated for by pre-calculation or pre-measurement, but there will still be some residual errors after correction. We consider phase errors up to 21° and examine how they degrade the radiation pattern. Figure 43 has a plot of the pattern of the worst case (21° fixed error) at 6 dB SNR. By comparing Figure 43 with Figure 41, we see that the effect of the fixed error on the receiving pattern is to increase the side lobe level and lower the main beam by 0.6 dB due to the increase of RMSE of the DOA.

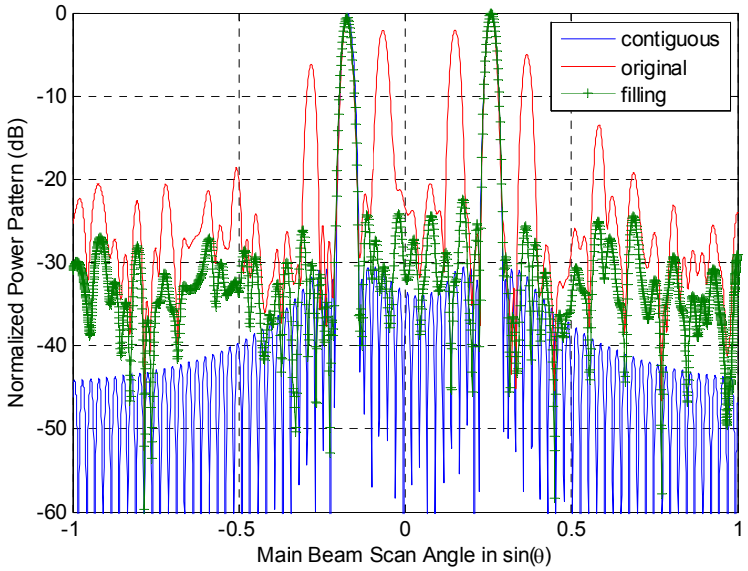

Figure 43. Pattern comparison of contiguous, original DDSA and virtual filled DDSA for 21° fixed error and with 6 dB SNR at each element. Taylor amplitude taper ($\bar{n}$ =5, SLL= -30 dB) has been applied.

We also consider the effect of signal angles on the RMSE of DOA with fixed errors uniformly distributed between -21° and 21° and 6 dB SNR per element. As can be seen in Figure 44, because the projected aperture area decreases at large signal angles, the RMSE of the DOA is increased.

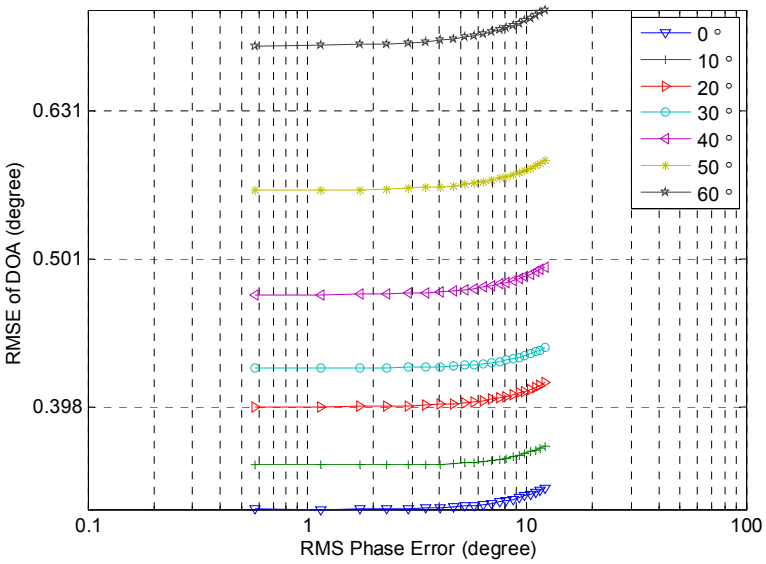

Figure 44. RMSE of DOA versus RMS phase errors from 0° to 12.1° and 6 dB SNR per element for different signal angles.

E. SUMMARY AND CONCLUSIONS

Filling the gaps between arrays with virtual elements for the purpose of receiving processing allows a synthesized antenna response that duplicates a contiguous array in a number of directions that is limited by the total number of elements used in the processing. The synthesized response has no grating lobes and can have low side lobes. As a first step, the signal amplitudes, phases and DOAs must be extracted from the element I and Q samples. This data is used generate I and Q samples that would be provided by virtual elements filling the gaps between distributed subarrays. Low side lobes and interference rejection were demonstrated for the virtual processed DDSA.

The MP method was found be to be well suited for this application. The MP technique was extended to handle multiple subarrays, for either single or multiple snapshots. Multiple snapshots provide improved stability in a low SNR situation. This method can deal with both coherent and non-coherent signals and requires fewer snapshots for accurate DOA estimation.

The proposed filling method allows suppression of undesired signals that would normally occur at grating lobe angles. It was shown that for high SNR the array response approaches that of a contiguous array of the same extent.

THIS PAGE INTENTIONALLY LEFT BLANK

VI. APPLICATIONS

A. THREE-STEP MODIFIED MATRIX PENCIL METHOD FOR DDSA

From the simulation results in Chapter V, it was shown that the modified MP for DDSA provides improved performance compared to the individual use of the arrays. The overall estimation accuracy can be further improved by adding a step, resulting in a Three-Step Modified Matrix Pencil method described in this chapter.

It is well known that the angular resolution of an array antenna is inversely proportional to its aperture size. It is true for the MP method that higher resolution requires larger array aperture, i.e., adding more radiation elements. However, a basic requirement for the MP method is to have a linear phase relationship between all array elements. For the DDSA case, the first workaround for the linear phase limitation is to cascade the subarray Hankel matrices as proposed in Chapter V. A second method proposed here, is to utilize the advantage of a large aperture and satisfy the linear phase requirement of MP method to gradually improve the DOAs estimation accuracy. The three steps are delineated in the following sections.

1. Preliminary DOA Estimation

A preliminary multiple single-snapshot DOA estimation using the modified MP method is the first step of the method. A fraction of the total snapshots is responsible for this preliminary estimation. For example, twenty single snapshots, out of a total of forty collected, can be used for the preliminary DOA estimation.

2. Signal Extraction and Virtual Filling

Using the DOAs estimated in step one, we can extract the signal parameters and then virtually fill the gaps between subarrays using the estimated parameters in the equations in Chapter V, Section C.

3. DOA Estimation Using Virtually Filled DDSA

The next step is to use the "filled" large array for the second improved DOA estimation. The filled array is analogous to a large continuous array, and the estimation results should be close to a real array with the same aperture size if the filling parameters are accurate enough. A large aperture provides better angular resolution. Therefore the system performance in terms of RMSE should be improved relative to the preliminary DOA estimation.

4. Final DOA Estimation

The final step is to use the improved estimated parameters from the previous step to fill the gaps again. Since more independent data points are used, the average SNR at each element improves. Higher SNR at each element will contribute to a lower RMSE of DOA estimation.

5. Simulation Results

Two equal amplitude signals with phases $\pi/5$ and $-4\pi/5$ are impinging on a five-subarray DDSA from the angles of -20° and 0° relative to broadside. The spacing between subarray centers is 18λ. Each subarray has 20 elements with 0.45λ element spacing. The performance comparison of modified MP method and three-step modified method, in terms of RMSE of DOA, is shown in Figure 45. Due to the increase of aperture size of the filled array 1, the RMSEs of DOAs are much smaller relative to the five subarray case.

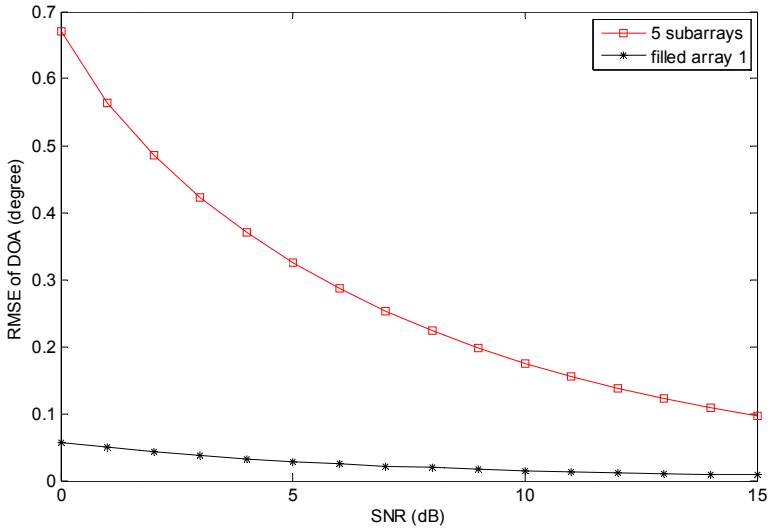

Figure 45. RMSE of DOA for five subarrays (modified MP) and filled array 1 (three-step modified method).

Now we use the results (DOAs, amplitudes and phases) from filled array 1 to virtually refill the gaps between subarrays and re-estimate the DOA using the MP method for single array. Improvement in terms of RMSE can be observed as seen in Figure 46. This is because of the improved accuracy of the filling data from the filled array 1 that lower the RMSE of DOA of filled array 2.

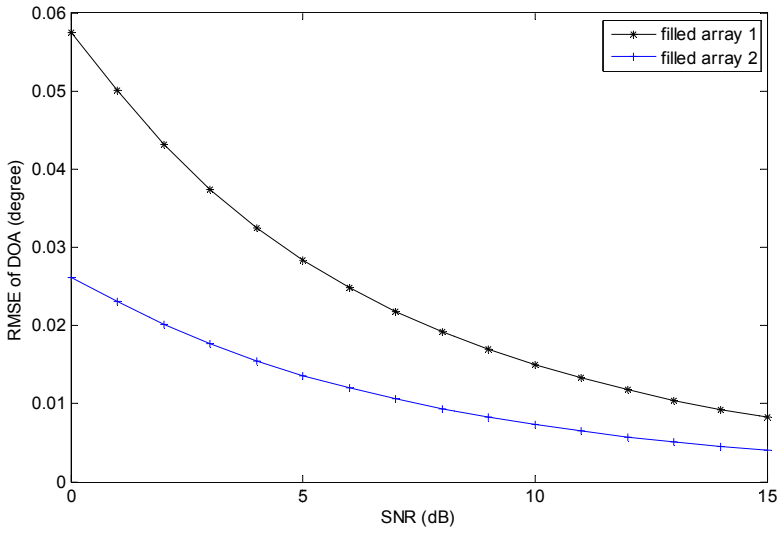

Figure 46. RMSE of DOA for filled array 1 and filled array 2.

6. Three-Step Modified MP for Close Targets

It is known that a larger aperture is the key solution to resolve two closely spaced targets. We would like to demonstrate the improved resolution for two close targets using the Three-Step Modified MP method and compare the result with that using modified MP method. Two equal amplitude signals with phases $\pi/5$ and $-4\pi/5$ are impinging on a five-subarray DDSA from the angles of -10° and -4° relative to the broadside. The subarray spacing between centers is 18λ. Each subarray has 20 elements with 0.45λ element spacing and 0 dB SNR per element. A total of 40 single-snapshots are used for both modified MP method and the Three-Step Modified MP method. The radiation power pattern using modified MP method is shown in Figure 47. In Figure 48, it can be seen that the grating lobes are suppressed further by using the Three-Step Modified MP method as the result of the higher accuracy of the parameters estimations.

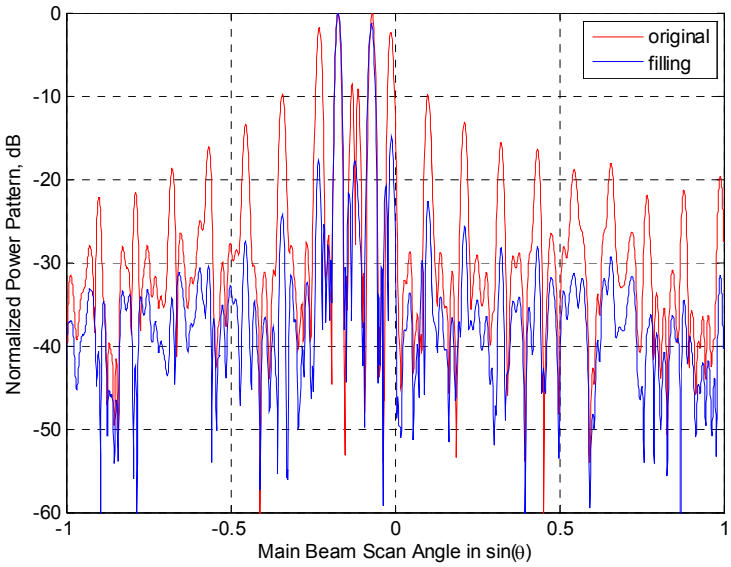

Figure 47. Normalized power pattern of two targets from -10° and -4° using the Modified MP method. Taylor amplitude taper ($\bar{n}$ =5, SLL=–30 dB) has been applied.

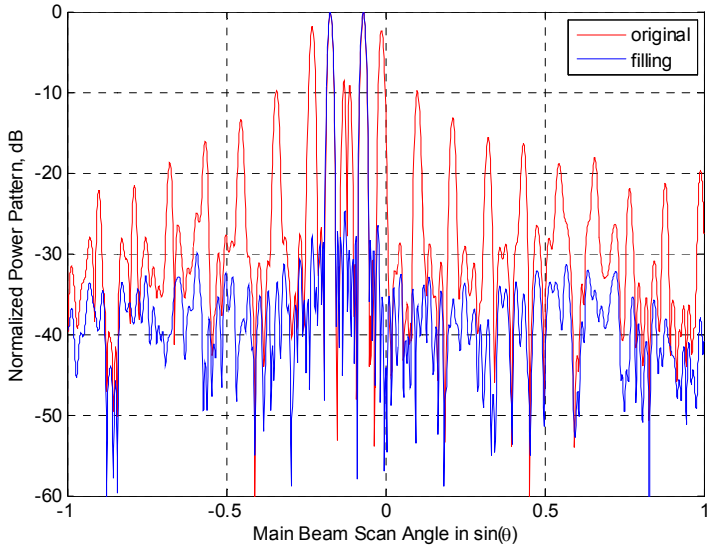

Figure 48. Normalized power pattern of two targets from -10° and -4° using the Three-Step Modified MP method. Taylor amplitude taper ($\bar{n}$ =5, SLL=–30 dB) has been applied.

B. COMBINATION OF RANDOM SUBARRAY SIZES AND FILLING METHOD

1. Introduction

We proposed the virtual filling method on the receiving side to mimic a contiguous array pattern and therefore side lobe taper can be applied to lower the side lobes. However, the virtual filling method cannot be used on the transmitting side, and the grating lobes from a DDSA on the transmitting side can only be addressed with traditional methods such as random subarray displacements, random/sequential subarray rotations and random subarray sizes, as discussed in Chapter IV. We choose random subarray sizes with fixed subarray gaps for our transmitting model because it has the following advantages:

- Since the gaps between subarrays are fixed, it is much easier to implement compared to random subarray gaps.
- Without subarray rotation, the virtual filling method can be applied much more easily.
- With random subarray sizes and fixed subarray gaps, the subarray phase centers are actually randomized and grating lobes are partially suppressed.

2. Simulation Results

A random sized 20-subarray DDSA with number of elements of 6, 8, 12, 10, 14, 10, 8, 14, 18, 16, 33, 21, 31, 47, 53, 39, 65, 21, 45, 29 was first chosen on the basis of the lowest GL level from a 100 Monte Carlo simulation trials that randomly assigned the number of elements of each subarray under the constraint that the total number of elements in the DDSA was 500. Element spacings are 0.48λ, and spacings between subarrays are 4.8λ. Two signals of equal power coming in from 10° and -25° relative to broadside are used for this simulation. The transmitting pattern is noiseless with a Taylor amplitude taper with parameters $\bar{n}$ =5, SLL= -20 dB. On the receiving side, a SNR of 6 dB at each element and a Taylor amplitude taper of -35 dB are used.

The radiation pattern of the periodic 20-subarray DDSA (25 elements in each subarray) is shown in Figure 49. The high grating lobes due to the large periodic spacing between subarrays are clearly seen. The pattern of the random 20-subarray case is shown in Figure 50. The randomness has lowered the grating lobes but also increased the average side lobe level. We can further lower the side lobe level on the receiving side by filling the gaps between subarrays so that an amplitude taper ($\bar{n}$ =5, SLL=–35 dB) can be applied as shown in Figure 51.

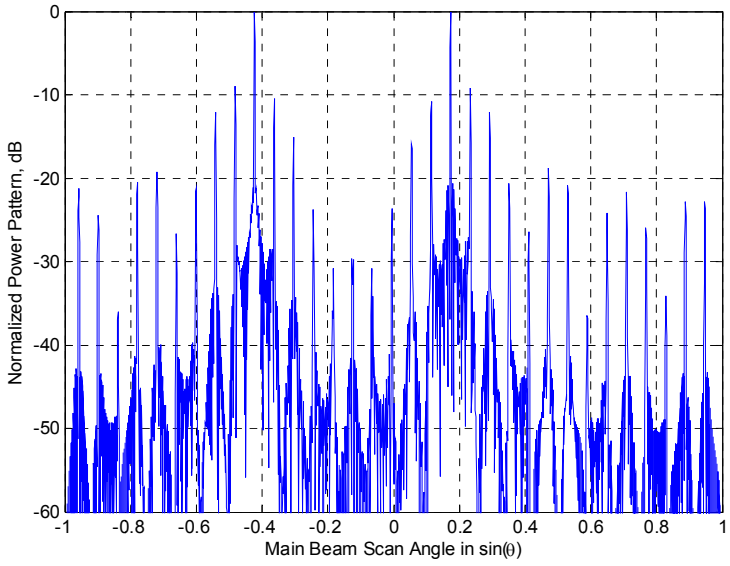

Figure 49. Periodic DDSA transmitting pattern of signals from 10° and -25° related to the broadside.

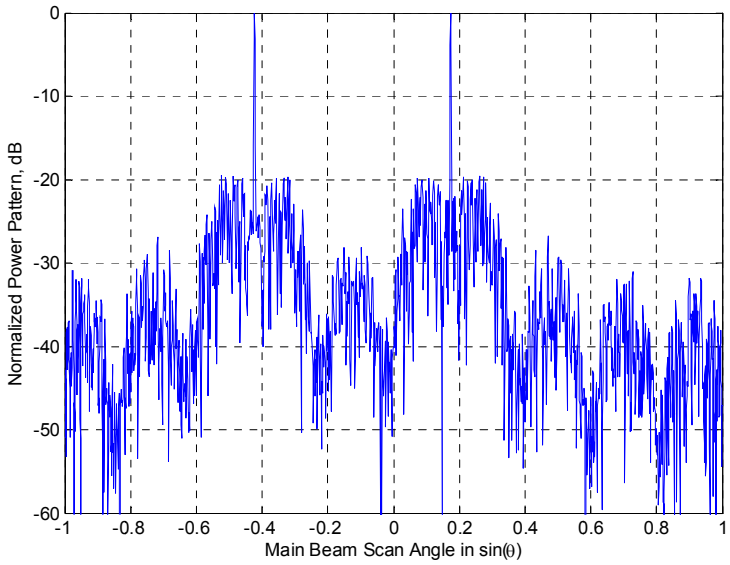

Figure 50. Random subarray sizes DDSA transmitting pattern of signals from 10° and -25° related to the broadside.

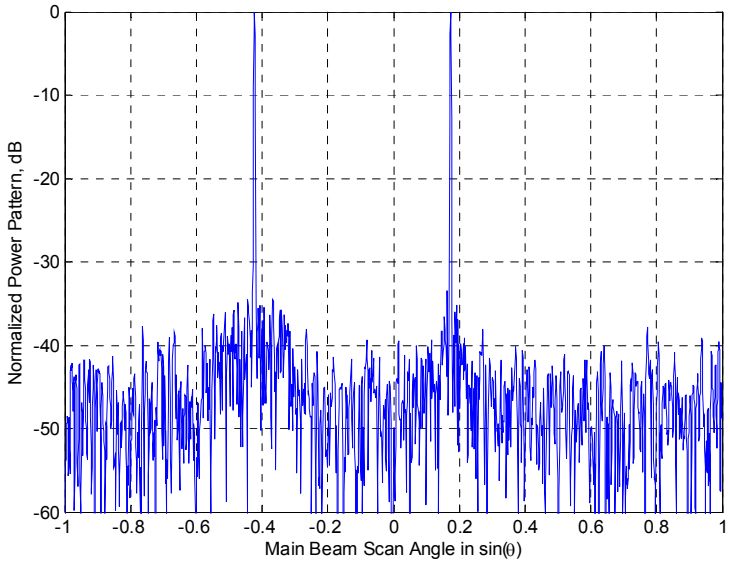

Figure 51. Random subarray sizes DDSA virtual filling receiving pattern of signals from 10° and -25° relative to the broadside. A 35 dB Taylor distribution was applied ($\bar{n}$ =5, SLL=-35 dB).

C. TWO-WAY PATTERN

1. Introduction

By applying pattern multiplication, the normalized two-way pattern is defined as

$$F_{norm_{2way}}(\theta,\phi) = F_{norm_{Tx}}(\theta,\phi) \times F_{norm_{Rx}}(\theta,\phi) \tag{56}$$

where $F_{norm_{Tx}}(\theta,\phi)$ is the normalized pattern of the transmitting DDSA array, and $F_{norm_{Rx}}(\theta,\phi)$ is the normalized pattern of receiving DDSA array. Using the two-way pattern multiplication approach, we see that the remaining DDSA transmitting grating lobes can be reduced by the pattern of the DDSA receiving array.

The two-way beam pattern design of a DDSA [5] can lead to an increase in the hardware complexity compared to separate transmitting and receiving systems and needs to be carefully designed to match the grating lobe and null locations on the two sides. Perfect suppression of the grating lobes by the nulls will only work for a limited number of cases. The method we propose uses a combination of random subarray sizes for the transmitting DDSA and virtual filling for the receiving DDSA, as seen in Figure 52; therefore, the hardware complexity is reduced. Because of the same aperture sizes, both transmitting and receiving patterns possess the same mainbeam beamwidth. The low sidelobe attribute of the receiving pattern can significantly reduce the grating lobes of the transmitting pattern after the multiplication has been done. Therefore no grating lobe and null matching is required.

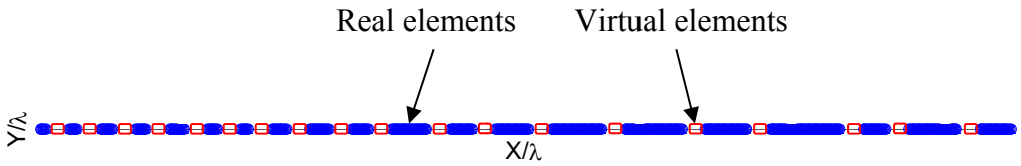

Figure 52. The transmitting DDSA model with real elements (in blue) and the receiving DDSA model with real and virtual elements (in blue and red respectively).

2. Simulation Results

For comparison purposes, a two-way pattern of the periodic DDSA is shown in Figure 53. The two-way pattern shown in Figure 54 is generated by multiplying the transmitting pattern shown in Figure 50 by the receiving pattern shown in Figure 51. The side lobe level has gone down to less than -50 dB without affecting the mainbeam.

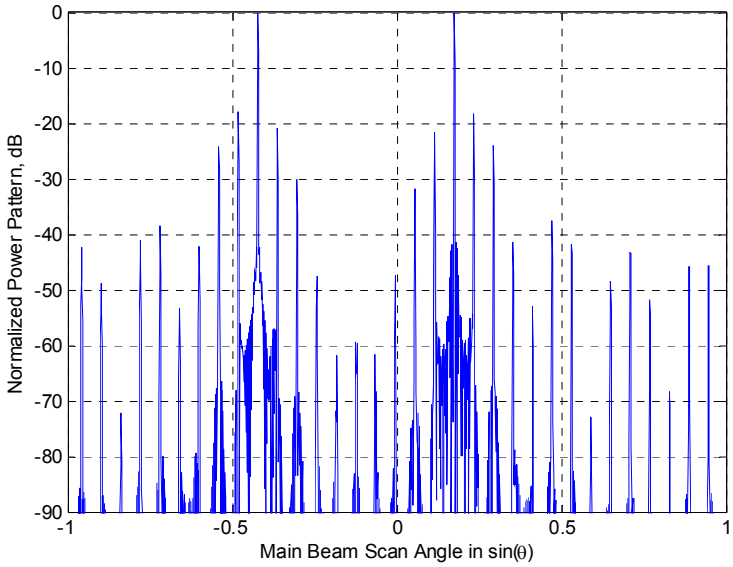

Figure 53. Periodic DDSA two-way pattern of signals from 10° and -25° related to the broadside.

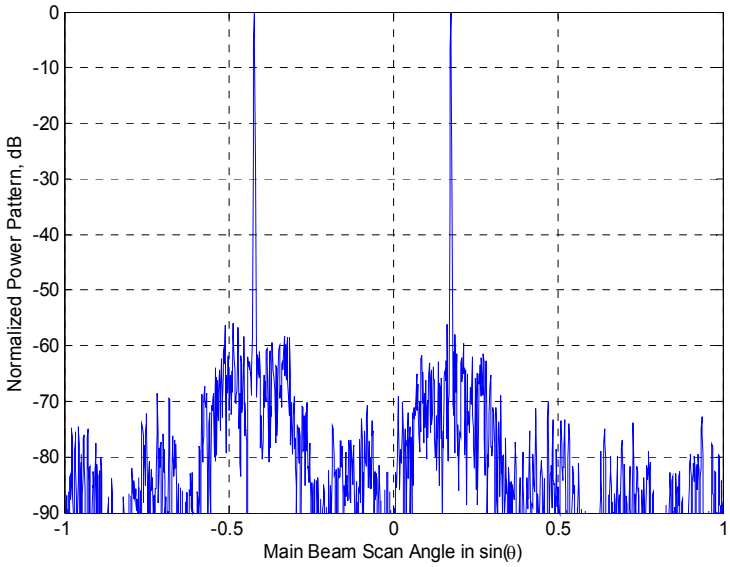

Figure 54. Random subarray sizes DDSA two-way pattern of signals from 10° and -25° related to the broadside.

D. SUMMARY AND CONCLUSIONS

In this chapter, the Three-Step Matrix Pencil method was proposed, and its effectiveness in terms of RMSE of DOA was demonstrated. For applications that require a highly accurate DOA estimation, the proposed method can utilize all available subarrays to achieve high accuracy.

Due to the limited options for grating lobe suppression of a DDSA when transmitting, a combination of conventional methods plays an important role in solving this problem. By using the combination of conventional methods on when transmitting and the virtual filling method when receiving, an improved two-way pattern with an ultra-low side-lobe level was demonstrated.

THIS PAGE INTENTIONALLY LEFT BLANK

VII. SUMMARY AND CONCLUSION

This research has focused on an important and emerging issue, which is grating lobe suppression for DDSAs. In a general sense, using more radiation elements in an array system can potentially increase the array gain when transmitting and SNR when receiving. However, because of the mechanical, structural and operational limitations discussed in Chapter I, the use of a large contiguous array on a platform can be restricted. The idea of using separated arrays that together form a DDSA is a potential solution to this dilemma. The critical issues that must be addressed are calibration, time/frequency synchronization, error correction and grating lobes.

This study focused on various methods to suppress the grating lobes of a DDSA on both the transmitting and receiving sides. Conventional techniques used to treat the grating lobe problem of a single sparse array were applied to DDSAs. Both periodic and random arrangements were considered and general equations for the pattern functions were derived.

Basic formulas for the DDSA radiation pattern were presented in Chapter II. Both periodic and aperiodic or random arrangements were considered and general equations were derived. Several methods of potential interest for grating lobe suppression including subarray rotation, multiplicative beamforming and randomness, were discussed in this chapter as well.

Several conventional methods for grating lobe suppression were examined in Chapter IV. To further improve the grating lobe suppression results, a combination of the conventional methods was introduced and simulated. As can be seen from the simulation results, each method provides some additional grating lobe suppression. By combining the methods, grating lobes are further lowered by around 8 dB (from −11 dB to −19 dB for the example presented). However, disadvantages such as polarization loss, hardware complexity, gain loss and limited suppression ability for large separations restrict the use of the methods, and therefore tradeoffs need to be made accordingly.

Filling gaps between arrays with virtual elements for the purpose of receiving processing allows a synthesized antenna response that duplicates a contiguous array in a number of directions that is limited by the total number of elements used in the processing. The synthesized response has no grating lobes and can have low side lobes, as seen in Chapter V. As a first step, the signal amplitudes, phases and DOAs must be extracted from the element *I* and *Q* samples. This data is used generate *I* and *Q* samples that would be provided by virtual elements filling the gaps between distributed subarrays. Low side lobes and interference rejection were demonstrated for the virtual processed DDSA.

The MP method was found be to be well suited for this application. The MP technique was extended to handle multiple subarrays, for either single or multiple snapshots. Multiple snapshots provide improved stability in a low SNR situation. This method can deal with both coherent and non-coherent signals and requires fewer snapshots for accurate DOA estimation, as was seen in Chapter V.

The proposed filling method allows suppression of undesired signals that would normally occur at grating lobe angles. It was shown that for high SNR the array response approaches that of a contiguous array of the same extent.

The Three-Step Matrix Pencil method was proposed in Chapter VI, and its effectiveness in terms of RMSE of DOA was demonstrated. For applications that require a high accuracy of DOA estimation, the proposed method can utilize all available subarrays to achieve the highest accuracy possible.

Due to the limited options for grating lobe suppression of a DDSA on the transmitting side, a combination of conventional methods plays an important role in solving this problem. By using the combination of conventional methods on the transmitting side and the virtual filling method on the receiving side, an improved two-way pattern with an ultra-low side-lobe level was demonstrated.

A. SIGNIFICANT CONTRIBUTIONS

The primary contributions of this dissertation come from the investigation of the grating lobe problem of DDSAs and the novel techniques proposed to deal with the grating lobe suppression on the receiving side along with the combination of conventional methods to improve the grating lobe level on the transmitting side.

One contribution of this research is a proposed hybrid approach that uses a combination of suppression techniques on both the transmitting and receiving sides. The result is improved two-way pattern performance.

Another contribution is the development of the new virtual filling processing method on the receiving side to suppress grating lobes and improve the signal-to-clutter ratio and signal-to-interference ratio.

A final contribution is the illustration of the relationship (and, hence, tradeoffs) between thermal noise, array errors, and the grating lobe suppression effectiveness. The consideration of array errors addresses the issue of array calibration and synchronization, which are critical concerns when multiple arrays operate coherently.

B. FUTURE RESEARCH

Future research should focus on subarrays with different array lattices and look at the potential application of the filling method. It is relatively straightforward to fill the gaps for DDSA with the same subarray types (i.e., the rectangular periodic planar array). For subarrays with different arrangements, optimal filling positions need to be determined for best grating lobe suppression performance. A similar question arises for DDSAs with subarray rotation, as well.

The mutual coupling effect between real array elements should be included in the simulation and possible compensation methods need to be developed in the future research.

Narrow band (single frequency) is assumed in this research. It would be of great interest to extend the methods developed here to broadband applications. On the transmitting side, broadband applications often assume small subarray sizes. For the same

number of elements in a DDSA, small subarray sizes will provide more subarrays or subarray centers; therefore, more randomization achieved. On the receiving side, parameter estimation techniques for broadband applications need to be examined.

For DDSA design, parameters that will affect the array performance are also the parameters that contribute to the grating lobe suppression effectiveness. For example, the sizes of subarray gaps, number of elements in each subarray, element spacing in each subarray, subarray rotation angles, array element types and array lattice are among these parameters. Therefore, the development of an optimization algorithm for choosing the optimal parameters for best grating lobe suppression results will benefit the design process going forward.

LIST OF REFERENCES

[1] J. E. Nilsson and H. Warston, "Radar with separated subarray antennas," in *Proc. of Int. Radar Conf.*, pp. 194-199, Sep. 2003.

[2] A. M. Haimovich, R. S. Blum, and L. J. Cimini, "MIMO radar with widely separated antennas," *IEEE Signal Processing Magazine*, vol. 25, pp. 116-129, 2008.

[3] R. C. Heimiller, J. E. Belyea, and P. G. Tomlinson, "Distributed array radar," *IEEE Transactions on Aerospace and Electronic Systems*, vol. AES-19, pp. 831-839, Nov. 1983.

[4] K. Nishizawa, K. Hirata, S.-i. Kan, H. Miyashita, and S. Makino, "Experimental investigations into grating lobe suppression in distributed array antennas," in *Int. Symp. on Antennas and Propagation*, pp. 201, Nov. 2006.

[5] C. Lin, "Distributed subarray antennas for multifunction phased-array radar," M.S. thesis, ECE, Naval Postgraduate School, Sep. 2003.

[6] W. Hao, F. Da-Gang, and Y. L. Chow, "Grating lobe reduction in a phased array of limited scanning," *IEEE Transactions on Antennas and Propagation*, vol. 56, pp. 1581-1586, June 2008.

[7] R. Willey, "Space tapering of linear and planar arrays," *IRE Transactions on Antennas and Propagation*, vol. 10, pp. 369-377, Jul. 1962.

[8] G. Burgstaller, "Wirelessly networked digital phased array: design and analysis of a 2.4 GHz demonstrator," M.S. thesis, Department of Electrical and Computer Engineering, Naval Postgraduate School, Sep. 2006.

[9] K. Phil-Su and L. Chang-Gun, "Coordinated search and track by multiple phased array radars," in *Proc. Real-Time and Embedded Technology and Applications Symp.*, pp. 227-235, May 2004.

[10] D. Jenn, Y. Loke, T. C. H. Matthew, Y. E. Choon, O. C. Siang, and Y. S. Yam, "Distributed Phased Arrays and Wireless Beamforming Networks," *Int. Journal of Distributed Sensor Networks*, vol. 5, pp. 283-302, Nov. 2009.

[11] C. S. Eng, "Digital antenna architectures using commercial off the shelf hardware," M.S. thesis, Department of Electrical and Computer Engineering, Naval Postgraduate School, Dec. 2003.

[12] B. D. Steinberg and E. Yadin, "Distributed airborne array concepts," *IEEE Transactions on Aerospace and Electronic Systems*, vol. AES-18, pp. 219-227, Mar. 1982.

[13] L. Ching-Tai and L. Hung, "Sidelobe reduction through subarray overlapping for wideband arrays," in *Proc. Radar Conf.*, pp. 228-233, May 2001.

[14] V. D. Agrawal, "Grating-lobe suppression in phased arrays by subarray rotation," *Proc. of the IEEE,* vol. 66, pp. 347-349, Mar. 1978.

[15] L. Songwen, "Grate lobes / side Lobes suppression for sparse array design by using genetic algorithms," in *2nd Int. Conf. on Innovations in Bio-inspired Computing and Applications*, pp. 371-373, Dec. 2011.

[16] A. P. Goffer, M. Kam, and P. R. Herczfeld, "Design of phased arrays in terms of random subarrays," *IEEE Transactions on Antennas and Propagation*, vol. 42, pp. 820-826, June 1994.

[17] L. C. Stange, C. Metz, E. Lissel, and A. F. Jacob, "Multiplicatively processed antenna arrays for DBF radar applications," *IEE Proc. Microwaves, Antennas and Propagation*, vol. 149, pp. 106-112, Apr. 2002.

[18] L. E. Miller and J. S. Lee, "Capabilities of multiplicative array processors as signal detector and bearing estimator," Defense Technical Information Center, Dec. 1974.

[19] W. Chen, X. Xu, S. Wen, and Z. Cao, "Super-resolution direction finding with far-separated subarrays using virtual array elements," *IET Radar, Sonar & Navigation*, vol. 5, pp. 824-834, Oct. 2011.

[20] R. O. Schmidt, "A signal subspace approach to multiple emitter location and spectral estimation," Stanford University, 1981.

[21] B. D. Rao and K. V. S. Hari, "Performance analysis of root-music," in *22nd Asilomar Conf. on Signals, Systems and Computers*, pp. 578-582, Dec. 1988.

[22] A. Paulraj, R. Roy, and T. Kailath, "Estimation of signal parameters via rotational invariance techniques- Esprit," in *19th Asilomar Conf. on Circuits, Systems and Computers*, pp. 83-89, Nov. 1985.

[23] T. K. Sarkar and O. Pereira, "Using the matrix pencil method to estimate the parameters of a sum of complex exponentials," *IEEE Antennas and Propagation Magazine*, vol. 37, pp. 48-55, Feb. 1995.

[24] K. Jinhwan and T. K. Sarkar, "High resolution DOA estimation using matrix pencil," in *IEEE Antennas and Propagation Society Int. Symp.*, vol. 1, pp. 423-426, June 2004.

[25] N. Yilmazer, S. Ari, and T. K. Sarkar, "Multiple snapshot direct data domain approach and ESPRIT method for direction of arrival estimation," *Digital Signal Processing,* vol. 18, pp. 561-567, Jul. 2008.

[26] F. Sarrazin, A. Sharaiha, P. Pouliguen, J. Chauveau, S. Collardey, and P. Potier, "Comparison between Matrix Pencil and Prony methods applied on noisy antenna responses," in *Loughborough Antennas and Propagation Conf.*, pp. 1-4, Nov. 2011.

[27] M. F. Khan and M. Tufail, "Comparative analysis of various Matrix Pencil methods for direction of arrival estimation," in *Int. Conf. on Image Analysis and Signal Processing*, pp. 496-501, Apr. 2010.

[28] N. Yilmazer, T. K. Sarkar, and M. Salazar-Palma, "DOA Estimation using Matrix Pencil and ESPRIT methods using single and multiple snapshots," in *URSI Int. Symp. on Electromagnetic Theory*, pp. 215-218, Aug. 2010.

[29] F. Ping and J. Zhanrong, "Parametric estimation of ultra wideband radar targets," *Journal of Systems Engineering and Electronics*, vol. 20, pp. 499-503, June 2009.

[30] F. A. Baqai and Y. Hua, "Matrix Pencil method for inverse synthetic aperture radar imaging," in *IEEE Region 10 Int.Conf. Technology Enabling Tomorrow: Computers, Communications and Automation towards the 21st Century*, vol. 1, pp. 403-407, Nov. 1992.

[31] C. Qi, "Performance comparison between matrix-pencil and MODE for 2-D harmonic retrieval," in *Proc. of the 5th Int. Symp. on Signal Processing and Its Applications*, vol. 1, pp. 207-210, Aug. 1999.

[32] C. K. E. Lau, R. S. Adve, and T. K. Sarkar, "Combined CDMA and Matrix Pencil direction of arrival estimation," in *Proc. Vehicular Technology Conf.*, vol. 1, pp. 496-499, Sep. 2002.

[33] J. Ruze, "Physical Limitations on Antennas," Research Laboratory of Electronics, Rep. 248, May 1952.

[34] D. E. N. Davies and C. R. Ward, "Low sidelobe patterns from thinned arrays using multiplicative processing," *IEE Proc. F Communications, Radar and Signal Processing*, vol. 127, pp. 9, Feb. 1980.

[35] R. H. Macphie and Y. Tae Ho, "On using the compound interferometer to obtain the power pattern of a conventional receiving array," *IEEE Transactions on Antennas and Propagation*, vol. 57, pp. 3356-3359, Oct. 2009.

[36] R. H. Macphie, "A mills cross multiplicative array with the power pattern of a conventional planar array," in *IEEE Antennas and Propagation Society Int. Symp.*, pp. 5961-5964, June. 2007.

[37] R. Guinvarc'h, R. Gillard, B. Uguen, and J. El-Khoury, "Improving the azimuthal resolution of HFSWR with multiplicative beamforming," *IEEE Geoscience and Remote Sensing Letters*, vol. 9, pp. 925-927, Sep. 2012.

[38] X. Lili, S. Qingqing, W. Xinbo, J. Huangfu, and L. Ran, "Performance enhancement of nulling antennas by utilizing the concept of multiplicative array," in *IEEE Int. Workshop on Antenna Technology*, pp. 52-55, Mar. 2012.

[39] W. C. Barott and P. G. Steffes, "Grating lobe reduction in aperiodic linear arrays of physically large antennas," *IEEE Antennas and Wireless Propagation Letters*, vol. 8, pp. 406-408, Sep. 2009.

[40] K. C. Kerby and J. T. Bernhard, "Sidelobe level and wideband behavior of arrays of random subarrays," *IEEE Transactions on Antennas and Propagation*, vol. 54, pp. 2253-2262, Aug. 2006.

[41] Y. Lo, "A mathematical theory of antenna arrays with randomly spaced elements," *IEEE Transactions on Antennas and Propagation*, vol. 12, pp. 257-268, May 1964.

[42] J. T. Bernhard, K. Kerby, G. Cung, and P. E. Mayes, "Wideband random phased arrays: theory and design," in *IEE Wideband and Multi-band Antennas and Arrays*, pp. 89-93, Sep. 2005.

[43] A. P. Goffer, M. Kam, and P. R. Herczfeld, "Wide-bandwidth phased arrays using random subarraying," in *20th European Microwave Conf.*, pp. 241-246, Sep. 1990.

[44] D. C. Jenn, "Transmission equation for multiple cooperative transmitters and collective beamforming," *IEEE Antennas and Wireless Propagation Letters*, vol. 7, pp. 606-608, Aug. 2008.

[45] H. Ochiai, P. Mitran, H. V. Poor, and V. Tarokh, "Collaborative beamforming for distributed wireless ad hoc sensor networks," *IEEE Transactions on Signal Processing*, vol. 53, pp. 4110-4124, Nov. 2005.

[46] M. F. A. Ahmed and S. A. Vorobyov, "Collaborative beamforming for wireless sensor networks with Gaussian distributed sensor nodes," *IEEE Transactions on Wireless Communications*, vol. 8, pp. 638-643, Feb. 2009.

[47] U. R. O. Nickel, "Properties of digital beamforming with subarrays," in *Int. Conf. on Radar*, pp. 1-5, Oct. 2006.

[48] S. Bolognani, S. Del Favero, L. Schenato, and D. Varagnolo, "Distributed sensor calibration and least-square parameter identification in WSNs using consensus algorithms," in *46th Annual Allerton Conf. on Communication, Control, and Computing*, pp. 1191-1198, Sep. 2008.

[49] M. S. Stankovic, S. S. Stankovic, and K. H. Johansson, "Distributed calibration for sensor networks under communication errors and measurement noise," in *IEEE 51st Annual Conf. on Decision and Control*, pp. 1380-1385, Dec. 2012.

[50] S. Coutts, K. Cuomo, J. McHarg, F. Robey, and D. Weikle, "Distributed coherent aperture measurements for next generation BMD radar," in *4th IEEE Workshop on Sensor Array and Multichannel Processing*, pp. 390-393, Jul. 2006.

[51] G. F. Sudha, "Distributed beamforming for randomly distributed sensors with position error correction," *Procedia Engineering,* vol. 30, pp. 8-8, Mar. 2012.

[52] B. Svensson, M. Lanne, and J. Wingard, "Element position error compensation in active phased array antennas," in *Proc. of the 4th European Conf. on Antennas and Propagation*, pp. 1-3, Apr. 2010.

[53] Z. Dengchang, A. Zhulin, and X. Yongjun, "Time synchronization in wireless sensor networks using max and average consensus protocol," *Int. Journal of Distributed Sensor Networks,* vol. 2013, pp. 10, Feb. 2013.

[54] E. H. Attia and K. Abend, "An experimental demonstration of a distributed array radar," in *AP-S. Digest Antennas and Propagation Society Int.Symp.*, vol. 3, pp. 1720-1723, June 1991.

[55] P. Djerf and I. Tornazakis, "Development of a distributed digital array radar (DDAR)," M.S. thesis, Department of Electrical and Computer Engineering, Naval Postgradute School, Sep. 2008.

[56] Y.-C. Tsai, "Development of the phase synchronization circuit for wirelessly distributed digital phased array," M.S. thesis, Department of Electrical and Computer Engineering, Naval Postgraduate School, Aug. 2009.

[57] K. N. K.Hirata, S.Matsuda, H.Miyashita and S.Makino, "Experimental evaluation of capon's beam former applied to a non-uniformly arranged distributed array," in *Int. Symp. on Antennas and Propagation*, pp. 202-203, Nov. 2006.

[58] H. Steyskal, J. K. Schindler, P. Franchi, and R. J. Mailloux, "Pattern synthesis for TechSat21 - a distributed space-based radar system," *IEEE Antennas and Propagation Magazine*, vol. 45, pp. 19-25, Aug. 2003.

[59] T. Liang and H. K. Kwan, "A novel approach to fast DOA estimation of multiple spatial narrowband signals," in *45th Midwest Symp. on Circuits and Systems*, vol. 1, pp. I-431-4, Aug. 2002.

THIS PAGE INTENTIONALLY LEFT BLANK

INITIAL DISTRIBUTION LIST

1. Defense Technical Information Center
   Ft. Belvoir, Virginia

2. Dudley Knox Library
   Naval Postgraduate School
   Monterey, California